National Library
of Canada

Acquisitions and
Bibliographic Services Branch

395 Wellington Street
Ottawa, Ontario
K1A 0N4

Bibliothèque nationale
du Canada

Direction des acquisitions et
des services bibliographiques

395, rue Wellington
Ottawa (Ontario)
K1A 0N4

Your file Votre référence

Our file Notre référence

NOTICE

The quality of this microform is heavily dependent upon the quality of the original thesis submitted for microfilming. Every effort has been made to ensure the highest quality of reproduction possible.

If pages are missing, contact the university which granted the degree.

Some pages may have indistinct print especially if the original pages were typed with a poor typewriter ribbon or if the university sent us an inferior photocopy.

Reproduction in full or in part of this microform is governed by the Canadian Copyright Act, R.S.C. 1970, c. C-30, and subsequent amendments.

AVIS

La qualité de cette microforme dépend grandement de la qualité de la thèse soumise au microfilmage. Nous avons tout fait pour assurer une qualité supérieure de reproduction.

S'il manque des pages, veuillez communiquer avec l'université qui a conféré le grade.

La qualité d'impression de certaines pages peut laisser à désirer, surtout si les pages originales ont été dactylographiées à l'aide d'un ruban usé ou si l'université nous a fait parvenir une photocopie de qualité inférieure.

La reproduction, même partielle, de cette microforme est soumise à la Loi canadienne sur le droit d'auteur, SRC 1970, c. C-30, et ses amendements subséquents.

Canada

BINUCLEAR AND TRINUCLEAR COMPOUNDS OF OSMIUM.

by

John Anthony Shipley

B. Sc., Simon Fraser University, 1982

THESIS SUBMITTED IN PARTIAL FULFILLMENT OF

THE REQUIREMENTS FOR THE DEGREE OF

DOCTOR OF PHILOSOPHY

in the Department

of

Chemistry

SIMON FRASER UNIVERSITY

July, 1992

ISBN 0-315-83762-4

APPROVAL

Name: John Anthony Shipley

Degree: Doctor of Philosophy

Title of Thesis: BINUCLEAR AND TRINUCLEAR COMPOUNDS OF OSMIUM

Examining Committee:

Chair: Dr. S. Holdcroft

Dr. R.K. Pomeroy, (Professor)
Senior Supervisor

Dr. D. Sutton, (Professor)
Committee Member

Dr. T.J. Burgford, (Assistant Professor)
Committee Member

Dr. F.W.B. Einstein, (Professor)
Internal Examiner

Dr. I.S. Butler
External Examiner
Department of Chemistry
McGill University
801 Sherbrooke Street West
Montreal, Quebec H3A 2K6 Canada

Date Approved: August 11, 1992

PARTIAL COPYRIGHT LICENSE

I hereby grant to Simon Fraser University the right to lend my thesis, project or extended essay (the title of which is shown below) to users of the Simon Fraser University Library, and to make partial or single copies only for such users or in response to a request from the library of any other university, or other educational institution, on its own behalf or for one of its users. I further agree that permission for multiple copying of this work for scholarly purposes may be granted by me or the Dean of Graduate Studies. It is understood that copying or publication of this work for financial gain shall not be allowed without my written permission.

Title of Thesis/Project/Extended Essay:

BINUCLEAR AND TRINUCLEAR COMPOUNDS OF OSMIUM

Author:

(signature)

John Anthony Shipley

(name)

AUGUST 19, 1992

(date)

ABSTRACT

The 18-electron osmium compounds, $Os(CO)_4(L)$ and $Os(CO)_3(L)_2$, (L = $CNBu^t$) have been synthesized from $Os(CO)_5$ or $Os_3(CO)_{12}$ and t-butyl isocyanide. These compounds react with $M(CO)_5$ (M = Cr, Mo, W) fragments to form complexes with unbridged, dative metal-metal bonds (i.e., $(OC)_4(L)Os$-$M(CO)_5$ and $(OC)_3(L)_2OsM(CO)_5$). Structural and spectroscopic evidence indicates that the isocyanide ligand always occupies a position cis to the metal-metal bond in contrast to the phosphine analogues (i.e., L = PR_3). For the $(OC)_4(L)OsM(CO)_5$ complexes there is only one isomer present in solution, but for the $(OC)_3(L)_2OsM(CO)_5$ complexes there is an equilibrium mixture of cis and trans diequatorial isomers in solution. Migration of the isocyanide ligand from M (M = Cr) to Os was found to be facile.

Also isolated in the reaction of $Os(CO)_4(L)$ with $W(CO)_5(THF)$ were the complexes $(OC)_4(L)OsOs(CO)_3(L)W(CO)_5$ and $(OC)_3(L)_2OsOs(CO)_4W(CO)_5$. The crystal structure of the former derivative reveals a linear arrangement of metal atoms with no bridging ligands. These complexes are believed to contain two dative metal-metal bonds in tandem (i.e., Os $\longrightarrow$ Os $\longrightarrow$ W). This is only the second example of a structurally characterized compound where this type of bonding has been proposed. The ^{13}C NMR spectrum indicated that the structure in solution is the same as that in the solid state.

The clusters $(\eta^5\text{-}C_5R_5)(OC)Ir[Os(CO)_4]_2$ (R = H, Me) were formed by the reaction of $(\eta^5\text{-}C_5R_5)Ir(CO)_2$ with $Os(CO)_4(\eta^2\text{-cyclooctene})$. The solid state structure of the pentamethylcyclopentadienyl derivative consists of a $(\eta^5\text{-}C_5Me_5)Ir(CO)$ unit and two $Os(CO)_4$ units bound in a triangular arrangement; there are no bridging carbonyls. Variable temperature ^{13}C NMR studies of the two clusters indicate CO exchange between the metal centers occurs above

-50 °C. The mode of collapse of the resonances was interpreted in terms of partial merry-go-round CO exchanges that occur in the two vertical planes that contain the Ir atom and one of the Os atoms. The activation barrier for the CO exchange in the cyclopentadienyl analogue was determined to be 14.2 kcal mol^{-1} at -10 °C, whereas a dramatically lower barrier ($\Delta G^{\neq}$ = 7.4 kcal mol^{-1}) was found for the pentamethylcyclopentadienyl derivative at -116 °C.

The substituted complexes $(\eta^5\text{-}C_5H_5)(OC)IrOs_2(CO)_7(L)$ (L = PMe_3, $P(OMe)_3$, $CNBu^t$) were prepared by removal of a carbonyl ligand from $(\eta^5\text{-}C_5H_5)(OC)Ir[Os(CO)_4]_2$ with Me_3NO followed by addition of the ligand L. Variable temperature ^{13}C NMR studies indicated CO exchange in these clusters above -30 °C. The lowest energy CO exchange process for the three clusters was interpreted in terms of a partial merry-go-round in one of the vertical planes containing the Ir atom and one of the Os atoms. The activation barriers for the CO exchange in the PMe_3 and $CNBu^t$ complexes were found to be lower than that for the unsubstituted parent cluster, with the $CNBu^t$ derivative having a particularly low barrier. Both of the phosphorus ligand derivatives were found to exist as a mixture of two isomers in solution. The activation barriers for the isomerization process for each cluster were determined; there was no significant difference between the barriers. A two dimensional NOE ^{13}C spectrum of the trimethylphosphine substituted derivative at -30 °C was used to confirm both the CO exchange mechanism for the cluster and the identity of the major isomer.

DEDICATION

To my wife, Alison, without whom this degree would not have been possible; for all your support and sacrifice during this lengthy pilgrimage, your time and effort with our children, your help with proofreading, to name a few. Here's to you!

To David and Laura; for daily reminding me of the important things in life and for your life, energy, and love.

ACKNOWLEDGEMENTS

I first wish to thank my senior supervisor, Dr. Roland Pomeroy, for all his confidence, encouragement, support and boundless optimism during my time as a graduate student. In 'putting up with' my many questions, he helped transform a biochemist into an 'inorganic-er'.

I would also like to express my thanks to the research group for their friendship and help in the lab: in order of appearance, Harry, Andrew, Victor, Mutley, Charles, Val, Weibin, and Anna.

I wish to thank Professor Fred Einstein, Dr. Ray Batchelor, and Dr. Andreas Riesen for the crystal structure determinations.

The skilled technical assistance of Mr. Fred Chin, Mr. Greg Owen, Mrs. Marcie Tracey, Mr. Miki Yang and the secretarial staff is gratefully acknowledged.

TABLE OF CONTENTS

Approval ii

Abstract iii

Dedication v

Acknowledgements vi

Table of Contents vii

List of Figures ix

List of Tables xi

General Introduction 1

1. Heterobimetallic and Heterotrimetallic Complexes with Dative Metal-Metal Bonds between Osmium and a Group 6 Metal. 2

   1.1 Introduction 2

   1.2 Experimental 6

   1.3 Results and Discussion 17

   1.4 Conclusion 47

2. Synthesis, Characterization, and Carbonyl Exchange in $(\eta^5\text{-}C_5R_5)(OC)Ir[Os(CO)_4]_2$ (R = H; R = Me). 49

   2.1 Introduction 49

   2.2 Experimental 51

   2.3 Results and Discussion 54

   2.4 Conclusion 68

3. Synthesis, Carbonyl Exchange, and Isomerization in $(\eta^5\text{-}C_5H_5)(OC)IrOs_2(CO)_7(L)$ (L = PMe_3, $P(OMe)_3$, $CNBu^t$). 69

3.1 Introduction 69

3.2 Experimental 70

3.3 Results and Discussion 74

3.4 Conclusion 108

Conclusions. 110

References. 112

LIST OF FIGURES

Figure		Page
Figure 1.1	Molecular structure of $(OC)_4(Bu^tNC)OsCr(CO)_5$ (**1-Cr**).	19
Figure 1.2	Carbonyl region of the ^{13}C NMR spectrum of $(OC)_4(Bu^tNC)Os$-$M(CO)_5$ (M = Cr, **1-Cr**; M = Mo, **1-Mo**; M = W, **1-W**).	22
Figure 1.3	Infrared spectrum of $(OC)_4(Bu^tNC)OsCr(CO)_5$ (**1-Cr**).	24
Figure 1.4	Infrared spectrum of $(OC)_4(Bu^tNC)OsM(CO)_5$ (M = Mo, **1-Mo**; M = W, **1-W**).	25
Figure 1.5	Carbonyl region of the ^{13}C NMR spectrum of [*trans-dieq*-$(OC)_3(Bu^tNC)_2Os]M(CO)_5$ (M = Cr, **2a-Cr**; M = Mo, **2a-Mo**; M = W, **2a-W**).	31
Figure 1.6	Infrared spectrum of [*trans-dieq*-$(OC)_3(Bu^tNC)_2Os]Cr(CO)_5$ (**2a-Cr**) and [*cis-dieq*-$(OC)_3(Bu^tNC)_2Os]Cr(CO)_5$ (**2b-Cr**).	32
Figure 1.7	Molecular structure of [*cis-dieq*-$(OC)_3(Bu^tNC)_2Os]Cr(CO)_5$ (**2b-Cr**).	35
Figure 1.8	Molecular structure of $(OC)_4(Bu^tNC)OsOs(CO)_3(CNBu^t)$-$W(CO)_5$ (**3a**).	40
Figure 1.9	Carbonyl region of ^{13}C NMR spectrum of $(OC)_4(Bu^tNC)OsOs(CO)_3(CNBu^t)W(CO)_5$ (**3a**) and [*cis-dieq*-$(OC)_3(Bu^tNC)_2Os]Os(CO)_4W(CO)_5$ (**3b**).	44
Figure 2.1	Molecular structure of $(\eta^5\text{-}C_5Me_5)(OC)Ir[Os(CO)_4]_2$ (**1***). ...	55
Figure 2.2	Variable-temperature ^{13}C NMR spectra of $(\eta^5\text{-}C_5H_5)(OC)Ir[Os(CO)_4]_2$ (**1**).	59
Figure 2.3	Calculated and observed ^{13}C NMR spectra for $(\eta^5\text{-}C_5H_5)(OC)Ir[Os(CO)_4]_2$ (**1**) at -10 °C; Calculated and observed ^{13}C NMR spectra for $(\eta^5\text{-}C_5Me_5)(OC)Ir$-$[Os(CO)_4]_2$ (**1***) at -116 °C.	63
Figure 2.4	Variable-temperature ^{13}C NMR spectra of $(\eta^5\text{-}C_5Me_5)(OC)Ir[Os(CO)_4]_2$ (**1***).	65

Figure 3.1 Variable temperature ^{13}C NMR spectra of $(\eta^5\text{-}C_5H_5)(OC)IrOs_2(CO)_7(PMe_3)$ (**1**). 75

Figure 3.2 ^{13}C NMR spectrum of $(\eta^5\text{-}C_5H_5)(OC)IrOs_2(CO)_7(PMe_3)$ (**1**) at -70 °C. 76

Figure 3.3 ^{13}C NOESY spectrum of $(\eta^5\text{-}C_5H_5)(OC)IrOs_2(CO)_7(PMe_3)$ (**1**) at -30 °C. 84

Figure 3.4 Variable Temperature ^{13}C NMR spectra of $(\eta^5\text{-}C_5H_5)(OC)IrOs_2(CO)_7[P(OMe)_3]$ (**2**). 87

Figure 3.5 ^{13}C NMR spectrum of $(\eta^5\text{-}C_5H_5)(OC)IrOs_2(CO)_7[P(OMe)_3]$ (**2**) at -50 °C. 88

Figure 3.6 Variable temperature ^{13}C NMR spectra of $(\eta^5\text{-}C_5H_5)(OC)IrOs_2(CO)_7(CNBu^t)$ (**3**). 92

Figure 3.7 ^{13}C NMR spectrum of $(\eta^5\text{-}C_5H_5)(OC)IrOs_2(CO)_7(CNBu^t)$ (**3**) at -80 °C. 93

Figure 3.8 Variable temperature ^1H NMR spectra of $(\eta^5\text{-}C_5H_5)(OC)IrOs_2(CO)_7(CNBu^t)$ (**3**). 99

Figure 3.9 Calculated and observed ^1H NMR spectra for $(\eta^5\text{-}C_5H_5)(OC)IrOs_2(CO)_7(CNBu^t)$ (**3**) at -60 °C. 100

Figure 3.10 Variable temperature ^1H NMR spectra of $(\eta^5\text{-}C_5H_5)(OC)IrOs_2(CO)_7(PMe_3)$ (**1**). 102

Figure 3.11 Calculated and observed ^1H NMR spectra for $(\eta^5\text{-}C_5H_5)(OC)IrOs_2(CO)_7(PMe_3)$ (**1**) at +35 °C. 103

Figure 3.12 Variable temperature ^1H NMR spectra of $(\eta^5\text{-}C_5H_5)(OC)IrOs_2(CO)_7[P(OMe)_3]$ (**2**). 106

Figure 3.13 Calculated and observed ^1H NMR spectra of $(\eta^5\text{-}C_5H_5)(OC)IrOs_2(CO)_7[P(OMe)_3]$ (**2**) at +25 °C. 107

LIST OF TABLES

Table		Page
Table 1.1	Analytical and Mass Spectral Data for New Compounds. ..	7
Table 1.2	Infrared Data For New Compounds.	8
Table 1.3	^{1}H and ^{13}C NMR Data for New Compounds.	9
Table 1.4	Bond Lengths (Å) and Selected Angles (deg) for $(OC)_4(Bu^tNC)OsCr(CO)_5$ (**1-Cr**).	20
Table 1.5	Bond Lengths (Å) and Selected Angles (deg) for [*cis-dieq*-$(OC)_3(Bu^tNC)_2Os]Cr(CO)_5$ (**2b-Cr**).	36
Table 1.6	Bond Lengths (Å) and Selected Angles (deg) for $(OC)_4(Bu^tNC)OsOs(CO)_3(CNBu^t)W(CO)_5$ (**3a**).	41
Table 2.1	Bond lengths (Å) and Selected angles (deg) for $(\eta^5\text{-}C_5Me_5)(OC)Ir[Os(CO)_4]_2$ (**1***).	56

GENERAL INTRODUCTION

One of the goals of organometallic chemistry is the synthesis and study of compounds with novel structural, bonding and fluxional character. Studies of these compounds in the solution and solid state often make use of such techniques as IR and NMR spectroscopy, and X-ray crystallography, respectively. This thesis reports the use of these techniques in the study of new binuclear and trinuclear compounds of osmium.

The first chapter deals with bimetallic and trimetallic compounds in which the unbridged metal-metal bonds present are considered to be rare examples of dative rather than nondative bonds.

The second and third chapters describe the synthesis of a number of $IrOs_2$ carbonyl clusters and a study of their stereochemical nonrigidity by variable temperature ^1H and ^{13}C NMR spectroscopy. The latter study was carried out to elucidate the mechanisms of the exchange processes and the effect of the substituted ligands on the activation barriers to the nonrigidity. The studies were also carried out to investigate the possible rotation of the Ir fragment relative to the rest of the cluster.

CHAPTER 1

HETEROBIMETALLIC AND HETEROTRIMETALLIC COMPLEXES WITH DATIVE METAL-METAL BONDS BETWEEN OSMIUM AND A GROUP 6 METAL.

1.1 Introduction

The concept of the donor-acceptor or dative bond in chemistry dates back to the 1920's and is associated with the names of Lewis, Sidgwick, and others.[1] Such a bond results from the interaction of a Lewis acid and a Lewis base. The prototypical example of a main group compound with a dative bond is H_3NBH_3 in which the ammonia is the Lewis base and borane is the Lewis acid.[2]

Dative bonds between metal atoms are also known. By far the most common type of metal-metal dative bond is that formed between a Lewis base transition metal fragment and a Lewis acid main group metal fragment. Two examples are $Fe(CO)_2(PMe_2Ph)_2[CS_2C_2(CO_2Me)_2](HgCl_2)$[3] in which the 18-electron Fe complex acts as the Lewis base to the Lewis acid $HgCl_2$, and in $(\eta^5\text{-}C_5H_5)Rh(PMe_3)_2(Al_2Me_2Cl_2)$[4] where the 18-electron Rh complex is the Lewis base towards the Al_2 Lewis acid.

Much less common are dative bonds between two transition metal atoms and they have been formulated in order that each metal attains an 18- or in some cases, a 16-electron configuration. Until recently, in those cases where a dative bond has been proposed, the metal-metal bond is bridged by other ligands. The first example of a complex in which a dative metal-metal bond was proposed was in complex I (R = OH, R' = Me).[5] An alternate electron counting scheme which would result in a non-dative, covalent Fe-Fe bond can, however, be proposed as shown in complex II.

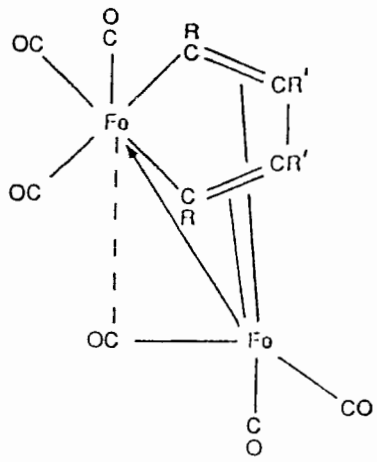

I

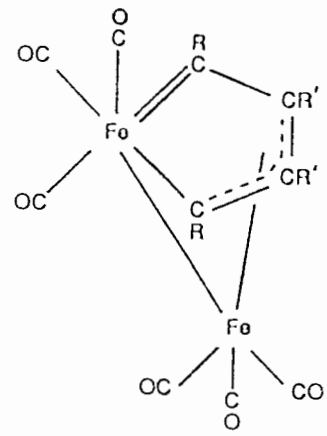

II

Similarly, Geoffroy and others have proposed dative metal-metal bonds in phosphido-bridged species;[6] an example is shown in III. Once again, an alternate counting scheme that yields a non-dative metal-metal bond can be formulated as shown in IV.

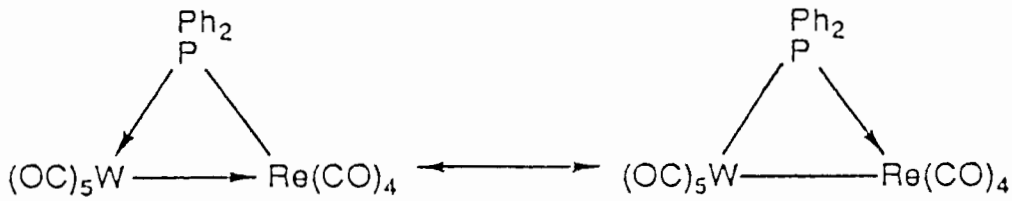

III IV

A dative metal-metal bond has also been proposed for the anionic hydride complexes $[(H)(OC)_4FeM(CO)_5]^-$ (M = Cr, W)[7] and the non hydride complexes $[(OC)_5M'M(CO)_5]^-$ (M' = Mn, Re; M = Cr, Mo, W).[8] The presence of a dative metal-metal bond in these complexes requires that the negative charge be localized on the group 7 or Fe metal atom, yielding an anionic 18-electron fragment and a neutral 16-electron group 6 metal fragment. This formulation is supported by ab initio calculations,[9] although it would seem at the same time to violate Paulings electroneutrality principle. An alternative formulation has the

metal-metal bond as a nondative bond and the negative charge equally distributed over the two metal centers.

The first example of a neutral transition metal complex in which a dative metal-metal bond could be unambiguously assigned was $(OC)_5OsOs(CO)_3(GeCl_3)(Cl)$.[10] The crystal structure showed no bridging ligands. The dative metal-metal bond results from the 18-electron $Os(CO)_5$ fragment acting as a two-electron donor to the 16-electron fragment $Os(CO)_3(GeCl_3)(Cl)$. Since this original discovery in 1983, a number of other bimetallic complexes containing unbridged donor-acceptor metal-metal bonds have been reported from this laboratory[11] and others.[12] As well, rare examples of cluster compounds with unsupported dative metal-metal bonds, have also been reported from this laboratory.[13]

One major area of work on the bimetallic complexes has been the study of the $(L)_x(OC)_{5-x}OsM(CO)_5$ (x = 1, 2; L = CO, PR_3, or $P(OR)_3$; M = Cr, Mo, or W) series.[11a,f] One part of this thesis reports the extension of this area to the synthesis of new mononuclear $Os(CO)_{5-x}(L)_x$ complexes and the investigation of their ability to act as donor fragments. *tert*-Butyl isocyanide was the ligand chosen for this study, since it is a sterically undemanding σ-donor ligand. (It was found for the phosphine and phosphite substituted bimetallic complexes that the bulkier the phosphorus ligand the more it preferred the axial rather than the radial site on the osmium atom.[11a]) Thus the initial objective was to prepare the isocyanide substituted osmium complexes. Surprisingly, no simple osmium isocyanide carbonyl complexes, $Os(CO)_{5-x}(CNR)_x$, had been reported, although many iron and ruthenium analogues were known.[14]

Having made the isocyanide substituted osmium fragments, they were then to be used in the synthesis of $(OC)_{5-x}(CNBu^t)_xOsM(CO)_5$ (x = 1, 2; M = Cr, Mo, W) complexes. Spectroscopic studies (^{13}C NMR and IR) along with X-ray

crystallographic structural studies were used to study their structure in solution and in the solid state, respectively, in an effort to make a comparison with the phosphorus ligand analogues.[15]

Another aspect of the work on the bimetallic complexes that was of interest was the ability of different ligands, in this case the isocyanide ligand, to migrate across the dative metal-metal bond. It was already known that CO migration between the two metal centers in the phosphine and phosphite analogues of $(L)(OC)_4OsM(CO)_5$ is facile in both directions.[11a] This was also found for $(Me_3P)(OC)_4OsOs_3(CO)_{11}$.[13a]

One recent unexpected result from the work on one of the phosphite substituted bimetallic complexes was the discovery of a trimetallic species with two dative metal-metal bonds in tandem.[16] This result prompted a reexamination of the products of the synthesis of $(OC)_4(Bu^tNC)OsW(CO)_5$. It was determined that indeed linear trimetallic complexes were byproducts of this synthesis. A crystal structure of one of these compounds showed a linear framework and two unbridged metal-metal bonds in tandem.[17]

Details of the syntheses, spectroscopic properties, and X-ray crystallographic structural studies that were determined on the bimetallic and trimetallic complexes reported in this thesis have either been published or are accepted for publication.[18,19]

1.2 Experimental

Unless otherwise stated, manipulations of starting materials and products were carried out under a nitrogen atmosphere with the use of standard Schlenk techniques. Hexane, tetrahydrofuran (THF) and dichloromethane were distilled under nitrogen from potassium, potassium benzophenone ketyl, and P_2O_5, respectively. The carbonyls $M(CO)_6$ (M = Cr, Mo, W), $Os_3(CO)_{12}$, cyclooctene, and t-butyl isocyanide were obtained commercially. Literature methods were used to prepare $Os(CO)_5$[20] and $M(CO)_5(THF)$.[11a] An external medium pressure mercury discharge lamp (200-W, Hanovia Model 654 A36) contained in a water-cooled quartz jacket was employed in the irradiations. There were ~ 5 cm between the source and the edge of the reaction vessel.

Infrared spectra (Table 1.2) were recorded on a Perkin-Elmer 983 Spectrometer; the internal calibration of the instrument was periodically checked against the known absorption frequencies of gaseous CO. Electron-impact (70 eV) mass spectra (Table 1.1) were obtained with a Hewlett-Packard 5985 GC-MS instrument; the most intense peak of the ions of highest mass in each spectrum matched that calculated for the parent ion of the compound in question. NMR spectra (Table 1.3) were recorded on either a Bruker WM400 spectrometer (operating frequencies: 400 MHz for ^1H and 100.6 MHz for ^{13}C) or a Bruker SY-100 spectrometer. The ^{13}C NMR spectra were obtained on samples enriched with ^{13}CO (about 30%) which, in turn, were prepared from ^{13}CO-enriched $M(CO)_5(THF)$.[11a] The microanalyses (Table 1.1) were obtained by M. K. Yang of the Microanalytical Laboratory of Simon Fraser University.

The three crystal structures reported in this chapter were determined by Professor F.W.B. Einstein and Dr. R.J. Batchelor at Simon Fraser University.

Preparation of $Os(CO)_4(CNBu^t)$. Method 1. The cyclooctene derivative $Os(CO)_4(\eta^2$-cyclooctene) was prepared from $Os_3(CO)_{12}$ by a procedure that was

Table 1.1 Analytical and Mass Spectral Data for New Compounds

	anal.						
	calcd			found			
	C	H	N	C	H	N	MS[a]
$Os(CO)_4(CNBu^t)$	28.05	2.35	3.63	28.25	2.54	3.70	387
$Os(CO)_3(CNBu^t)_2$	35.45	4.12	6.36	35.65	4.08	6.29	442
$(OC)_4(Bu^tNC)OsCr(CO)_5$ **(1-Cr)**	29.12	1.57	2.42	29.35	1.69	2.50	579
$(OC)_4(Bu^tNC)OsMo(CO)_5$ **(1-Mo)**	27.06	1.46	2.25	27.25	1.48	2.05	623
$(OC)_4(Bu^tNC)OsW(CO)_5$ **(1-W)**	23.71	1.28	1.97	23.66	1.36	2.09	709
$(OC)_3(Bu^tNC)_2OsCr(CO)_5$ **(2a-Cr)**	34.18	2.87	4.43	34.56	2.97	4.18	634
$(OC)_3(Bu^tNC)_2OsCr(CO)_5$ **(2b-Mo)**	34.18	2.87	4.43	34.34	2.78	4.27	634
$(OC)_3(Bu^tNC)_2OsMo(CO)_5$ **(2a-Mo)**	31.96	2.86	4.14	31.76	2.67	3.93	678
$(OC)_3(Bu^tNC)_2OsMo(CO)_5$ **(2b-Mo)**	31.96	2.86	4.14	31.97	2.62	4.30	678
$(OC)_3(Bu^tNC)_2OsW(CO)_5$ **(2a-W)**	28.28	2.37	3.66	28.48	2.46	3.69	764
$(OC)_3(Bu^tNC)_2OsW(CO)_5$ **(2b-W)**	28.28	2.37	3.66	28.24	2.32	3.67	764
$(OC)_4(Bu^tNC)OsOs(CO)_3(CNBu^t)W(CO)_5$ **(3a)**	24.77	1.70	2.63	25.03	1.85	2.40	[b]
$(OC)_3(Bu^tNC)_2OsOs(CO)_4W(CO)_5$ **(3b)**	24.77	1.70	2.63	24.90	1.66	2.50	[b]

[a] M^+ ion [b] satisfactory mass spectrum not obtained

Table 1.2 Infrared Data for New Compounds

	solvent[b]	ν(CN), cm^{-1}	ν(CO), cm^{-1}
$Os(CO)_4(L)$	hex	2195 (w)	2061 (s), 1996 (m), 1960 (vs)
$Os(CO)_3(L)_2$	hex	2136 (m)	1925 (vs)
$(OC)_4(L)OsCr(CO)_5$ **(1-Cr)**	hex	2206 (w)	2099 (m), 2040 (m), 2031 (vs), 2021 (vs), 1961 (w), 1921 (vs), 1914 (vs)
	dich	2214 (w)	2102 (m), 2030 (vs), 1915 (vs)
$(OC)_4(L)OsMo(CO)_5$ **(1-Mo)**	hex	2205 (w)	2095 (m), 2048 (m), 2033 (m), 2019 (s), 2014 (s), 1973 (w),1933 (vs), 1925 (s), 1914 (s)
	dich	2211 (w)	2097 (m), 2047 (s), 2013 (s), 1926 (vs), 1888 (m)
$(OC)_4(L)OsW(CO)_5$ **(1-W)**	hex	2207 (w)	2099 (m), 2046 (m), 2039 (m), 2022 (s), 1963 (vw), 1922 (vs),1915 (s), 1909 (sh)
	dich	2214 (m)	2102 (m), 2044(m), 2022 (s), 1915 (vs), 1884 (sh)
$(OC)_3(L)_2OsCr(CO)_5$ **(2a-Cr)**[c]	hex	2174 (m)	2060 (vw), 2014 (s), 1995 (s), 1909 (s), 1902 (vs)
	dich	2181 (s)	2062 (vw), 2012 (vs), 1993 (s), 1904 (vs), 1870 (sh),
$(OC)_3(L)_2OsCr(CO)_5$ **(2b-Cr)**	dich	2208 (m), 2184 (m)	2061 (s), 2012 (vs), 1994 (sh), 1942 (wv), 1899 (vs), 1867 (sh)
$(OC)_3(L)_2OsMo(CO)_5$ **(2a-Mo)**[c]	hex	2170 (m)	2059 (w), 2026 (m), 1987 (s), 1921 (vs), 1913 (s), 1902 (s)
	dich	2176 (s)	2058 (m), 2026 (s), 1984 (s), 1915 (vs), 1872(m)
$(OC)_3(L)_2OsMo(CO)_5$ **(2b-Mo)**	dich	2204 (m), 2177 (m)	2058 (s), 2027 (s), 1994 (s), 1914 (vs), 1871 (m)
$(OC)_3(L)_2OsW(CO)_5$ **(2a-W)**[c]	hex	2173 (m)	2062 (vw), 2027 (m), 1995 (s), 1910 (vs), 1903 (s), 1899 (sh)
	dich	2180 (m)	2062 (w), 2027 (m), 1989 (s), 1908 (vs), 1866 (m)
$(OC)_3(L)_2OsW(CO)_5$ **(2b-W)**	dich	2207 (m), 2182 (m)	2062 (s), 2027 (s), 2003(s), 1951 (vw), 1904 (vs), 1865 (m)
$(OC)_4(L)OsOs(OC)_3(L)W(CO)_5$ **(3a)**	dich	2216 (w), 2170 (w)	2102 (m), 2047 (s), 2013 (s), 1954 (s), 1899 (s), 1847 (m, br)
$(OC)_3(L)_2OsOs(OC)_4W(CO)_5$ **(3b)**	dich	2216 (w), 2195 (w)	2089 (s), 2056 (s), 2031 (s), 2016 (s), 1968 (vs), 1900 (s), 1856 (m, br)

[a] L = Bu^{t}NC. [b] hex = hexane; dich = dichloromethane. [c] weak absorptions may be due to isomer b

Table 1.3 ^1H and ^{13}C NMR Data for New Compounds

	^1H	^{13}C					
		$M(CO)_5$		Os Carbonyls			
	δ[a]	δ(ax-CO)[b]	δ(eq-CO)[b]	δ(CO)[b,c]			
$Os(CO)_4(L)$	1.53			187.4			
$Os(CO)_3(L)_2$	1.48			193.4			
$(OC)_4(L)OsCr(CO)_5$ (**1-Cr**)	1.55[d]	229.6	222.7	187.1	180.0	165.4	
$(OC)_4(L)OsMo(CO)_5$ (**1-Mo**)	1.55[d]	216.2	210.3	187.0	179.7	166.8	
$(OC)_4(L)OsW(CO)_5$ (**1-W**)	1.55[d]	203.9 (176)[e]	202.2 (125)[e]	184.0	177.8	165.7	
$(OC)_3(L)_2OsCr(CO)_5$ (**2a-Cr**)[f]	1.47	231.7	225.5	194.1	168.0		
$(OC)_3(L)_2OsCr(CO)_5$ (**2b-Cr**)	1.54	231.9	226.1	188.0	167.2		
$(OC)_3(L)_2OsMo(CO)_5$ (**2a-Mo**)[f]	1.47	217.4	212.0	193.9	169.3		
$(OC)_3(L)_2OsMo(CO)_5$ (**2b-Mo**)[g]	1.53	217.7	212.8	188.0	168.4		
$(OC)_3(L)_2OsW(CO)_5$ (**2a-W**)[f]	1.47	205.9 (179)[e]	204.1 (126)[e]	190.5	168.3		
$(OC)_3(L)_2OsW(CO)_5$ (**2b-W**)	1.53	206.2 (178)[e]	204.6 (126)[e]	185.3	167.3		
$(OC)_4(L)OsOs(OC)_3(L)W(CO)_5$ (**3a**)	1.54, 1.46	207.4 (177)[e]	204.9 (125)[e]	197.5 (2)	192.2 (1)	180.9 (2)	177.0 (1)
				162.5 (1)			
$(OC)_3(L)_2OsOs(OC)_4W(CO)_5$ (**3b**)	1.54	204.4 (179)[e]	204.4 (124)[e]	196.3 (4)	179.2 (2)	162.9(1)	
$(OC)_7(L)_2Os_2W(CO)_5$ (**3c**)	h	i	204.1	195.8 (4)	183.0 (2)	163.8(1)	

[a] In $CDCl_3$ solution (room temperature). [b] ^{13}CO-enriched samples in CH_2CD_2/CD_2Cl_2 at -30 or -40 °C, except for the isomers of **3**, which were obtained at 0 °C. [c] Figures in parentheses for osmium carbonyls are relative intensities. [d] Spectrum at -40 °C. [e] J_{W-C} [f] Spectrum contained signals assigned to isomer **b**. [g] Spectrum contained a weak signal assigned to isomer **a**. [h] not measured. [i] expected signal due to axial carbonyl on tungsten not seen.

a modification of that of Burke:[21] A quartz Carius tube fitted with a Teflon valve was charged with $Os_3(CO)_{12}$ (138 mg, 0.152 mmol), cyclooctene (1.92 mL, 14.7 mmol) and benzene (60 mL). The vessel was cooled to -196 °C and evacuated; the solution was degassed with one freeze-pump-thaw cycle. The vessel was pressurized with CO (1 atm) and the solution irradiated through a GWV filter ($\lambda > 370$ nm) for 23 h. The solvent and excess cyclooctene were removed on the vacuum line; the remaining solid was extracted with hexane (2 x 20 mL). The extracts were combined and placed along with further hexane (35 mL) and Bu^{t}NC (64 μL, 0.57 mmol) in a round-bottom flask (80 mL capacity) fitted with a Teflon valve. The flask was heated in the dark at 55 - 65 °C for 24 h. The solvent and excess Bu^{t}NC were removed on the vacuum line and the remaining solid subjected to sublimation (25 °C, 0.1 mm Hg) to a water-cooled probe whereupon $Os(CO)_4(CNBu^t)$ was obtained as a white solid. The yield of $Os(CO)_4(CNBu^t)$ was 50 mg (28%).

Method 2. To a 100 mL three-necked flask was added $Os(CO)_5$ (~155 mg, 0.47 mmol) in hexane/benzene (1/1, v/v, 50mL), Bu^{t}NC (50 μL, 0.48 mmol) and the catalyst $CoCl_2 \cdot 2H_2O$ (~5mg). The solution was refluxed for 20 min during which time the color of the solution changed from green to yellow. An infrared spectrum of the solution at this stage indicated the presence of $Os(CO)_4(CNBu^t)$ and $Os(CO)_3(CNBu^t)_2$, but not of $Os(CO)_5$. The solvent and any remaining Bu^{t}NC were removed on the vacuum line, and the desired product isolated as in Method 1. The yield of $Os(CO)_4(CNBu^t)$ was 52 mg (28%).

Preparation of $Os(CO)_3(CNBu^t)_2$. To a 200 mL, three-necked flask was added $Os(CO)_5$ (263 mg, 0.80 mmol) in hexane/benzene (1/1, v/v, 100 mL), Bu^{t}NC (70 μL, 0.67 mmol) and $CoCl_2 \cdot 2H_2O$ (~5 mg). The solution was refluxed for 20 min at which time the flask and contents were cooled and more Bu^{t}NC (70 μL, 0.67 mmol) added; the solution was refluxed for a further 20 min. An infrared

spectrum of the solution at this stage indicated the reaction was complete (the solution had turned from pale green to yellow). The solvent and any unreacted Bu^tNC were removed on the vacuum line. The remaining solid was extracted with hexane (4 x 20 mL). The hexane extracts were combined and evaporated to dryness to yield crude $Os(CO)_3(CNBu^t)_2$ (80 mg, 23%). The analytical sample was obtained as bright yellow, air stable crystals, by sublimation (with some decomposition) of the crude product at 80-90 °C (0.1 mm Hg) followed by recrystallization of the sublimed product from hexane.

Preparation of $(OC)_4(Bu^tNC)OsM(CO)_5$ (M = Cr, Mo, W). A solution of $M(CO)_5(THF)$ was prepared by prolonged irradiation of $M(CO)_6$ (M = Cr, 0.20 mmol; M = Mo, 0.60 mmol; M = W, 0.40 mmol) and THF (30 mL).[11a] The solution was reduced in volume to 1-2 mL and immediately cooled to -196 °C. A solution of $Os(CO)_4(CNBu^t)$ (40 mg, 0.10 mmol) in hexane (10 mL) was added to the frozen $M(CO)_5(THF)$/THF and the resulting mixture allowed to warm with stirring. The treatment varied somewhat depending on the group 6 metal: for the chromium case the mixture was allowed to warm to room temperature, for the molybdenum case to 0 °C, and for the tungsten case to room temperature followed by a further 20 min stirring. After this treatment, the isolation of the product was identical in each case. The solvent was removed on the vacuum line and the residue extracted with hexane (4 x 10 mL). The extracts were combined and evaporated to dryness. The residue was subjected to sublimation (0.1 mm Hg) at room temperature (M = Cr) or 40 °C (M = Mo,W) to a water-cooled probe which removed $M(CO)_6$. The residue remaining after the sublimation was crystallized from hexane/CH_2Cl_2 (7/1) to give analytically pure $(OC)_4(Bu^tNC)Os$-$M(CO)_5$. The yields were 65 - 80% for M = Cr, 55 - 60% for M = Mo, and 30 - 40% for M = W. The chromium compound was bright yellow, the molybdenum compound colorless or pale yellow, and the tungsten compound

pale yellow. All compounds could be handled in air for short periods without apparent decomposition; prolonged exposure did, however, result in decomposition. A later check of the mass spectra for the 'bare' OsM^+ ion revealed that only for **1-W** was the lower mass range studied. A peak centered at about m/e 374, corresponding to the Os-W^+ ion was seen in the mass spectrum of **1-W**.

Preparation of Isomer a of $(OC)_3(Bu^tNC)_2OsM(CO)_5$ (M = Cr, Mo, W). A solution of $M(CO)_5(THF)$ in THF (30 mL) was prepared as above from $M(CO)_6$ (M = Cr, 0.20 mmol; M = Mo, 0.55 mmol; M = W, 0.30 mmol). The solution was reduced in volume to 1 - 2 mL and cooled to -196 °C. A solution of $Os(CO)_3(CNBu^t)_2$ (40mg, 0.091 mmol) in hexane (10 mL) was added to the frozen $M(CO)_5(THF)$/THF. The solution was allowed to warm with stirring, to room temperature (M = Cr), to 0 °C (M = Mo) or to room temperature with further stirring at room temperature for 10 min (M = W). The solvent was then removed on the vacuum line. The residue was extracted repeatedly with hexane. The hexane extracts were combined and evaporated to dryness. The remaining solid (i.e., that had originally dissolved in hexane) was chromatographed on Florisil (14 x 1 cm). Elution with hexane removed $M(CO)_6$. The desired product, $(OC)_3(Bu^tNC)_2OsM(CO)_5$ (mainly isomer **a** but with some isomer **b**) was obtained by elution with hexane/CH_2Cl_2 (4/1). The analytical samples were obtained by recrystallization from hexane/CH_2Cl_2 (7/1). As such, the samples consisted mainly of isomer **a** but they also had small amounts of isomer **b** (e.g., see Figure 1.5).

The residue that remained after the hexane extraction described above was chromatographed on silica gel (15 x 1 cm) with hexane/CH_2Cl_2 (3/1) as the solvent to yield small amounts of isomer **b** of $(OC)_3(Bu^tNC)_2OsM(CO)_5$ (see below). In the tungsten case elution with hexane/CH_2Cl_2 (1/1) gave a yellow

band from which a yellow solid was isolated. The solid was a mixture of two isomers of a compound having two unbridged dative metal-metal bonds in tandem. This compound will be discussed later in this chapter.

The (combined isomer **a** and **b**) yields and colors of the $(OC)_3(Bu^tNC)_2Os$-$M(CO)_5$ complexes were similar to those for the analogous $(OC)_4(Bu^tNC)Os$-$M(CO)_5$ derivatives given above.

Preparation of Isomer b of $(OC)_3(Bu^tNC)_2OsM(CO)_5$ (M = Cr, Mo, W). A saturated solution of isomer **a** of $(OC)_3(Bu^tNC)_2OsM(CO)_5$ in hexane was prepared in an 80 mL round-bottom flask fitted with a Teflon valve. The solution was cooled to -196 °C, evacuated, and degassed by three freeze-pump-thaw cycles. The solution was stirred in the dark at room temperature for 7 - 10 d. During this time the less soluble isomer **b** precipitated from solution. The supernatant solution was removed and the precipitate was washed several times with hexane to remove traces of isomer **a** and dried on the vacuum line. In the case of the molybdenum complex partial decomposition to a black material accompanied the isomerization. The desired product was separated from the decomposition product by dissolving it in hexane/CH_2Cl_2 (3/1) and passing the solution through a short column (1 x 1 cm) of silica gel. Removal of the solvent on the vacuum line gave the crude product. The analytical samples of isomer **b** of the $(OC)_3(Bu^tNC)_2OsM(CO)_5$ (M = Cr, Mo, W) complexes were obtained by recrystallization from hexane/CH_2Cl_2. As such they were pure isomer **b** as indicated by ^{13}C NMR spectroscopy.

Determination of the Isomer Ratio at Equilibrium for the $(CO)_3(Bu^tNC)_2OsM(CO)_5$ (M = Cr, Mo, W) Complexes. Recrystallized isomer **b** of $(CO)_3(Bu^tNC)_2OsM(CO)_5$ was dissolved in CH_2Cl_2 contained in a round-bottom flask fitted with a Teflon valve. The solution was stirred under vacuum in the dark at room temperature for a period of 3 - 7 d. The isomerization was

monitored by infrared spectroscopy (in the 1800 - 2250 cm^{-1} region). When there was no further change in the infrared spectrum of the reaction mixture, the solvent was removed under reduced pressure. The residue was dissolved in $CDCl_3$ and a ^1H NMR spectrum of the solution was recorded at room temperature. The **a:b** isomer ratio was obtained from the areas of the ^1H NMR signal of each isomer.

For the molybdenum derivative, equilibrium was reached within 41 h, whereas for the chromium and tungsten compounds, equilibrium was attained after 3 - 5 d. The approximate **a:b** isomer ratio was 1:2.6, 1:1.8, 1:2.3 for the chromium, molybdenum and tungsten derivatives, respectively.

Reaction of $Os(CO)_4(CNBu^t)$ with $Cr(CO)_4(CNBu^t)(THF)$. A hexane solution of Bu^tNC was added to an approximately equimolar quantity of $Cr(CO)_5(THF)$ maintained at -196 °C. The frozen mixture was warmed to room temperature and the solvent removed on the vacuum line. The residue was sublimed at room temperature (0.1 mm Hg) to a probe at -78 °C to give a pale yellow solid identified by infrared spectroscopy as $Cr(CO)_5(CNBu^t)$.[22] A solution of $Cr(CO)_5(CNBu^t)$ in THF was placed in a Pyrex Carius tube fitted with a Teflon valve; the solution was cooled to -196 °C, evacuated and degassed with two freeze-pump-thaw cycles. The stirred solution was then subjected to UV irradiation at room temperature. The conversion of $Cr(CO)_5(CNBu^t)$ to $Cr(CO)_4(CNBu^t)(THF)$ was monitored by infrared spectroscopy. A small amount of $Cr(CO)_5(THF)$ was also produced. When the conversion was judged complete, the solution was reduced in volume and cooled to -196 °C. A hexane solution of $Os(CO)_4(CNBu^t)$ was added to the frozen solution of $Cr(CO)_4(CNBu^t)(THF)$. An approximate molar ratio for $Os(CO)_4(CNBu^t)$:$Cr(CO)_4(CNBu^t)(THF)$ of 1:2 was employed. The frozen mixture was warmed to room temperature with stirring at which point the solvent

was removed under vacuum. The remaining solid was chromatographed on a silica gel column. Elution with hexane removed unreacted $Cr(CO)_5(CNBu^t)$. Elution with hexane/CH_2Cl_2 (5/1, v/v) separated a yellow band which was collected in three fractions. The first fraction contained mostly $(OC)_4(Bu^tNC)OsCr(CO)_5$ (**1-Cr**). The remaining two fractions also contained small amounts of **1-Cr** in addition to the desired product. The impurity of **1-Cr** was removed by washing the solid several times with hexane. The bright yellow residue was identified as $(OC)_3(Bu^tNC)_2OsCr(CO)_5$, **2b-Cr** (i.e., the thermodynamically preferred isomer). The yield was estimated to be ~60%.

Preparation of $(OC)_4(Bu^tNC)OsOs(CO)_3(CNBu^t)W(CO)_5$ (3a) and $(OC)_3(Bu^tNC)_2OsOs(CO)_4W(CO)_5$ (3b). During the preparation of **1-W**, a bright yellow solid, later found to be a mixture of isomers **3a** and **3b**, was isolated. This mixture was synthesized and isolated in the following manner. A solution of $W(CO)_5(THF)$ was prepared as above from $W(CO)_6$ (120 mg, 0.341 mmol) and THF (30 mL). The solution was reduced in volume to ~2 mL and immediately cooled to -196 °C. A solution of $Os(CO)_4(CNBu^t)$ (40 mg, 0.10 mmol) in hexane (10 mL) was added to the frozen $W(CO)_5(THF)$/THF and the resulting mixture allowed to warm with stirring to room temperature. The stirring was continued for a further 20 min at this temperature. The solvent was then removed on the vacuum line and the remaining solid was chromatographed on a silica gel column (15 x 1 cm). Elution with hexane removed $W(CO)_6$; elution with hexane/CH_2Cl_2 (5/1) afforded the binuclear species **1-W**. The desired products eluted as a yellow band with hexane/CH_2Cl_2 (1/1). Collection of this fraction and removal of the solvent gave $(OC)_7(Bu^tNC)_2Os_2W(CO)_5$ (**3**) (11 mg, 20%) as a mixture of the isomers **3a** and **3b**. Trace amounts of a third compound (**3c**) also believed to be an isomer of $(OC)_7(Bu^tNC)_2Os_2W(CO)_5$ were also present. The **3a**:**3b** ratio appeared somewhat variable as ascertained by IR spectroscopy, but

was determined in one preparation as approximately 1:1 by ^{1}H NMR spectroscopy.

Attempts to separate the isomers by chromatography were unsuccessful. Partial separation was, however, achieved by fractional recrystallization: Solids from four such preparations described above were combined and recrystallized from hexane/CH_2Cl_2. The first batch of crystals obtained by this recrystallization consisted essentially of **3b**. A further recrystallization of these crystals from hexane/CH_2Cl_2 gave **3b** that was pure by ^{13}C NMR spectroscopy. The supernatant solution from the first recrystallization was evaporated to dryness and the residue was recrystallized from a minimum of hexane/CH_2Cl_2. This afforded a yellow sample that by ^{13}C NMR spectroscopy consisted of mainly isomer **3a**, but also **3b** (<10%) and traces of **3c**.

1.3 Results and Discussion

$Os(CO)_{5-x}(CNBu^t)$ (x=1,2) Compounds. The derivative $Os(CO)_4(CNBu^t)$ was prepared by the methods summarized in eq 1and 2.

$$Os_3(CO)_{12} + \text{excess COE} \xrightarrow[\text{hexane}]{\lambda > 370\ nm} 3\ Os(CO)_4(COE) \qquad (1a)$$

$$Os(CO)_4(COE) + CNBu^t \xrightarrow[55 - 65\ ^\circ C]{\text{hexane}} Os(CO)_4(CNBu^t) \qquad (1b)$$

COE = cyclooctene

$$Os(CO)_5 + xCNBu^t \longrightarrow Os(CO)_{5-x}(CNBu^t)_x \qquad (2)$$

x = 1,2

The derivative $Os(CO)_3(CNBu^t)_2$ was also prepared by the method shown in eq 2. The reaction in eq 2 was carried out in hexane/benzene at reflux temperature with a catalyst of $CoCl_2 \cdot 2H_2O$. Iron analogues had been prepared by this method.[23] The pattern of the CO-stretches in the infrared spectrum of $Os(CO)_4(CNBu^t)$ in hexane (Table 1.2) is typical of an $M(CO)_4L$ compound that has trigonal bipyramidal coordination about the Os atom ator1 with L in an axial position.[23-25] The single carbonyl and isocyanide(CN) stretches exhibited by $Os(CO)_3(CNBu^t)_2$ in hexane are consistent with trigonal bipyramidal coordination around M with both isocyanide ligands in axial sites.[23,25]

$(OC)_4(Bu^tNC)OsM(CO)_5$ (M = Cr, 1-Cr; M = Mo, 1-Mo; M = W, 1-W) Complexes. These complexes were prepared by the method indicated in eq 3 (x = 1). The complexes are moderately stable in air and range in color from

$$Os(CO)_{5-x}(CNBu^t)_x + M(CO)_5(THF) \longrightarrow (OC)_{5-x}(Bu^tNC)_xOsM(CO)_5 \qquad (3)$$

x = 1: M = Cr, Mo, W	**1-Cr**, **1-Mo**, **1-W**
x = 2	**2-Cr**, **2-Mo**, **2-W**

colorless or pale yellow (molybdenum and tungsten derivatives) to bright yellow (chromium derivative).

The structure of **1-Cr** was determined by X-ray crystallography. A view of the molecule showing the disorder in the Bu^t group is given in Figure 1.1; some bond length and angle data are given in Table 1.4. As can be seen from the figure, the 18-electron compound $Os(CO)_4(CNBu^t)$ acts as a two electron donor ligand towards the chromium atom in the $Cr(CO)_5$ fragment via an unbridged, dative metal-metal bond. The isocyanide ligand in **1-Cr** is cis to the metal-metal bond which is in contrast to $(Me_3P)(OC)_4OsCr(CO)_5$ where the phosphine ligand is trans to the osmium- chromium bond.[11a] The Os-Cr bond length in **1-Cr** is 2.966 (2) Å whereas in $(Me_3P)(OC)_4OsCr(CO)_5$ it is 2.979 (2) Å. Although the difference is small, it does suggest that $Os(CO)_4(CNBu^t)$ is a slightly better donor ligand to $Cr(CO)_5$ than is $Os(CO)_4(PMe_3)$. This is contrary to expectations given that $CNBu^t$ is a poorer donor ligand than PMe_3. (The CO-stretching frequencies of 2061, 1980, 1939 cm^{-1} of $Os(CO)_4(PMe_3)$[24] may be compared to corresponding values given in Table 1.2 for $Os(CO)_4(CNBu^t)$.) A similar situation was found when comparing the dative OsOs bond lengths in $(OC)_4(Bu^tNC)Os$-$Os_3(CO)_{11}$ and $(Me_3P)(OC)_4OsOs_3(CO)_{11}$.[13b] At that time, it was rationalized that with the better π-accepter ligand CO trans to the dative metal-metal bond the repulsive interactions between the filled metal d-orbitals across the bond would be lessened. In addition, the system avoids the better π-acceptor carbonyl ligands competing for the same π-electron density on the osmium atom when the non-carbonyl ligand and the 16-electron unit are in a cis configuration. The same arguments can be applied to **1-Cr** and $(Me_3P)(OC)_4OsCr(CO)_5$.

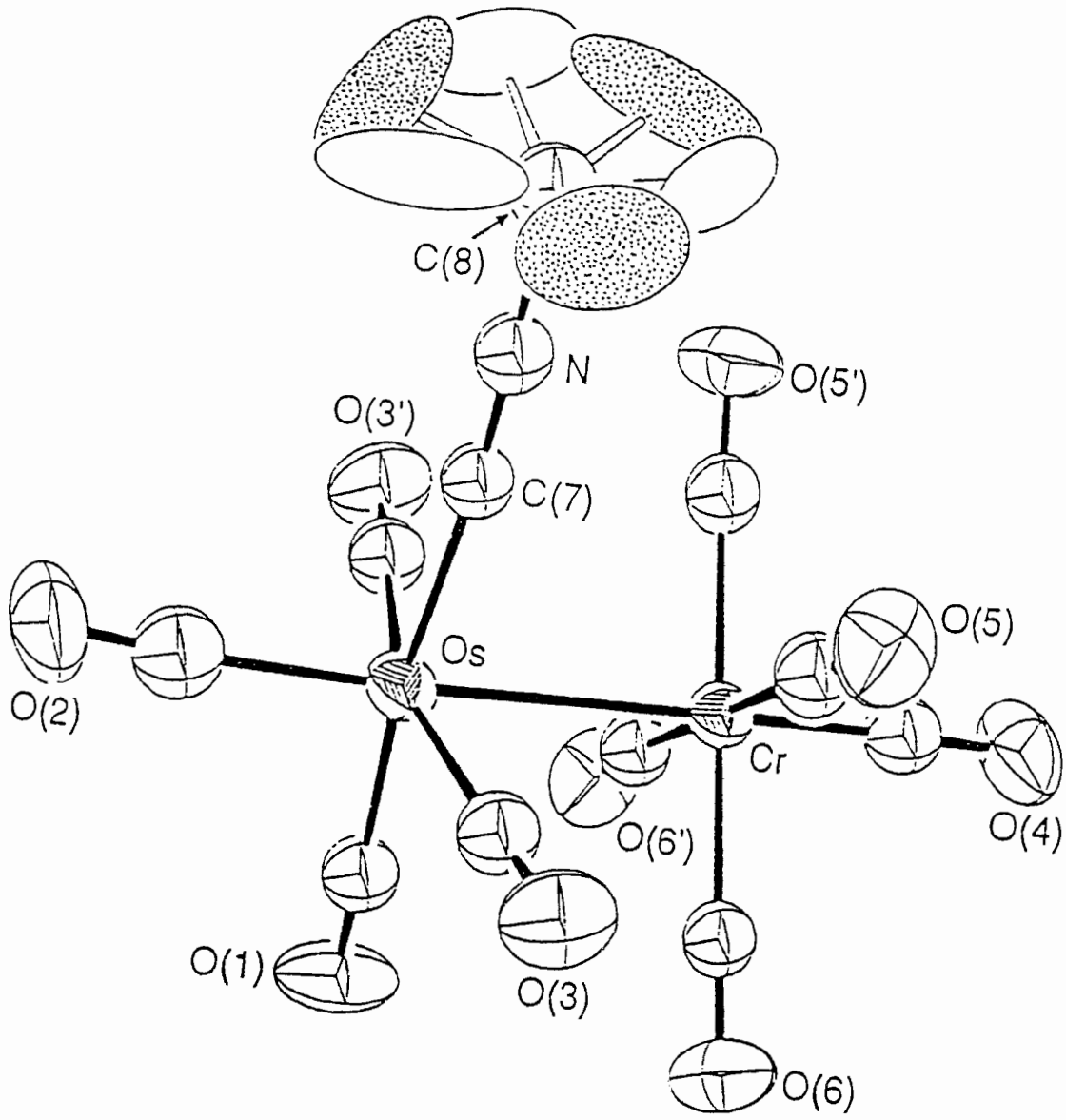

Figure 1.1 Molecular structure of **1-Cr**.

Table 1.4 Bond Lengths (Å) and Selected Angles (deg) for **1-Cr**

		Bond Lengths	
Os - Cr	2.966 (2)	Os - C(1)	1.945 (10)
Os - C(2)	1.934 (12)	Os - C(3)	1.972 (7)
Os - C(7)	2.011 (9)	Cr - C(4)	1.815 (10)
Cr - C(5)	1.896 (7)	Cr - C(6)	1.896 (7)
C(1) - O(1)	1.139 (11)	C(2) - O(2)	1.160 (13)
C(3) - O(3)	1.115 (8)	C(4) - O(4)	1.172 (12)
C(5) - O(5)	1.146 (8)	C(6) - O(6)	1.139 (7)
N - C(7)	1.169 (11)	N - C(8)	1.466 (10)
C(8) - C(9)	1.464[a]	C(8) - C(10)	1.492[a]
C(8)-C(11)	1.465[a]		
		Angles	
C(1) - Os - Cr	84.5 (3)	C(2) - Os - Cr	176.2 (3)
C(2) - Os - C(1)	99.3 (4)	C(3) - Os - Cr	80.0 (2)
C(3) - Os - C(1)	89.5 (3)	C(3) - Os - C(2)	99.9 (2)
C(7) - Os - Cr	87.7 (3)	C(7) - Os - C(1)	172.2 (4)
C(7) - Os - C(2)	88.4 (4)	C(3) - Os - C(3′)	160.0 (3)
C(7) - Os - C(3)	89.2 (4)	C(4) - Cr - Os	179.0 (3)
C(5) - Cr - Os	89.5 (2)	C(5) - Cr - C(4)	91.2 (3)
C(5) - Cr - C(5′)	88.5 (4)	C(6) - Cr - Os	90.4 (2)
C(6) - Cr - C(4)	88.9 (3)	C(6) - Cr - C(5)	91.2 (3)
C(6) - Cr - C(5′)	179.6(3)	C(6) - Cr - C(6′)	89.2 (4)
C(8) - N - C(7)	175.8(7)	O(1) - C(1) - Os	179.3 (10)
O(2) - C(2) - Os	175.8(9)	O(3) - C(3) - Os	179.0 (7)
O(4) - C(4) - Cr	177.2(9)	O(5) - C(5) - Cr	177.0 (7)
O(6) - C(6) - Cr	174.8(6)	N - C(7) - Os	175.5 (8)
C(9) - C(8) - N	170.0[a]	C(10) - C(8) - N	106.9[a]
C(10) - C(8) - C(9)	111.8[a]	C(11) - C(8) - N	107.0[a]
C(11) - C(8) - C(9)	111.9[a]	C(11) - C(8) - C(10)	111.9[a]

[a] Parameters subjected to restraints during refinement.

As observed in other molecules with unbridged dative metal-metal bonds,[11a,d] there is an inward leaning of the equatorial ligands on the donor half of the molecule (e.g.C(3)-Os-C(3') = 160.0 (3)°). This inward leaning is not present in the equatorial carbonyls of the acceptor half of the molecule (e.g., C(6)-Cr-C(5') 179.6 (3)°). The Cr-C distance (1.815 (10) Å) trans to the metal-metal bond is significantly shorter than the two other independent Cr-C distances (both 1.896 (7) Å). This has been observed in other complexes with dative metal-metal bonds, and is taken to indicate that the 18-electron compound is a weak donor ligand.[11d] A repulsive π-interaction between the d-orbitals on the metal atoms would also be expected to increase the metal to carbonyl dπ to π^* bonding to the trans carbonyl and thus shorten the Cr-C bond to that carbonyl. A repulsive π-interaction between the metal d-orbitals would also be expected to shorten the Os-C bond trans to the dative OsCr bond, but this bond is not significantly shorter than the equatorial Os-C bonds. The dimensions of the $Os(CO)_4(CNBu^t)$ ligand in **1-Cr** are similar to those of the same ligand in $(OC)_4(Bu^tNC)OsOs_3(CO)_{11}$.[13b]

The spectroscopic properties of the $(OC)_4(Bu^tNC)OsM(CO)_5$ complexes (Table 1.2) are consistent with these complexes having the same structure in solution as that found for **1-Cr** in the solid state, except that there is rotation about the Os-M bond in solution. The carbonyl regions of the ^{13}C NMR spectra of the $(OC)_4(Bu^tNC)OsM(CO)_5$ complexes are shown in Figure 1.2. The two signals in an intensity ratio of 1:4 in the 230 - 200 ppm region are assigned to the axial and radial carbonyls, respectively, of the $M(CO)_5$ moiety. The equivalence of the four radial carbonyls of the $M(CO)_5$ moiety indicates that there is rapid rotation on the NMR time scale about the Os-M bond. The typical upfield shift on going to the derivative with the group 6 metal lower in the periodic table

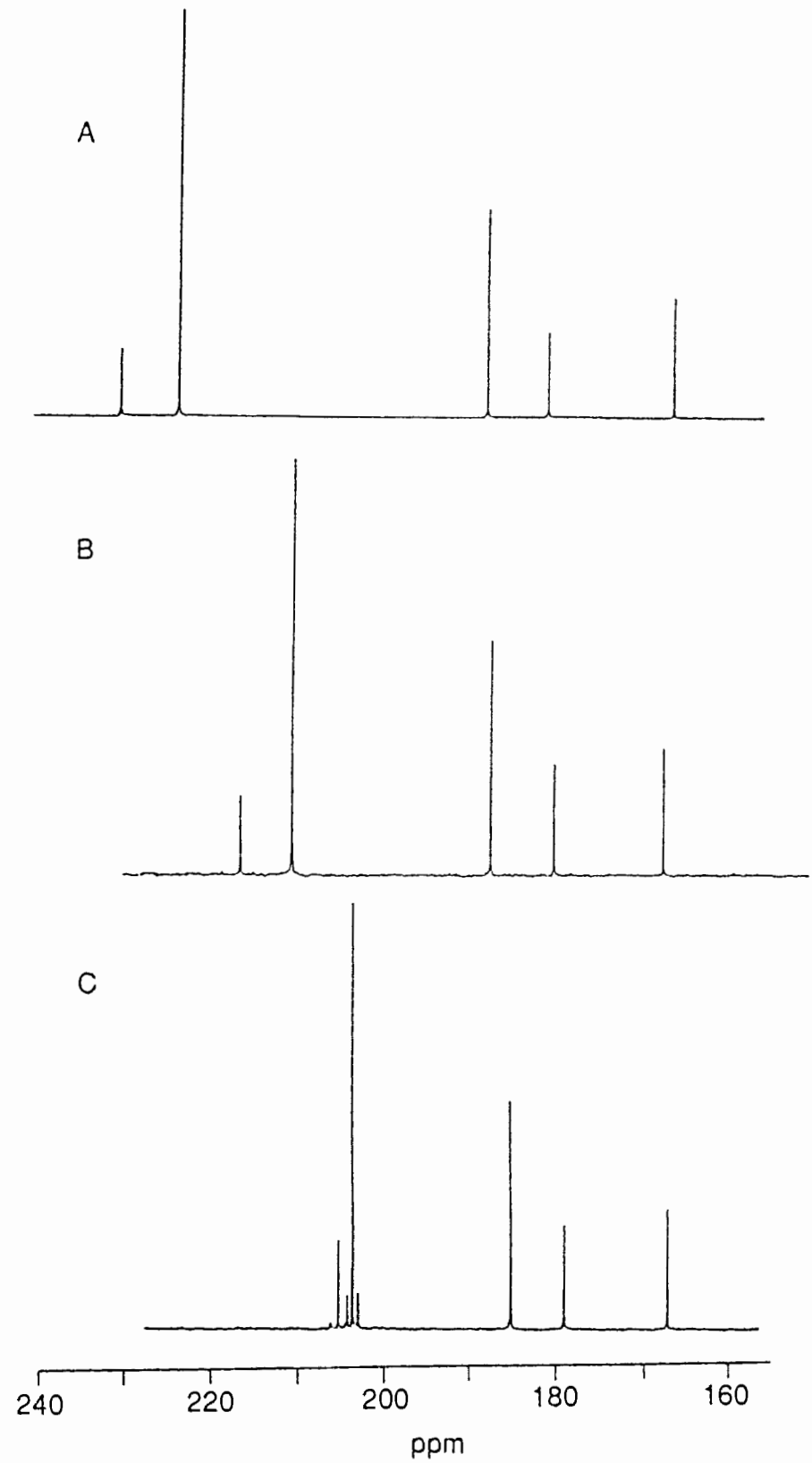

Figure 1.2 Carbonyl region of the ^{13}C NMR spectrum of A: **1-Cr**, B: **1-Mo**, and C: **1-W** (CH_2Cl_2/CD_2Cl_2, 1/4, at -30 °C or -40 °C).

is apparent.[26] The signals due to the carbonyls bound to tungsten show the expected coupling to ^{183}W.

In the 190 - 160 ppm region of the spectra there are three signals in an approximate 2:1:1 ratio as expected for an $Os(CNBu^t)(CO)_4$ moiety with the isocyanide ligand in a position cis to the OsM bond (Figure 1.2). The signal to highest field is attributed to the carbonyl ligand trans to the dative metal-metal bond. In all complexes prepared in this laboratory that contain a carbonyl ligand trans to a dative metal-metal bond, the ^{13}C NMR resonance of this carbonyl carbon occurs at an unusually high field.[10,11a,11d,13b] (In the spectra of the minor isomer of $(OC)_4(R_3P)OsM(CO)_5$ (i.e. where the PR_3 is cis to the OsM bond), the assignment of the signals due to the $Os(PR_3)(CO)_4$ fragment is unambiguous because of the small cis and large trans couplings to the phosphorus atom.[11a]) The other signal of intensity 1 in the spectra of the $(OC)_4(Bu^tNC)OsM(CO)_5$ complexes is therefore assigned to the carbonyl trans to the Bu^tNC ligand, and that of intensity 2 to the carbonyls cis to this ligand.

Unlike the $(R_3P)(OC)_4OsM(CO)_5$ complexes,[11a] the isocyanide analogues are soluble in hexane such that infrared spectra with well resolved CO-stretching vibrations can be obtained. The infrared spectrum of **1-Cr** in hexane is shown in Figure 1.3; the corresponding spectra of **1-Mo** and **1-W** are given in Figure 1.4. In comparing these spectra with those of $(\eta^5\text{-}C_5Me_5)(OC)_2IrW(CO)_5$[11c] and $(R_3P)(OC)_4OsM(CO)_5$,[11a] one finds that the bands below 2000 cm^{-1} can be attributed to vibrations that mainly involve the carbonyls of the $M(CO)_5$ unit, and the bands in the 2000 - 2125 cm^{-1} region as due mainly to the carbonyls of the $Os(CO)_4(L)$ (L = PR_3 or $CNBu^t$), or $(\eta^5\text{-}C_5Me_5)Ir(CO)_2$ moieties. This is consistent with the expected polarity of the donor-acceptor metal-metal bond (i.e., $(\delta+)Os \longrightarrow M(\delta-)$).[11a] The carbonyl (and isocyanide) stretching frequencies

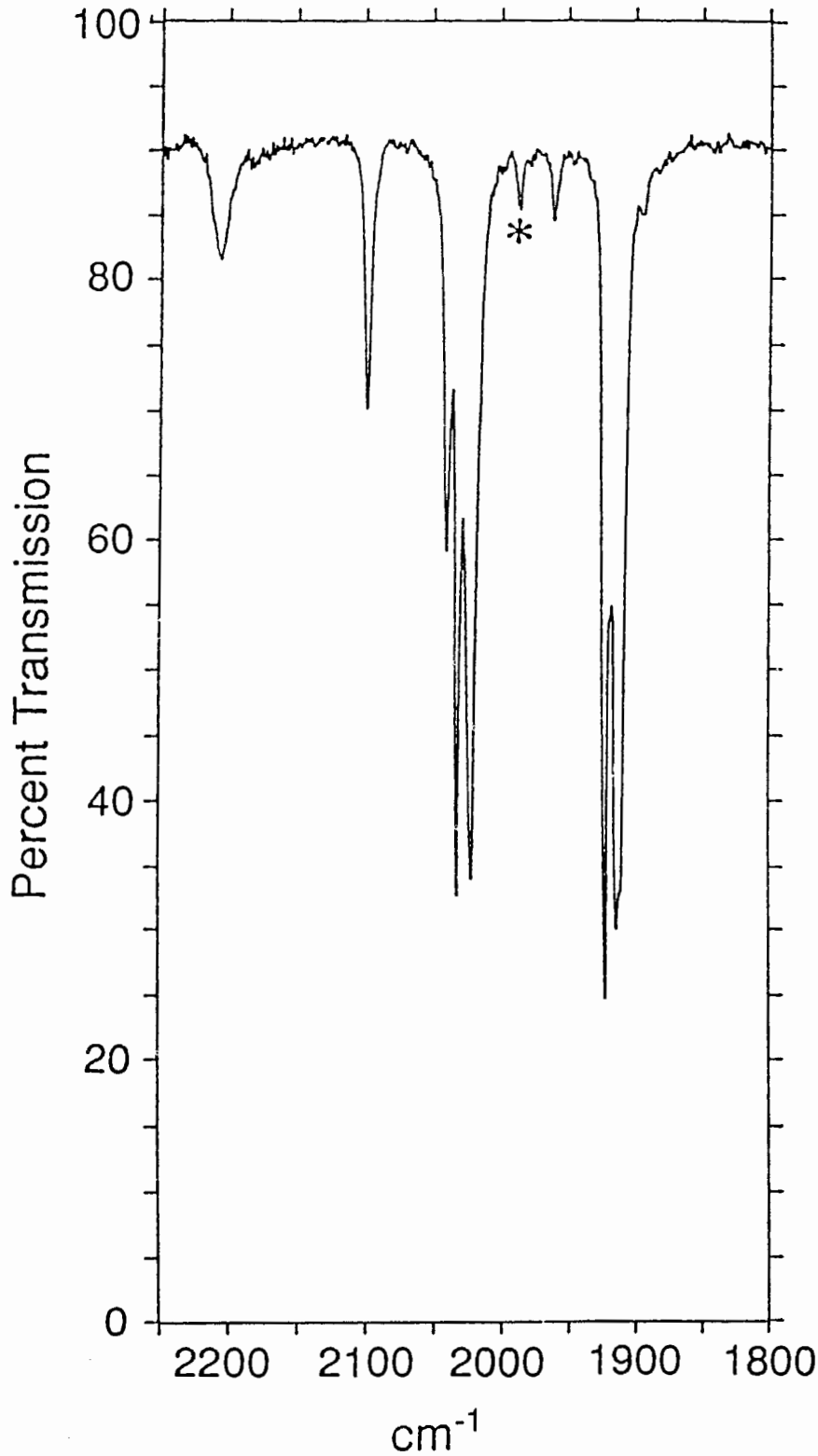

Figure 1.3 Infrared spectrum of **1-Cr** in hexane. (The peak marked with an asterisk is due to $Cr(CO)_6$.)

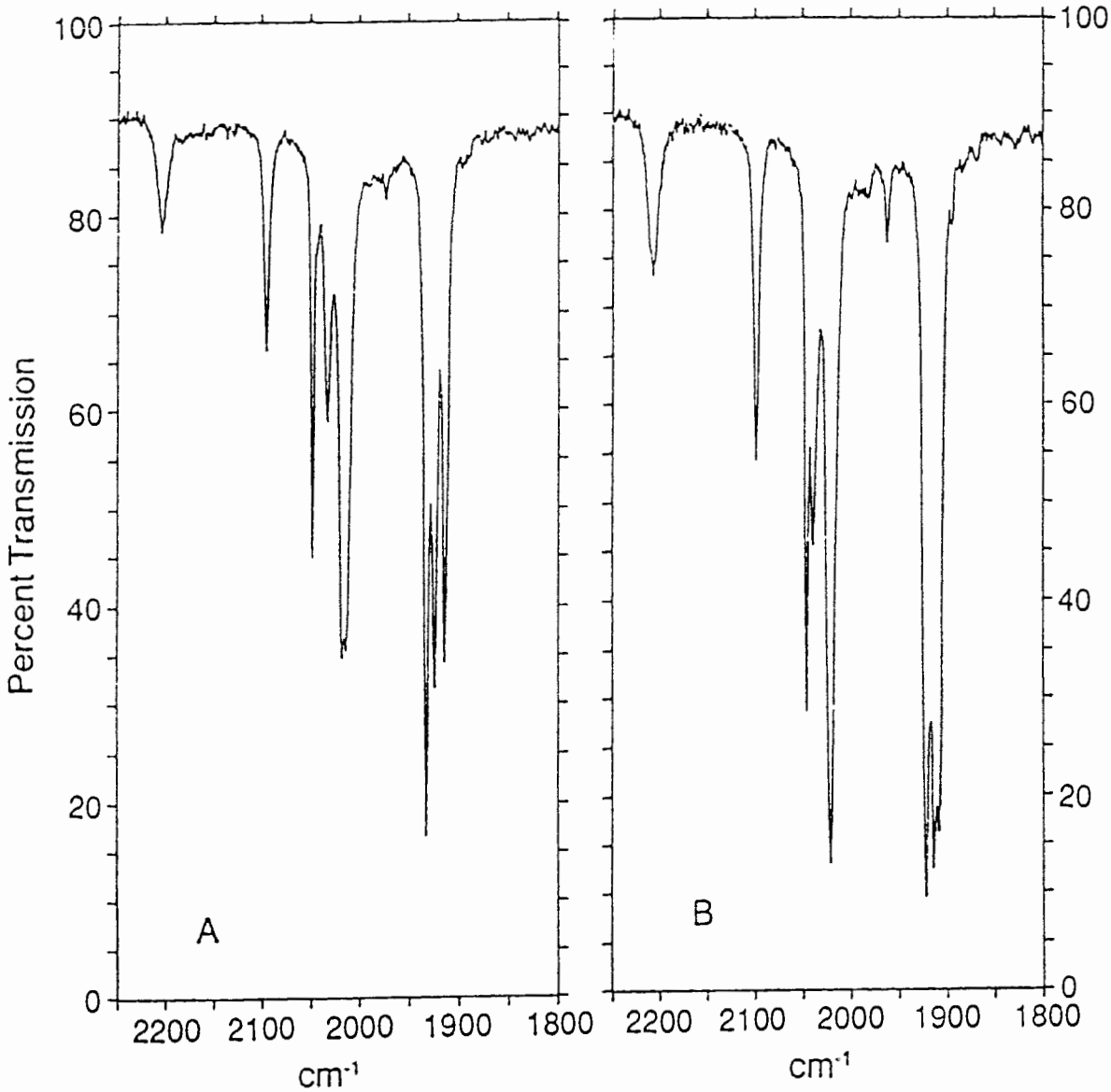

Figure 1.4 Infrared spectrum of A: **1-Mo** and B: **1-W** (both samples in hexane).

shift to higher values on going from the free $Os(CO)_4(CNBu^t)$ molecule to the coordinated state (Table 1.2), consistent with less backbonding to the CO (and $CNBu^t$) groups in the latter state. As well, the carbonyl stretching frequencies of the group 6 carbonyl unit shift to lower values on going from the parent $M(CO)_6$ (M = Cr, 1987; M = Mo,1989; M = W, 1983 cm^{-1}) to the coordinated $M(CO)_5(L')$ ($L' = Os(CO)_4(CNBu^t)$) complex, which is also consistent with greater back-bonding to the carbonyls in the latter compound.

The *cis*-$Os(CO)_4(X)(Y)$ and $M(CO)_5(L')$ fragments are expected to have four and three infrared-active CO-stretches, respectively.[27] This is observed for **1-Cr** (Figure 1.3) although the CO-stretch at the lowest frequency does have a shoulder. The spectra of **1-Mo** and **1-W** (Figure 1.4), however, show more than the expected number of bands (two and one more, respectively). For the $M(CO)_5(L')$ unit the extra band(s) could be due to lowering of the C_{4v} symmetry of the unit due to the asymmetry of the L' ligand. This cannot be the case for the $Os(CO)_4(X)(Y)$ fragment since four carbonyl stretches are the maximum number allowed, regardless of the symmetry of X and Y.

The appearance of an extra absorption band of the $Os(CO)_4(X)(Y)$ unit in **1-Mo** (i.e., the lowest frequency carbonyl band is split compared to that of **1-Cr** and **1-W**) can be attributed to the presence of different conformers of **1-Mo** in solution. (Note: The ^{13}C NMR spectrum of **1-Mo** shows there is only one isomer present in solution.) It is known that different conformers of a molecule can give rise to splitting of the carbonyl absorptions in the infrared spectra of metal carbonyl compounds.[28] In one conformer of **1-Mo** one of the methyls of the tert-butyl group could eclipse the axial CO bound to the osmium atom, whereas in the second conformer two of the methyls could be in staggered positions with respect to this carbonyl. It is not unprecedented for a symmetric ligand to give rise to a splitting of CO-stretches.[28c,d] Although there are two conformers

present in the solid state structure of **1-Cr** (Figure 1.1), they are mirror images of each other and would therefore give the same infrared spectrum if they were present in solution.

An alternate interpretation is that since the **1-M** molecule as a whole has C_s symmetry there should be a maximum of nine carbonyl stretches in the IR spectrum. According to this interpretation, **1-Cr** and **1-W** have two and one fewer carbonyl bands, respectively, due to accidental degeneracy of some of these bands.

There is no evidence in the ^{13}C NMR spectra of the $(OC)_4(Bu^tNC)Os$-$M(CO)_5$ complexes for the isomer with the isocyanide ligand trans to the dative metal-metal bond (Figure 1.2). This is in contrast to the $(R_3P)(OC)_4OsM(CO)_5$ complexes where the isomer with the phosphine or phosphite ligand trans to the metal-metal bond is the major,or in some cases, the only isomer present in solution.[11a] The crystal structures of the $(Me_3P)(OC)_4OsM(CO)_5$ (M = Cr, W) complexes show that this isomer is also adopted in the solid state.[11a]

Similar behavior has been found in metal carbonyl compounds with nondative metal-metal bonds. For example, in compounds of the type $M'_2(CO)_{10-x}(L)_x$ (M' = Mn, Re; L = PR_3, x = 1,2; L = CNR, x = 1 - 4) when L is a phosphorus-donor ligand, these ligands are found in both radial and axial sites, with large PR_3 ligands preferring the less hindered axial sites.[29] For the derivatives with L = RNC, the isocyanide ligands are found exclusively in the radial positions.[30] Similarly in cluster complexes of the type $Os_3(CO)_{12-x}(L)_x$ (x = 1 - 6) phosphorus donor ligands are invariably found in equatorial sites[31] whereas isocyanide ligands usually adopt axial sites.[32] The latter results have been rationalized on the basis that the axial site is electronically preferred, but the equatorial site is sterically favored.

In solution at room temperature the isomers of $(Me_3P)(OC)_4OsW(CO)_5$ were shown to be in dynamic equilibrium by the NMR spin saturation transfer technique. This observation is consistent with isomerization proceeding via an intermediate with bridging carbonyls which also exchanges the carbonyls on osmium and tungsten.[11a] When the $(OC)_4(Bu^tNC)OsM(CO)_5$ complexes were prepared from ^{13}CO-enriched $M(CO)_5(THF)$ and unenriched $Os(CO)_4(CNBut)$ it was found that the ^{13}C-carbonyls were scrambled over both the Os and M sites. This is also consistent with terminal-bridge carbonyl exchange, although as pointed out for $(OC)_4(Bu^tNC)OsOs_3(CO)_{11}$ there must also be a second process that exchanges the carbonyl trans to the Bu^tNC ligand with the other carbonyls.[13b]

The isocyanide ligand is also known to readily act as a bridging ligand,[33] but there was no evidence for isomers of $(OC)_4(Bu^tNC)OsM(CO)_5$ with the Bu^tNC ligand bound to the group 6 metal atom. To determine whether this was due to kinetic or thermodynamic reasons, the reaction of $Os(CO)_4(CNBu^t)$ with $Cr(CO)_4(CNBu^t)(THF)$ was carried out. The product was identified spectroscopically as [*cis-dieq*-$(OC)_3(Bu^tNC)_2Os$]$Cr(CO)_5$ (**2b-Cr**,see below). The cis, diequatorial rather than the trans, diequatorial isomer (**2a-Cr**, see below) is the expected product if the isocyanide migration occurs via an intermediate that has a carbonyl ligand (from the osmium moiety) and the isocyanide ligand bridging in a plane that is perpendicular to the Os-$CNBu^t$ bond.

Thus it appears that the isomer with the isocyanide ligand located on the donor metal atom is thermodynamically preferred to one where the isocyanide ligand is bound to the acceptor metal atom. This might be expected given that the Bu^tNC is a better donor ligand than CO.[33,34] It is interesting that the reaction of $(\eta^5\text{-}C_5Me_5)Ir(CO)_2$ with $[(\mu\text{-}Cl)Rh(PR_3)_2]_2$ (R = O-Pr^i) gives $(\eta^5\text{-}C_5Me_5)(R_3P)(OC)IrRh(CO)(PR_3)(Cl)$ that contains an unbridged IrRh dative bond and where

there has been a migration of a PR_3 ligand to the donor metal atom accompanied by migration of a carbonyl to the acceptor metal atom.[12a]

The mass spectrum of **1-W** was analyzed in detail. Besides the parent ion, it showed ions corresponding to the stepwise loss of the CO and $CNBu^t$ ligands. The spectrum also showed a peak centered at about m/e 374, assigned to the 'bare' Os-W^+ ion. This was interpreted as a crude indication that the Os-W bond is a fairly strong bond since it is strong enough to survive the loss of all the CO and $CNBu^t$ ligands.

The **1-M** isocyanide derivatives do not appear to possess as rich a chemistry as their phosphine or phosphite counterparts. For example, photolysis of $(L)(OC)_4OsM(CO)_5$ (L = PMe_3, $P(OMe)_3$, $P(OCH_2)_3Me$; M = Cr, Mo, or W) yielded the deep red trimetallic clusters $(OC)_5M[Os(CO)_3(L)]_2$.[35] However, photolysis of **1-W** resulted only in its decomposition. In addition, the linear trimetallic complex, $(OC)_3(Pc)_2OsOs(CO)_4W(CO)_5$ (Pc = $P(OCH_2)_3CMe$) can be prepared by heating $Os(CO)_4(Pc)$ and $(Pc)(OC)_4OsW(CO)_5$ to 90 °C.[16] Heating a mixture of $Os(CO)_4(CNBu^t)$ and **1-W** to 60 °C failed to produce the analogous trimetallic isocyanide complex, although it was later found to be a byproduct of the **1-W** preparation. The failure of the thermal route may be due to instability of the isocyanide substituted trimetallic complexes at 60 °C (see below).

$(OC)_3(Bu^tNC)_2OsM(CO)_5$ (M = Cr, Mo, W) Complexes. These complexes were prepared by the method used for the monoisocyanide derivatives except that $Os(CO)_3(CNBu^t)_2$ replaced $Os(CO)_4(CNBu^t)$ (i.e., eq 3, x=2).

If it is assumed that the isocyanide ligands remain attached to the osmium atom in the products, then there are three possible isomers of the formula $(OC)_3(Bu^tNC)_2OsM(CO)_5$; these are shown below as **a**, **b**, and **c** with L = Bu^tNC (this assumes that there are no bridging ligands and each metal has

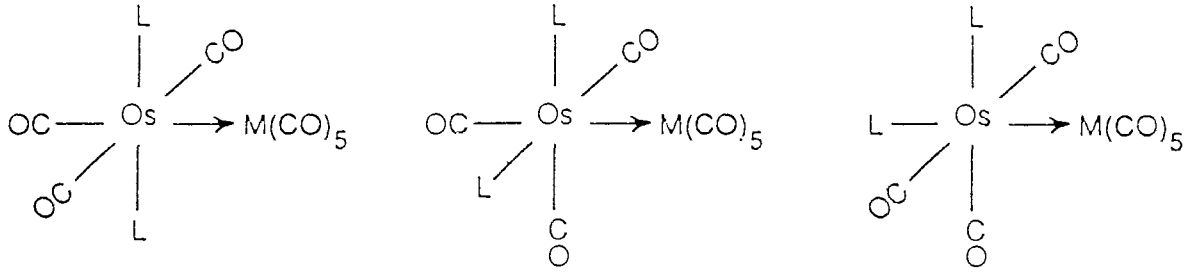

approximate octahedral coordination). The ^{13}C NMR spectra of the products formed initially in the reaction (**2a-M**) have, besides the typical pattern for the $M(CO)_5$ unit, a 2:1 pattern in the region associated with resonances of carbonyls bound to osmium (see Figure 1.5). Furthermore, the signal of intensity 1 appears at high fields which, as discussed above, is characteristic of a carbonyl ligand trans to a dative metal-metal bond. Structure **c** may therefore be ruled out. The ^{13}C NMR spectra are, however, consistent with either structure **a** or **b** for the kinetic products. The infrared spectra (e.g., Figure 1.6A) in the region 2150 - 2250 cm^{-1} exhibited only one CN stretching absorption which is consistent with **a** for the structure of the initial products. This would have been the expected structure given the diaxial arrangement of the isocyanide substituents in the starting complex $Os(CO)_3(CNBu^t)_2$.

When the **2a-M** complexes were stirred in hexane at room temperature for 7 - 10 d, they rearranged to a second isomer (**2b-M**) which precipitated from solution. Since the **2b-M** products were much less soluble in hexane than the **2a-M** isomers, they could be obtained pure by recrystallization from CH_2Cl_2/hexane.

The ^{13}C NMR spectra of the **2b-M** complexes are similar to those of the corresponding **2a-M** complexes (Table 1.3, see also Figure 1.5). Thus the spectra of the **2b-M** compounds had the typical $M(CO)_5$ pattern as well as a 2:1

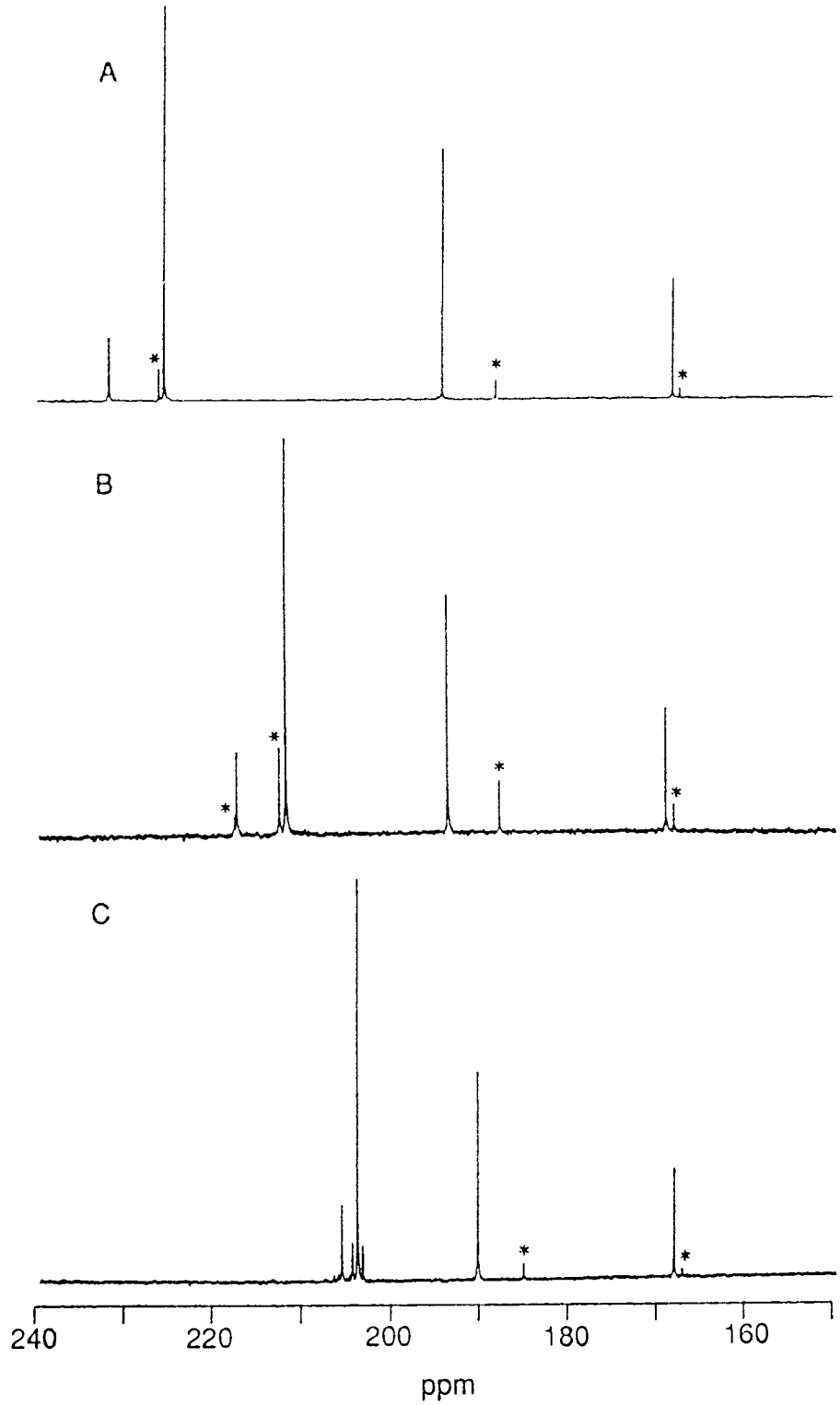

Figure 1.5 Carbonyl region of the ^{13}C NMR spectrum of A: **2a-Cr**, B: **2a-Mo**, and C: **2a-W** (CH_2Cl_2/CD_2Cl_2, 4/1, at -30 °C). The peaks marked with an asterisk are due to trace amounts of the corresponding **2b** isomer.

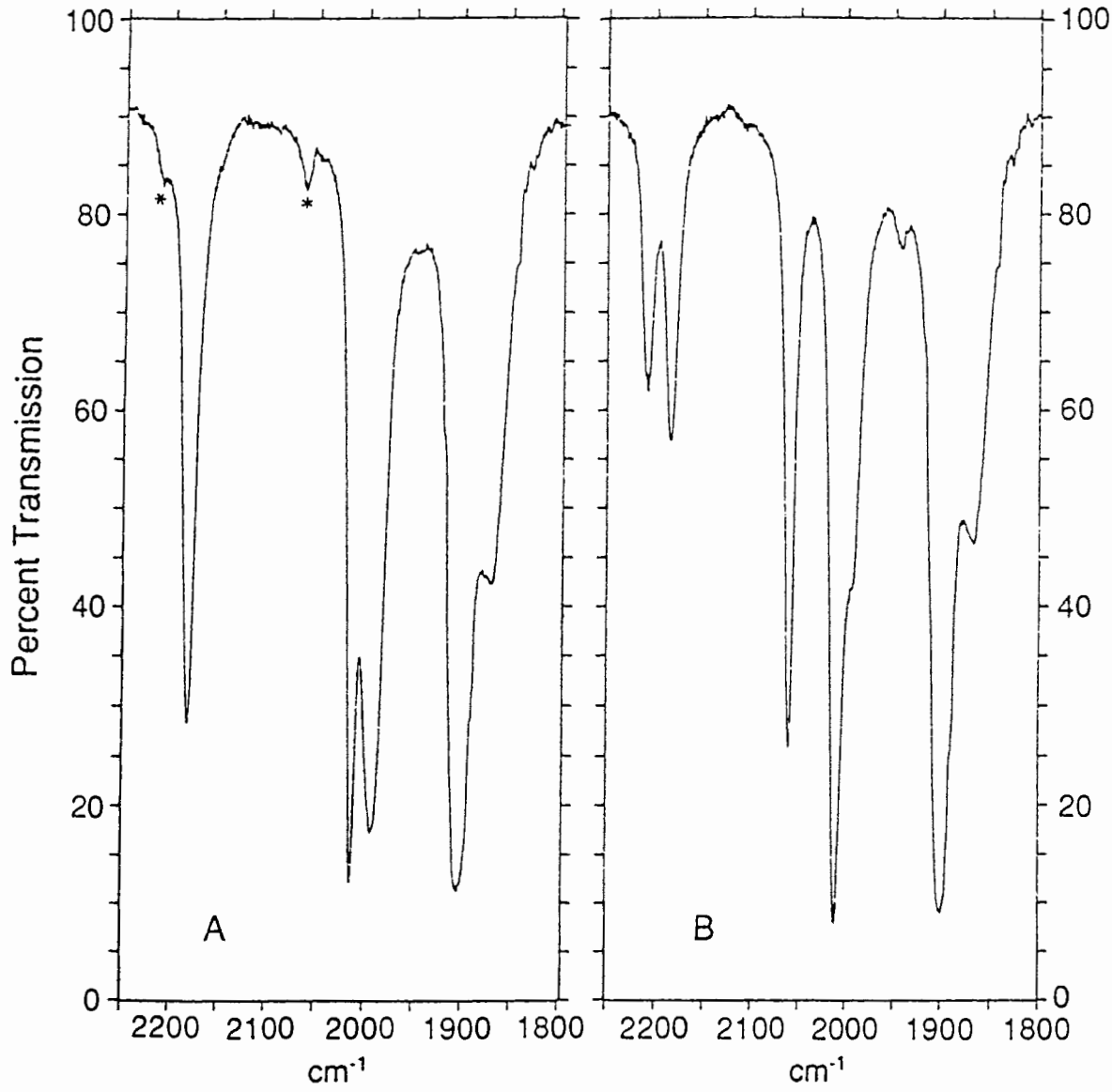

Figure 1.6 Infrared spectrum of A: **2a-Cr** and B: **2b-Cr** (both samples in CH_2Cl_2). The peaks marked with an asterisk may be due to **2b-Cr**.

pattern for the carbonyls bound to osmium. A resonance of intensity 1 appeared in the 170 - 165 ppm region which, as mentioned earlier, is consistent with a carbonyl trans to a dative metal-metal bond. Furthermore, the **2b-M** isomers exhibit two infrared CN stretches (Table 1.2, see also Figure 1.6B). The spectroscopic properties of these complexes are, therefore, consistent with structure **b** with the isocyanide ligands cis to one another and cis to the Os-M bond. (The pattern of the carbonyl stretches in the 1975 - 2100 cm^{-1} region of the infrared spectra of the **2b-M** complexes is also consistent with a *fac*-$Os(CO)_3(X)_2(Y)$ arrangement of ligands.)

Configuration **b** might be expected to be favored over configuration **a** for electronic reasons since in **b** all the carbonyl ligands are trans to poorer π-acceptor ligands. In $Re_2(CO)_6(CNC_6H_3Me_2)_4$ each rhenium atom has two radial isocyanide ligands that are also mutually cis.[30] The difference in the stability of the **2b-M** and **2a-M** isomers must, however, be small. This is because when the pure **2b-M** complexes were stirred in CH_2Cl_2 at room temperature (~ 25 °C) they isomerized over 2 - 10 d to give an equilibrium mixture that contained significant concentrations of the corresponding **2a-M** isomer. The **a**:**b** isomer ratios as determined by ^1H NMR spectroscopy at room temperature were 1:2.6, 1:1.8, and 1:2.3 for **2-Cr**, **2-Mo**, and **2-W** respectively.

The mechanism of the isomerization between **2a-M** and **2b-M** has not been studied. If, however, the formation of the complexes involves the reaction of $Os(CO)_3(CNBu^t)_2$ with the intermediate $M(CO)_5$ (derived from $M(CO)_5(THF)$), then by the principle of microscopic reversibility the isomerization cannot involve the dissociation of $(OC)_3(Bu^tNC)_2OsM(CO)_5$ into these two species. If the isocyanide ligands remain on osmium, as appears probable, the isomerization also cannot proceed via an intermediate with two bridging carbonyls as is thought to occur in the $(PR_3)(OC)_4OsM(CO)_5$ complexes.[11a] A mechanism that

does account for the isomerization is a trigonal twist at the osmium atom that takes a *mer*-$Os(CO)_3(CNBu^t)_2[M(CO)_5]$ configuration to the fac isomer. Trigonal twist mechanisms have been proposed before to account for nondissociative isomerizations of metal carbonyls.[36]

The structure of **2b-Cr** was confirmed by X-ray crystallography. A view of the molecule is given in Figure 1.7; bond length and angle data are given in Table 1.5. In a similar manner to **1-Cr**, the 18-electron compound $Os(CO)_3(CNBu^t)_2$ acts as a two-electron donor ligand to the chromium atom via an unbridged dative metal-metal bond. The comparable bond lengths in **2b-Cr** and **1-Cr** are equal within error. For example, the Os-Cr bond length in **2b-Cr** is 2.9693 (12) Å whereas in **1-Cr** it is 2.966 (2) Å. As found for **1-Cr**, the equatorial carbonyls on the osmium atom lean towards the chromium atom (the CO_{eq}-Os-Cr angles are approximately 80°). The isocyanide ligands, however, do not lean inwards (the appropriate C-Os-Cr angles are approximately 88°).

The results for the $(OC)_3(Bu^tNC)_2OsM(CO)_5$ complexes are in contrast to the unpublished results for $(OC)_3(Me_3P)_2OsM(CO)_5$.[11f] In CH_2Cl_2 solution $(OC)_3(Me_3P)_2OsM(CO)_5$ exists as a mixture of isomers **a** and **c** (L = PMe_3) in an approximate 1:1 ratio with no evidence for isomer **b**. In the solid state $(OC)_3(Me_3P)_2OsM(CO)_5$ has structure **a** and the Os-W bond (3.1417 (6) Å) is markedly longer than that in $(Me_3P)(OC)_4OsM(CO)_5$ (3.0756 (5) Å) where the PMe_3 ligand is trans to the metal-metal bond.[11a,f] The long Os-W bond in $(OC)_3(Me_3P)_2OsM(CO)_5$ suggests it is weak probably due to steric interactions between the methyl groups and the equatorial carbonyls on the tungsten atom. Interestingly, the chromium or molybdenum analogues of $(OC)_3(Me_3P)_2Os$-$M(CO)_5$ could not be synthesized.

The stability of complexes **1-Cr** and **2-Cr** may also be compared to $(OC)_5OsCr(CO)_5$ which decomposes in solution at room temperature with a half

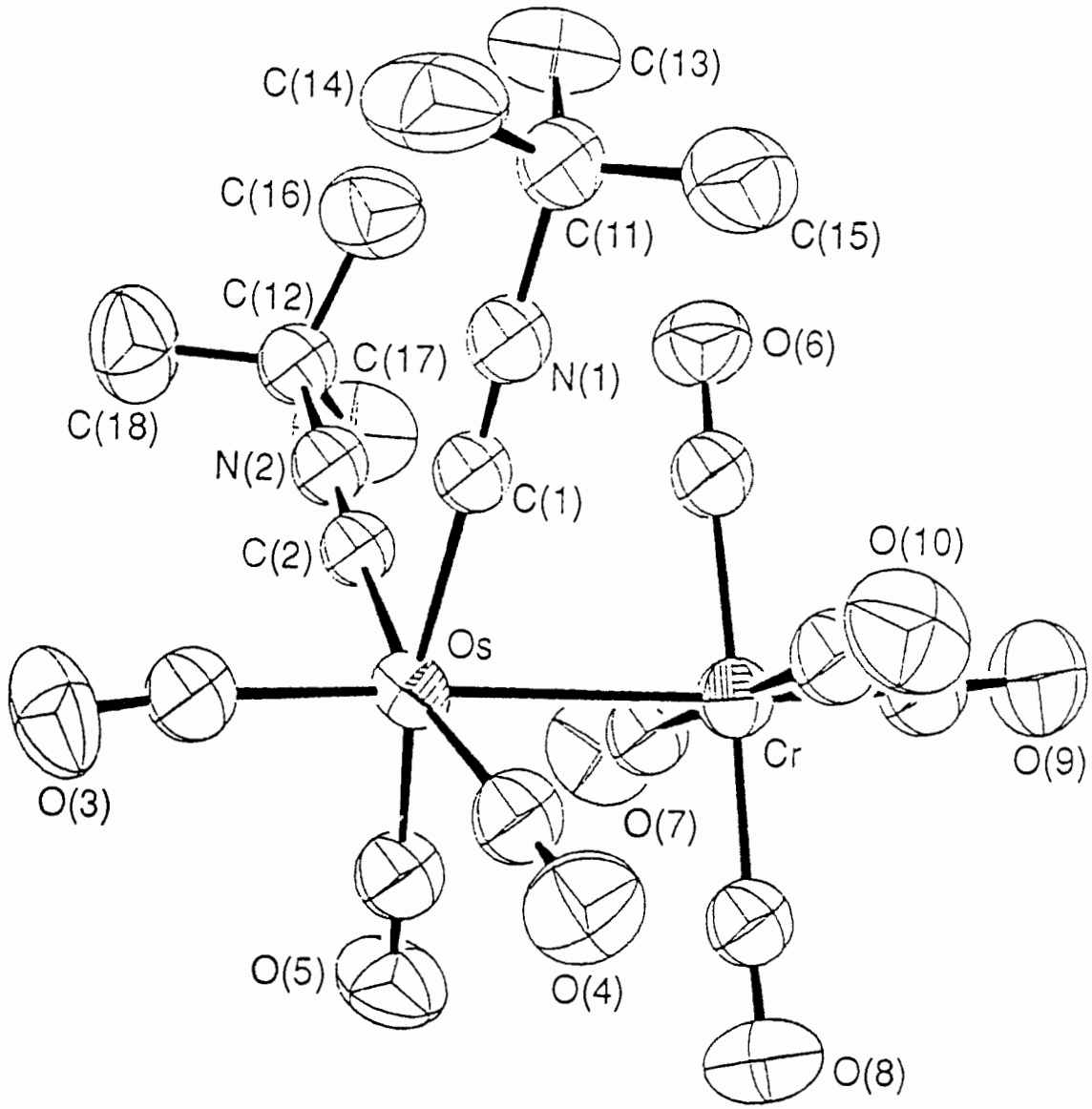

Figure 1.7 Molecular structure of **2b-Cr**.

Table 1.5 Bond Lengths (Å) and Selected Angles (deg) for **2b-Cr**

Bond Lengths

Os - Cr	2.9693 (12)	Os - C(3)	1.894 (9)
Os - C(1)	2.011 (7)	Os - C(4)	1.923 (8)
Os - C(2)	2.018 (7)	Os - C(5)	1.869 (8)
Cr - C(6)	1.890 (8)	Cr - C(9)	1.825 (9)
Cr - C(7)	1.897 (8)	Cr - C(10)	1.864 (8)
Cr - C(8)	1.884 (8)	C(7) - O(7)	1.138 (10)
C(3)- O(3)	1.158 (10)	C(8) - O(8)	1.146 (10)
C(4)- O(4)	1.140 (10)	C(9) - O(9)	1.153 (10)
C(5)- O(5)	1.187 (9)	C(10) - O(10)	1.156 (10)
C(6)- O(6)	1.130 (9)	C(2) - N(2)	1.156 (9)
C(1)- N(1)	1.160 (9)	N(2) - C(12)	1.466 (9)
N(1)- C(11)	1.462 (9)	C(12) - C(16)	1.493 (11)
C(11)- C(13)	1.522 (12)	C(12) - C(17)	1.491 (11)
C(11)- C(14)	1.505 (11)	C(12) - C(18)	1.499 (12)
C(11)- C(15)	1.496 (12)		

Angles

Cr - Os - C(1)	88.05 (19)	C(1) - Os - C(5)	166.4 (3)
Cr - Os - C(2)	87.46 (19)	C(2) - Os - C(3)	94.3 (3)
Cr - Os - C(3)	177.14 (24)	C(2) - Os - C(4)	167.0 (3)
Cr - Os - C(4)	79.96 (23)	C(2) - Os - C(5)	89.1 (3)
Cr - Os - C(5)	78.99 (24)	C(3) - Os - C(4)	98.4 (3)
C(1)- Os- C(2)	86.1 (3)	C(3) - Os - C(5)	98.8 (3)
C(1)- Os- C(3)	94.3 (3)	C(4) - Os - C(5)	91.6 (3)
C(1)- Os- C(4)	90.3 (3)	C(6) - Cr - C(9)	90.3 (3)
Os - Cr - C(6)	86.22 (23)	C(6) - Cr - C(10)	90.6 (3)
Os - Cr - C(7)	90.94 (25)	C(7) - Cr - C(8)	90.1 (3)
Os - Cr - C(8)	90.69 (23)	C(7) - Cr - C(9)	89.7 (3)
Os - Cr - C(9)	176.5 (3)	C(7) - Cr - C(10)	179.4 (3)
Os - Cr - C(10)	89.45 (24)	C(8) - Cr - C(9)	92.8 (3)

Table 1.5 cont'd

C(6) - Cr - C(7)	89.0 (3)	C(8) - Cr - C(10)	90.3 (3)
C(6) - Cr - C(8)	176.8 (3)	C(9) - Cr - C(10)	89.9 (3)
C(1) - N(1) - C(11)	178.9 (7)	C(2) - N(2) - C(12)	177.4 (7)
Os - C(1) - N(1)	176.0 (6)	Os - C(2) - N(2)	177.8 (6)
Os - C(3) - O(3)	173.9 (7)	Os - C(5) - O(5)	177.5 (7)
Os - C(4) - O(4)	177.9 (7)	Cr - C(8) - O(8)	177.1 (7)
Cr - C(6) - O(6)	176.9 (7)	Cr - C(9) - O(9)	177.6 (7)
Cr - C(7) - O(7)	176.8 (7)	Cr - C(10) - O(10)	178.7 (7)
N(1) - C(11) - C(13)	107.3 (6)	N(2) - C(12) - C(16)	107.5 (6)
N(1) - C(11) - C(14)	107.8 (6)	N(2) - C(12) - C(17)	107.0 (6)
N(1) - C(11) - C(15)	108.5 (6)	N(2) - C(12) - C(18)	107.5 (6)
C(13) - C(11) - C(14)	110.7 (7)	C(16) - C(12) - C(17)	112.8 (7)
C(13) - C(11) - C(15)	113.7 (7)	C(16) - C(12) - C(18)	111.8 (7)
C(14) - C(11) - C(15)	111.7 (7)	C(17) - C(12) - C(18)	110.0 (7)

life of approximately 2 min.[11a] (The molybdenum and tungsten analogues of $(OC)_5OsCr(CO)_5$ have not been prepared.) It therefore appears that $Os(CO)_4(CNBu^t)$ and $Os(CO)_3(CNBu^t)_2$ are superior donor ligands than $Os(CO)_5$ and $Os(CO)_3(PMe_3)_2$, and are at least as good donor ligands as $Os(CO)_4(PMe_3)$. It is generally accepted that isocyanide ligands are better σ-donors than carbonyl ligands.[33,34] Furthermore, the rod-like Bu^tNC ligand[36] can readily adopt a site that is cis to the metal-metal dative bond without too much steric interaction with the equatorial carbonyls on the group 6 atom. For reasons discussed above, this appears to be the site that is electronically favored by the poorer π-acceptor ligand. It is interesting that $(OC)_3[MeC(CH_2O)_3P]_2OsOs(CO)_4W(CO)_5$, which has two unbridged dative metal-metal bonds (i.e., Os ⟶ Os ⟶ W), is a remarkably stable molecule.[16] The X-ray structure of this compound reveals that the sterically-undemanding $P(OCH_2)_3CMe$ ligands[38] occupy positions that are mutually trans but are also cis to the OsOs dative bond.[16]

$(OC)_7(Bu^tNC)_2Os_2W(CO)_5$ Complexes. The main product of the addition of $Os(CO)_4(CNBu^t)$ to $W(CO)_5(THF)$ was $(OC)_4(Bu^tNC)OsW(CO)_5$ (**1-W**) (see above). However, $(OC)_4(Bu^tNC)OsOs(CO)_3(CNBu^t)W(CO)_5$ (**3a**) and $(OC)_3(Bu^tNC)_2OsOs(CO)_4W(CO)_5$ (**3b**), were also isolated (combined yield of 20%) from the same reaction (eq 4).The ratio of the complexes **3a**:**3b** produced

$$Os(CO)_4(CNBu^t) + W(CO)_5(THF) \longrightarrow \underset{\textbf{1-W}}{(OC)_4(Bu^tNC)OsW(CO)_5} + \underset{\textbf{3a}}{(OC)_4(Bu^tNC)OsOs(CO)_3(CNBu^t)W(CO)_5} + \underset{\textbf{3b}}{(OC)_3(Bu^tNC)_2OsOs(CO)_4W(CO)_5} \quad (4)$$

by this method was estimated to be approximately 1:1 by ^{1}H NMR spectroscopy. Compounds **3a** and **3b** were separated from **1-W** by chromatography; they were separated from each other by fractional crystallization (**3b** is much less soluble in hexane/CH_2Cl_2 than **3a**). In this way samples of **3b** could be obtained that were pure by ^{13}C NMR spectroscopy. The best samples of **3a**, however, contained **3b** (<10%) and traces of a third compound, **3c**, also believed to be an isomer of $(OC)_7(Bu^tNC)_2Os_2W(CO)_5$ (see below).

The structure of **3a** was determined by X-ray crystallography. A view of the molecule is shown in Figure 1.8; bond length and angle data are given in Table 1.6. An electron count for each metal atom in **3a** indicates that both metal-metal bonds should be regarded as dative bonds in order for each metal atom to achieve an 18-electron configuration (i.e., as shown below).

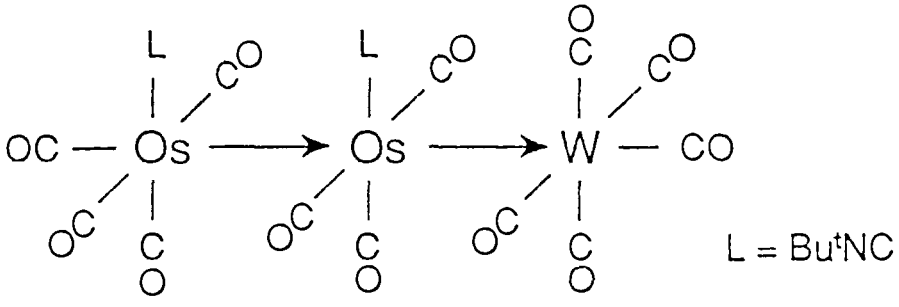

Two dative metal-metal bonds in tandem are believed to be present in $(OC)_3[MeC(CH_2O)_3P]_2OsOs(CO)_4W(CO)_5$ (**4**). The compound **3a** represents only the second example where this type of bonding has been supported by an X-ray crystal structure.[16]

It has been previously pointed out that the dative metal-metal bonds in **4** and complexes such as $(Me_3P)(OC)_4OsW(CO)_5$ are somewhat longer than comparable (nondative) bonds in compounds where the atoms are part of a closed polyhedron of metal atoms.[16] They are, however, of similar length to nondative metal-metal bonds between the same elements in compounds with a linear arrangement of metal atoms. This is also true of the metal-metal bond

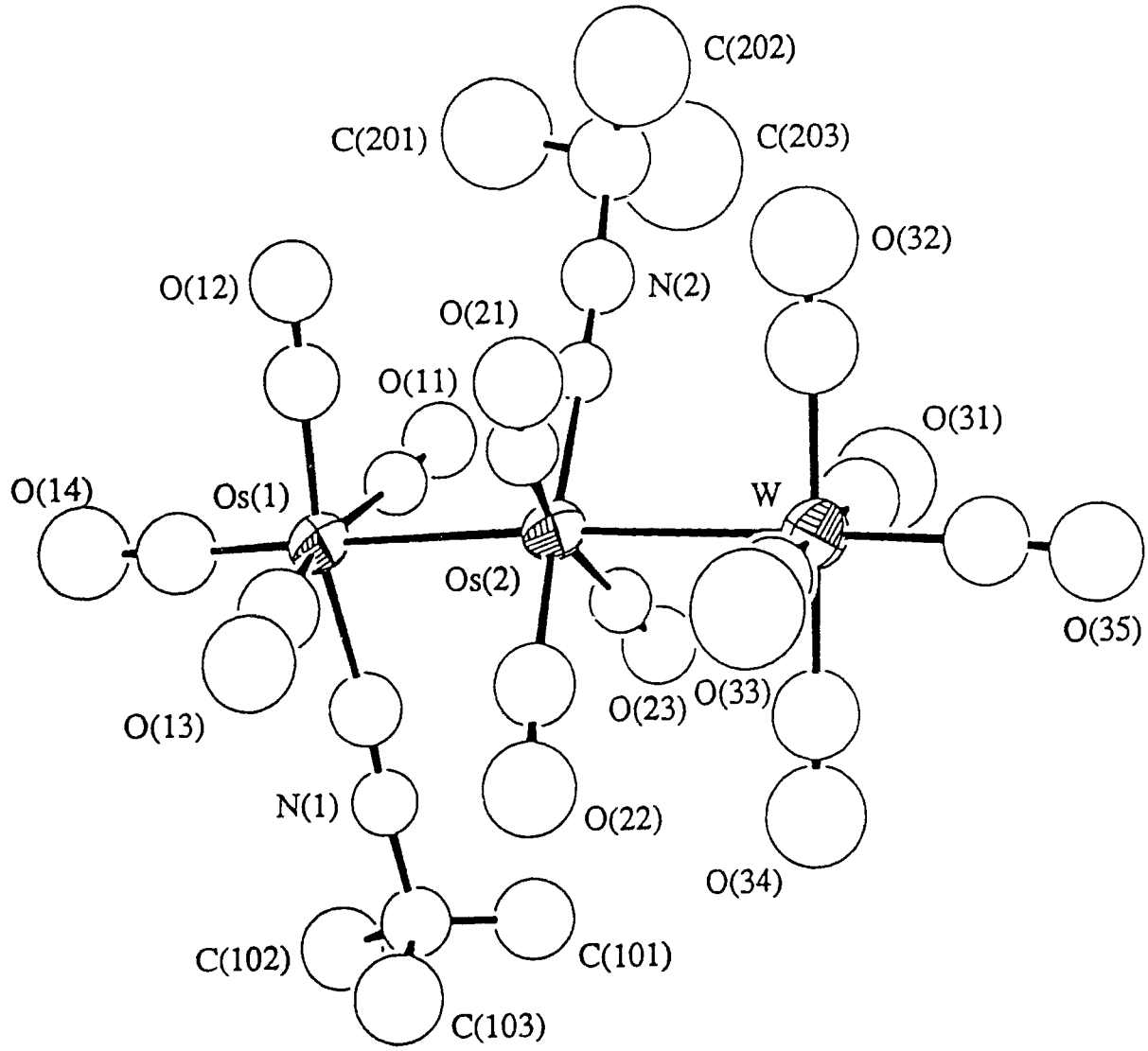

Figure 1.8 Molecular structure of **3a**.

Table 1.6 Bond Lengths (Å) and Selected Angles (deg) for **3a**

Bond distances

Os(1)-Os(2)	2.9066(15)	Os(2)-W	3.0335(16)
Os(1)-C(1)	2.027(22)	Os(2)-C(2)	1.958(20)
N(1)-C(1)	1.13(3)	N(2)-C(2)	1.17(3)
N(1)-C(100)	1.49(3)	N(2)-C(200)	1.50(4)
<Os-C(O)>	1.86 (range: 1.84(3) - 1.89(3))		
<W-C>	1.93 (range: 1.87(3) - 2.00(3))		
<C-O>	1.19 (range: 1.15(3) - 1.23(3))		
<C-C>	1.47 (range: 1.41(6) - 1.50(6))		

Bond angles

Os(1)-Os(2)-W	174.27(4)	C(11)-Os(1)-C(12)	89.6(9)
Os(2)-Os(1)-C(11)	85.1(6)	C(11)-Os(1)-C(13)	164.7(10)
Os(2)-Os(1)-C(12)	84.4(7)	C(11)-Os(1)-C(14)	98.5(11)
Os(2)-Os(1)-C(13)	79.8(8)	C(11)-Os(1)-C(1)	89.7(9)
Os(2)-Os(1)-C(14)	176.4(9)	C(12)-Os(1)-C(13)	91.1(10)
Os(2)-Os(1)-C(1)	86.1(6)	C(12)-Os(1)-C(14)	96.4(11)
Os(1)-Os(2)-C(21)	100.6(7)	C(12)-Os(1)-C(1)	170.5(9)
Os(1)-Os(2)-C(22)	93.3(8)	C(13)-Os(1)-C(14)	96.6(12)
Os(1)-Os(2)-C(23)	93.1(6)	C(13)-Os(1)-C(1)	87.0(10)
Os(1)-Os(2)-C(2)	90.8(6)	C(14)-Os(1)-C(1)	93.1(11)
W-Os(2)-C(21)	85.0(7)	C(21)-Os(2)-C(22)	89.9(10)
W-Os(2)-C(22)	85.6(8)	C(21)-Os(2)-C(23)	166.2(9)
W-Os(2)-C(23)	81.3(6)	C(21)-Os(2)-C(2)	88.4(8)
W-Os(2)-C(2)	90.4(6)	C(22)-Os(2)-C(23)	91.1(10)
Os(2)-W-C(31)	91.2(8)	C(22)-Os(2)-C(2)	175.8(10)
Os(2)-W-C(32)	89.2(9)	C(23)-Os(2)-C(2)	89.6(8)
Os(2)-W-C(33)	90.7(8)	C(31)-W-C(32)	89.4(11)
Os(2)-W-C(34)	89.0(8)	C(31)-W-C(33)	176.6(11)

Table 1.6 cont'd

Os(2)-W-C(35)	177.9(7)	C(31)-W-C(34)	87.9(11)
C(32)-W-C(35)	92.8(11)	C(31)-W-C(35)	89.6(12)
C(33)-W-C(34)	89.4(11)	C(32)-W-C(33)	93.4(11)
C(33)-W-C(35)	88.4(11)	C(32)-W-C(34)	176.8(11)
C(34)-W-C(35)	89.0(11)	C(1)-N(1)-C(100)	179(5)
Os(1)-C(1)-N(1)	177.1(19)	C(2)-N(2)-C(200)	177.0(22)
Os(2)-C(2)-N(2)	175.6(18)		
<M[a]-C-O>	176 (range: 171(2) - 179(2))		
<N-C-C>	107 (range: 103(3) - 110(3))		
<C-C-C>	111 (range: 105(3) - 120(3))		

[a] M = Os or W.

lengths in **3a**. The Os-Os bond length in **3a** of 2.9066 (15) Å is, for example, somewhat longer than the average Os-Os bond length in $Os_3(CO)_{12}$ (2.877 Å),[39] but slightly shorter than the Os-Os distance in $Os_3(CO)_{12}(SiCl_3)_2$ (2.912 (1) Å)[40] and $Os_3(CO)_{12}(I)_2$ (2.935 (2) Å).[41] That the Os-Os distance in **3a** is shorter than that in **4** (2.940 (1) Å) may indicate that there are fewer repulsive interactions between the radial ligands in **3a** than in **4**. The Os-W length in **3a** (3.0335 (16) Å) may be compared to that in **4** (3.039 (1) Å)[39] and that in $(Me_3P)(OC)_4OsW(CO)_5$ (3.0756 (5) Å).[11a]

As found for binuclear compounds with unbridged, dative metal-metal bonds such as **1-Cr** and **2b-Cr** (see above), there is an inward leaning of the radial carbonyls on the donor metal atom toward the acceptor metal atom in **3a** (the appropriate Os(2)-Os(1)-C angles are in the range 79.8 (8) - 85.1 (6)°; the W-Os(2)-C angles are in the range 81.3 (6) - 85.6 (8)°). On the other hand, the corresponding angles for the radial carbonyls on the terminal acceptor-metal are close to 90° (the relevant Os(2)-W-C angles range from 89.0 (8) to 91.2 (8)°).

The ^{13}C NMR spectrum of **3a** in CH_2Cl_2/CD_2Cl_2 (Figure 1.9A) exhibits a 1:4:2:1:2:1:1 pattern of signals in the CO region; the ^1H NMR spectrum contains 2 singlets. These spectra indicate that the structure found for the molecule in the solid state is also adopted in solution. The assignments of the ^{13}C NMR resonances readily follows from intensity considerations, satellites due to coupling to ^{183}W, and by comparison of the spectrum with the ^{13}C NMR spectra of **1-W**, **3b** (see below), and **4**[16] where the assignment is unambiguous. As previously noted , the ^{13}C NMR resonances of carbonyls trans to dative metal-metal bonds appear at unusually high fields. In **3a** this resonance appears at δ 162.5.

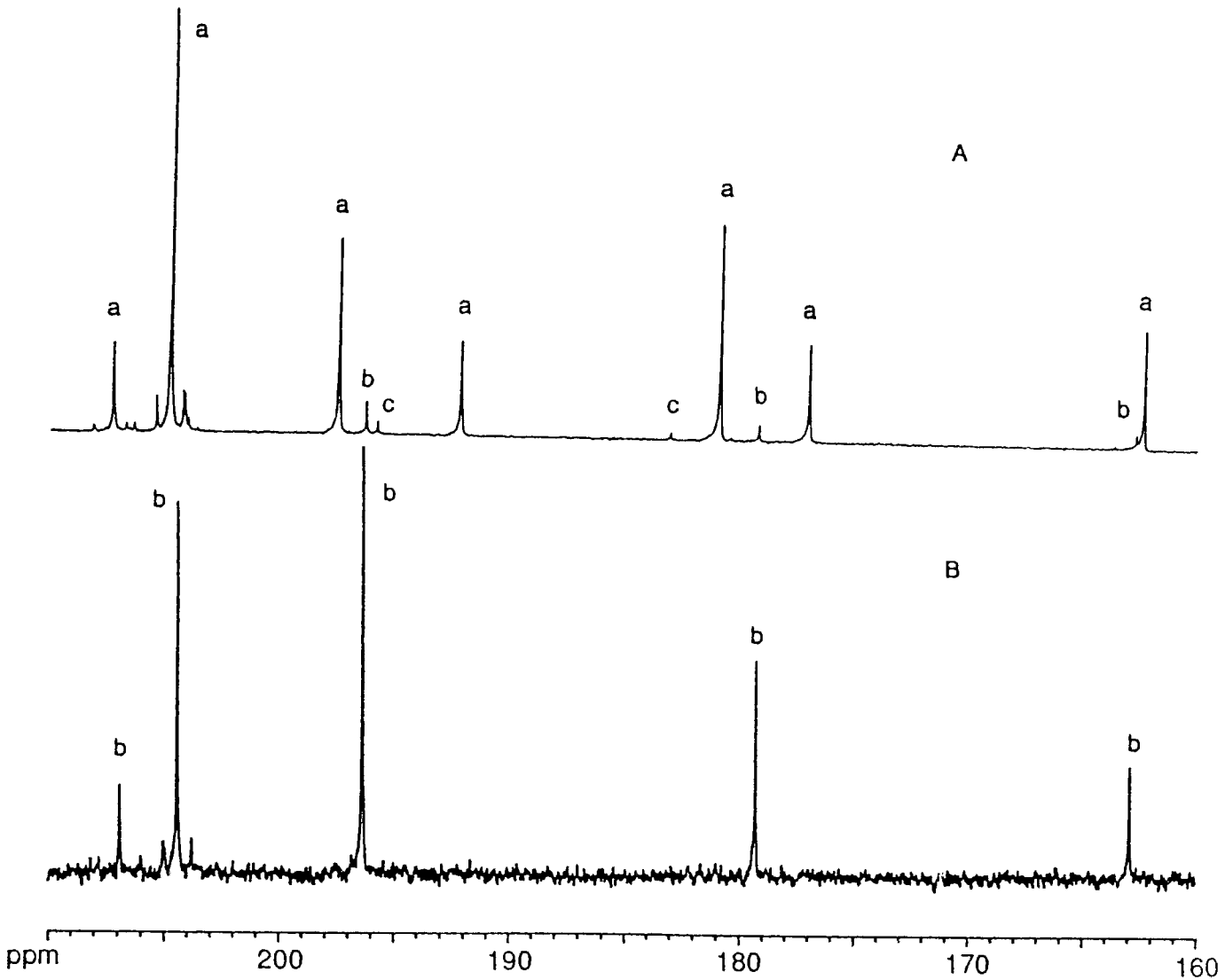

Figure 1.9 Carbonyl region of ^{13}C NMR spectrum of A: **3a** and B: **3b** (a = **3a**, b = **3b**, c = **3c**; CH_2Cl_2/CD_2Cl_2, 4/1, at 0 °C).

The compound **3b** is assigned a structure similar to that of **3a**, but with both isocyanide ligands on the terminal osmium atom in a cis arrangement as shown below. The assignment comes from the 1:4:4:2:1 pattern of peaks in the

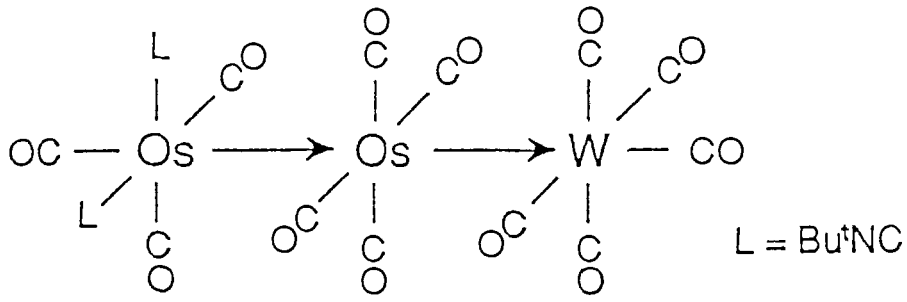

carbonyl region of the ^{13}C NMR spectrum of the compound in CH_2Cl_2/CD_2Cl_2 (Figure 1.9B), and the two CN stretches in the infrared spectrum, consistent with a cis arrangement of the Bu^tNC ligands.

There was also evidence in the ^{13}C NMR spectrum of **3a** (Figure 1.9A) for a third compound (**3c**). The pattern of the signals, with the exception that one signal of intensity 1 was not observed, was consistent with **3c** having a structure similar to that proposed for **3b**, but with the isocyanide ligands in a trans arrangement. Again, the presence of a resonance at an unusually high field (δ 163.8) rules out the possibility of the $CNBu^t$ ligand being trans to the Os-Os bond.

Comparison of the ^{13}C NMR spectra of **3a**, **3b** and **3c** (Figure 1.9 and Table 1.3) shows that there are definite, well separated regions for the carbonyls of the two different osmium atoms. The resonances attributed to the carbonyls on the central osmium atom occur between δ 198 and 192 while those attributed to the radial carbonyls of the terminal osmium atom are found between δ 183 and 177. In addition, the signals assigned to the axial carbonyl of the terminal osmium atom occur between δ 164 and 162.

That there might be isomerization occurring between the two isomers having the isocyanides on the terminal osmium (i.e., **3b** and **3c**) was considered:

this type of isomerization was observed for $(OC)_3(Bu^tNC)_2OsM(CO)_5$ (**2-M**) (see above). However, whereas the two isomers of **2-M** (i.e., **2a-M** and **2b-M**) were in dynamic equilibrium in solution at room temperature, this was not the case for **3b** and **3c**: A sample of pure **3b** was unchanged (by ^{13}C NMR spectroscopy) after it had stirred in CH_2Cl_2 at room temperature for 7 d.

The possible isomerization of **3a** in solution was also studied by ^{13}C NMR spectroscopy: A sample containing approximately equal amounts of **3a** and **3b** (each ^{13}CO-enriched) was stirred in CH_2Cl_2 at room temperature for 9 d. The intensities of the ^{13}C NMR resonances of the sample before and after this treatment were compared to those of an internal standard of ^{13}CO-enriched $Os_3(CO)_{12}$. From this comparison, it was judged that **3a** had almost completely decomposed during this period but the concentration of **3b** and **3c** was unchanged.

These results indicate that the formation of **3b** from $Os(CO)_4(CNBu^t)$ and $W(CO)_5(THF)$ (i.e., as in eq 4) does not involve the initial formation of **3a** followed by its isomerization to **3b**. This has parallels to observations regarding the synthesis of **4** in that $(L')(OC)_4OsOs(CO)_3(L')W(CO)_5$ (L' = $P(OCH_2)_3CMe$) did not isomerize to **4** under the same conditions used to prepare **4** from $Os(CO)_4(L')$ and $(L')(OC)_4OsW(CO)_5$.[16] It is perhaps more surprising in the present case since Bu^tNC has been shown to migrate across a dative metal-metal bond from the acceptor metal atom to the donor metal atom (see above). The $P(OCH_2)_3CMe$ ligand is not known to act as a bridging ligand.

It is interesting that **3b** is more stable in solution than **3a**. This observation can be compared with the finding reported above that [*cis-dieq*-$(OC)_3(Bu^tNC)_2Os]Cr(CO)_5$ (**2b-Cr**) is thermodynamically more stable than $(OC)_4(Bu^tNC)OsCr(CO)_4(CNBu^t)$.

1.4 Conclusion

Simple mononuclear osmium isocyanide complexes of the type $Os(CO)_{5-x}(CNBu^t)_x$ (x = 1, 2) have been prepared from $Os(CO)_5$ (or for x = 1, $Os(CO)_4(\eta^2$-cyclooctene)) and Bu^tNC. Both of these mononuclear complexes were used to prepare bimetallic complexes with dative metal-metal bonds that are analogous to the previously known phosphine and phosphite analogues.[11a] However, unlike the phosphorus ligand analogues, the non-carbonyl ligand was never found trans to the Os-M bond in the bimetallic isocyanide complexes. It is thought that the small rod-like $CNBu^t$ ligand can easily adopt a site that is cis to the metal-metal bond; this site is believed to be electronically preferred but is more sterically hindered than the axial position.

On the question of the types of ligands that can migrate across a dative metal-metal bond, it has been established that CO can easily migrate.[11a] As well, there is at least one case of a phosphite, namely $P(o\text{-}Pr^i)_3$, that has migrated from the acceptor to the donor metal atom in a complex with a dative metal-metal bond.[12a] It has now been established that the $CNBu^t$ ligand can also migrate from the acceptor to the donor metal atom. The latter site therefore appears to be the thermodynamically preferred site for the isocyanide ligand.

Preliminary investigations indicate that the **1-M** complexes are not as synthetically useful as their phosphine or phosphite analogues. However, the greater solubility of **1-M** complexes in hexane allows the structure of the complexes in solution to be studied in more detail by IR spectroscopy. This was not possible for the phosphorus ligand compounds.[11a] In addition, the CN stretching vibration of the isocyanide ligand provided additional structural information which was not possible with the complexes having phosphorus ligands. Indeed, the two isomers of **2-M** (**2a-M** and **2b-M**), which gave the same ^{13}C NMR pattern, were distinguished by the number of CN stretches in their IR

spectra.

From comparison of various compounds of the type $Os(CO)_{5-x}(L)_x$ (L = CO, PMe_3, $CNBu^t$; x = 1,2), it appears that for these compounds to be optimal donor ligands, L should be a good σ-donor and also be small so that it can occupy a site cis to the dative metal-metal bond. In the only examples of compounds with two, unbridged dative metal-metal bonds synthesized to date, the L ligands ($CNBu^t$ and $P(OCH_2)_3CMe$) are both sterically undemanding. Furthermore, the crystal structures of both compounds (**3a** and **4**) studied to date show that the L ligands are cis to the dative metal-metal bonds.[16]

Although the bimetallic (**1-M** and **2-M**) and the trimetallic complexes (**3**) are similar in that they all have dative metal-metal bonds, there are considerable differences between them. For example, **3a** is not in equilibrium with **3b**, even though it has been shown that $CNBu^t$ can migrate across an OsCr dative metal-metal bond. More surprisingly, **3b** and **3c** are not in equilibrium, even though **2a-M** and **2b-M** are found to be in equilibrium.

To date, the longest chain of dative metal-metal bonds in tandem is two. It may be that with a judicious choice of L donor ligand and reaction conditions that complexes with longer chains can be synthesized.

CHAPTER 2

SYNTHESIS, CHARACTERIZATION AND CARBONYL EXCHANGE IN $(\eta^5\text{-}C_5R_5)(OC)Ir[Os(CO)_4]_2$ (R = H; R = Me).

2.1 Introduction

The concept of the isolobal analogy in organometallic chemistry was made popular by Hoffmann.[42] This concept has been skillfully exploited by Stone in the rational synthesis of heterometallic clusters.[43] One isolobal relationship that had been verified is that between $(\eta^5\text{-}C_5H_5)M(CO)$ (M = Co or Rh) and $M'(CO)_4$ (M' = Fe or Os); synthetic examples include $(\eta^5\text{-}C_5H_5)Co\text{-}Fe_2(CO)_9$,[44] $(\eta^5\text{-}C_5H_5)RhFe_2(CO)_9$,[45] and $(\eta^5\text{-}C_5H_5)(OC)Rh[Os(CO)_4]_2$.[46] It was of interest to extend this relationship to M = Ir, by synthesizing $(\eta^5\text{-}C_5R_5)(OC)Ir\text{-}[Os(CO)_4]_2$ (R = H, Me). The synthetic approach was to use $Os(CO)_4\text{-}(\eta^2\text{-cyclooctene})$[21] as a 'building block' for polymetallic compounds.

The $(\eta^5\text{-}C_5R_5)(OC)Ir[Os(CO)_4]_2$ clusters were of interest because of the CO exchange they would undoubtedly exhibit. Ligand exchange processes in carbonyl clusters are common.[47,48] In some cases, the CO exchange occurs on the NMR time scale and as a result can be studied by using variable temperature ^{13}C NMR. Shore and co-workers had reported the ^{13}C NMR spectra of $(\eta^5\text{-}C_5H_5)(OC)Rh[Os(CO)_4]_2$, but even at -95 °C the carbonyl exchange in the cluster was still rapid.[46] It was therefore impossible to propose mechanisms for the carbonyl exchange in this $(\eta^5\text{-}C_5H_5)MM'_2(CO)_9$ cluster.

It is generally found in metal carbonyl clusters that barriers to carbonyl exchange increase upon going to the metal lower in the periodic table. Thus it was hoped that study of the NMR spectra of the iridium analogues,

$(\eta^5\text{-}C_5R_5)(OC)Ir[Os(CO)_4]_2$ (R = H, Me), would allow more detail on the fluxional processes of these types of clusters to be obtained. Some time after the project had been started, Takats and Washington reported the ^{13}C NMR spectra of $(\eta^5\text{-}C_5H_5)(OC)Rh[Os(CO)_4]_2$ and its pentamethylcyclopentadienyl analogue.[49] They found that the former compound was rigid at -115 °C in THF and they were able to propose a mechanism for the CO exchange. The ^{13}C NMR studies on the Ir analogues synthesized here essentially confirm the results of their work.

Another reason to study the $(\eta^5\text{-}C_5R_5)(OC)Ir[Os(CO)_4]_2$ clusters was to investigate the possible rotation of organometallic fragments that are isolobal with $Os(CO)_4$ in trinuclear clusters that have two $Os(CO)_3(L)$ (L = two-electron donor ligand) groups. A large difference in the ease of rotation of the formally isolobal fragments $M(CO)_5$ (M = Cr, Mo, W) and $Os(CO)_4$ had previously been found. For example, while there is apparent rapid rotation of the $Cr(CO)_5$ unit in $(OC)_5Cr[Os(CO)_3(PMe_3)]_2$ even at -122 °C,[50] the $Os(CO)_4$ units in the two isomers of $(OC)_4Os\{Os(CO)_3[P(OMe)_3]\}_2$ are rigid at -66 °C.[47] Other fragments that are formally isolobal with $M(CO)_5$ and $Os(CO)_4$ include $(\eta^5\text{-}C_5R_5)M(CO)$ (M = Rh, Ir; R = H, Me). Takats and Washington found that the $(\eta^5\text{-}C_5H_5)Rh(CO)$ group in $(\eta^5\text{-}C_5R_5)(OC)Rh[Os(CO)_4]_2$ was rigid with respect to the rest of the molecule at -115 °C.[49]

The details of the syntheses, characterization, and the spectroscopic studies along with the crystal structure of $(\eta^5\text{-}C_5Me_5)(OC)Ir[Os(CO)_4]_2$ are described in this chapter.[51] These results have been recently published.[52]

2.2 Experimental

Unless otherwise stated, manipulations of starting materials and products were carried out under a nitrogen atmosphere with the use of standard Schlenk techniques. Hexane and dichloromethane were distilled from potassium and P_2O_5, respectively. Dicarbonyl(cyclopentadienyl)iridium, $(\eta^5\text{-}C_5H_5)Ir(CO)_2$, was prepared from $[Ir(CO)_3(Cl)]_n$ and TlC_5H_5;[53] the method of Maitlis[54] was used to synthesize $(\eta^5\text{-}C_5Me_5)Ir(CO)_2$ with the exception that $[(\eta^5\text{-}C_5Me_5)Ir(Cl)_2]_2$ was prepared with the use of pentamethylcyclopentadiene.[53] Other reagents were available commercially.

Infrared spectra were recorded on a Perkin-Elmer 983 spectrometer; the internal calibration of the instrument was checked against the known absorption frequencies of gaseous CO. The ^1H NMR spectra were recorded on a Bruker SY-100 NMR spectrometer. The variable temperature ^{13}C NMR spectra were obtained by Andrew K. Ma using a Bruker WMX400 NMR spectrometer (operating frequency: 100.6 MHz) on ^{13}CO-enriched samples (~30% ^{13}C). The ^{13}CO-enriched samples were synthesized from ^{13}CO-enriched $Os_3(CO)_{12}$ that had been prepared by heating $Os_3(CO)_{12}$ in toluene at 125 °C under ~1.5 atm of ^{13}CO (99% ^{13}C) for 3 d. The NMR line-shape simulations shown in Figure 2.3 were carried out by Andrew K. Ma using a computer program written by Professor R. E. D. McClung of the University of Alberta. The electron impact (70 eV) mass spectra were obtained with a Hewlett-Packard 5985 GC-MS instrument; the pattern of the ions at highest mass in each spectrum matched that calculated for the parent ion of the compound in question. Microanalyses were performed by M.K. Yang of the Microanalytical Laboratory of Simon Fraser University.

The crystal structure reported in this chapter was determined by Professor F.W.B. Einstein and Dr. A. Riesen at Simon Fraser University.

Preparation of $(\eta^5\text{-}C_5H_5)(OC)Ir[Os(CO)_4]_2$ (1). A modified procedure of that by Burke[21] was used to prepare $Os(CO)_4(\eta^2\text{-cyclooctene})$: A Carius tube fitted with a Teflon valve was charged with $Os_3(CO)_{12}$ (50 mg, 0.055 mmol), cyclooctene (0.68 mL, 5.2 mmol) and hexane (45 mL). The tube was cooled to -196 °C and evacuated; the solution was degassed with one freeze-pump-thaw cycle. The vessel was pressurized with CO (1 atm). The stirred solution was irradiated with a Hanovia 200 W ultraviolet lamp through a GWV filter ($\lambda >$ 370 nm). After 7 h irradiation, the solution was filtered and transferred to a round-bottom flask (~80 mL volume, fitted with a Teflon valve). The hexane and excess cyclooctene were removed on the vacuum line. The residue that contained the $Os(CO)_4(\eta^2\text{-cyclooctene})$ was suspended in hexane (30 mL) and $(\eta^5\text{-}C_5H_5)Ir(CO)_2$ (21 mg, 0.075 mmol) added. The vessel was cooled to -196 °C and evacuated; the solution was degassed with one freeze-pump-thaw cycle. The flask was wrapped in aluminum foil and heated at 55 - 65 °C for 25 h. After this treatment the initially pale yellow solution had become pale red. The solvent was removed on the vacuum line and the residue extracted with hexane (4 x 2 mL). The extracts were filtered (which removed most of the $Os_3(CO)_{12}$, the other major product). The extracts were combined and the solvent removed on the vacuum line. The remaining solid was subjected to sublimation (0.1 mm Hg) at 55 - 65 °C which removed unreacted $(\eta^5\text{-}C_5H_5)Ir(CO)_2$ and $Os(CO)_4$-$(\eta^2\text{-cyclooctene})$. An alternate method involved cooling the reaction solution to 4 °C to precipitate most of the $Os_3(CO)_{12}$ byproduct. The solution was then decanted and the solvent removed under vacuum. The remaining solid was sublimed as described above.

After sublimation, the residue was chromatographed on silica gel (10 x 1cm). Elution with hexane gave a yellow band followed by an orange-red band of the desired product. The latter band was collected and the solvent removed

on the vacuum line to give $(\eta^5\text{-}C_5H_5)(OC)Ir[Os(CO)_4]_2$ (21 mg, 28% based on the $Os_3(CO)_{12}$ used). The analytical sample was recrystallized from toluene to give red, air-stable crystals of **1**; IR (hexane) ν(CO) 2108 (m), 2062 (s), 2028 (s), 2013 (vs), 1995 (s), 1983 (m), 1957 (m) cm^{-1}; MS (EI) *m/z* 890 (M^+); ^1H NMR ($CDCl_3$) δ 5.45 (s); ^{13}C NMR (CH_2Cl_2/CD_2Cl_2, 4/1; CO region, -48 °C) δ 185.3 (2C), 183.4 (2C),174.3 (1C), 169.9 (2C). Anal. Calcd for $C_{14}H_5IrO_9Os_2$: C, 18.90; H, 0.57. Found: C, 19.14; H, 0.56.

The synthesis of $(\eta^5\text{-}C_5Me_5)(OC)Ir[Os(CO)_4]_2$ (**1***) followed a similar procedure. The yield starting with 105 mg (0.116 mmol) of $Os_3(CO)_{12}$ and 50 mg (0.140 mmol) $(\eta^5\text{-}C_5Me_5)Ir(CO)_2$ was 45 mg (27%). The analytical sample (as red, air-stable crystals) was obtained by recrystallization from hexane: IR (hexane) ν(CO) 2099 (m), 2053 (s), 2019 (vs), 2007 (vs), 2000 (sh), 1985 (s), 1973 (m), 1944 (m) cm^{-1}; MS (EI) *m/z* 960 (M^+); ^1H NMR ($CDCl_3$) δ 2.11 (s); ^{13}C NMR ($CHFCl_2/CD_2Cl_2$; CO region; -129 °C) δ 185.9, 179.1, 173.3, 170.2 Anal. Calcd for $C_{19}H_{15}IrO_9Os_2$: C, 23.77; H, 1.58. Found: C, 23.99; H, 1.64.

2.3 Results and Discussion

The clusters $(\eta^5\text{-}C_5R_5)(OC)Ir[Os(CO)_4]_2$ (R = H: **1**; R = Me: **1***) were prepared in ~28% yield by the reaction of $(\eta^5\text{-}C_5R_5)Ir(CO)_2$ with $Os(CO)_4$-$(\eta^2$-cyclooctene)[21] in hexane at 55 - 65 °C (eq 1).

$$Os(CO)_4(\eta^2\text{-cyclooctene}) + (\eta^5\text{-}C_5R_5)Ir(CO)_2 \xrightarrow{55\text{-}65\ ^\circ C} (\eta^5\text{-}C_5R_5)(OC)Ir[Os(CO)_4]_2 \quad (1)$$

R = H, **1**; R = Me, **1***

Shore and co-workers prepared $(\eta^5\text{-}C_5H_5)(OC)Rh[Os(CO)_4]_2$ (**1-Rh**) by the reaction of $Os_3(\mu\text{-}H)_2(CO)_{10}$ with $(\eta^5\text{-}C_5H_5)Rh(CO)_2$.[46] The preparation of **1*** by reacting $Os_3(\mu\text{-}H)_2(CO)_{10}$ and $(\eta^5\text{-}C_5Me_5)Ir(CO)_2$ was previously attempted in this laboratory, but it was unsuccessful. Heating $Os(CO)_5$ and $(\eta^5\text{-}C_5Me_5)Ir(CO)_2$ together in hexane also failed to produce **1***. However, trace amounts of **1*** were observed in the prolonged reaction of $Os_3(CO)_{10}(cyclooctene)_2$ with $(\eta^5\text{-}C_5Me_5)Ir(CO)_2$. In this reaction **1*** presumably results from the disintegration of a tetranuclear cluster ($(\eta^5\text{-}C_5Me_5)IrOs_3(CO)_{10}$ has been isolated from the same reaction[55]). This last reaction therefore resembles the formation of **1*-Rh** from $Os_2(\mu\text{-}\eta^1,\eta^1\text{-}CH_2CH_2)(CO)_8$ and $[Rh(\mu\text{-}CO)(\eta^5\text{-}C_5Me_5)]_2$.[49]

Like **1-Rh** and **1*-Rh**, the iridium analogues are deep red, air-stable, crystalline solids. The infrared spectra in the carbonyl stretching region of **1** and **1*** are similar to those reported by Washington and Takats for **1-Rh**, and **1*-Rh**.[49] There is no evidence in the spectra for bridging carbonyls.

Structure of 1*. A view of the molecule is shown in Figure 2.1; bond lengths and selected angles are given in Table 2.I. As can be seen from Figure 2.1, **1*** may be regarded as derived from $Os_3(CO)_{12}$[39] in which one of the $Os(CO)_4$ units has been replaced by the formally isolobal fragment

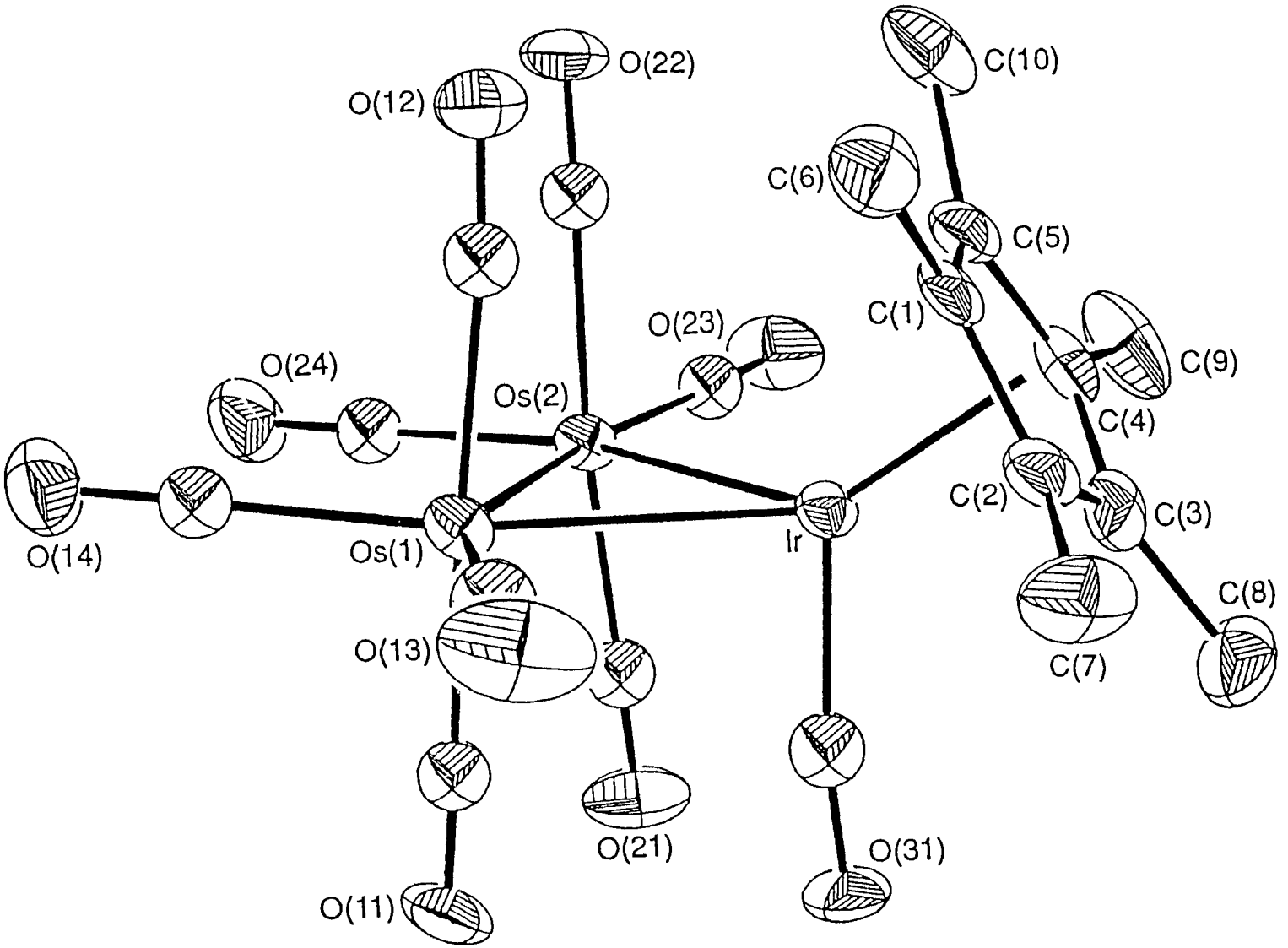

Figure 2.1 Molecular structure of **1***.

Table 2.1 Bond lengths (Å) and Selected angles (deg) for **1***.

Bond Lengths

Ir-Os(1)	2.7902 (5)	C(12)-O(12)	1.13 (1)
Ir-Os(2)	2.8124 (5)	C(13)-O(13)	1.13 (1)
Os(1)-Os(2)	2.8536 (5)	C(14)-O(14)	1.12 (1)
Ir-C(1)	2.324 (8)	C(21)-O(21)	1.14 (1)
Ir-C(2)	2.217 (9)	C(22)-O(22)	1.11 (1)
Ir-C(3)	2.17 (1)	C(23)-O(23)	1.12 (1)
Ir-C(4)	2.227 (9)	C(24)-O(24)	1.14 (1)
Ir-C(5)	2.301 (9)	C(31)-O(31)	1.23 (1)
Ir-C(31)	1.85 (1)	C(1)-C(2)	1.42 (1)
Os(1)-C(11)	1.96 (1)	C(1)-C(5)	1.42 (1)
Os(1)-C(12)	1.96 (1)	C(1)-C(6)	1.51 (1)
Os(1)-C(13)	1.92 (1)	C(2)-C(3)	1.42 (2)
Os(1)-C(14)	1.92 (1)	C(2)-C(7)	1.51 (1)
Os(2)-C(21)	1.95 (1)	C(3)-C(4)	1.44 (2)
Os(2)-C(22)	1.97 (1)	C(3)-C(8)	1.50 (2)
Os(2)-C(23)	1.91 (1)	C(4)-C(5)	1.45 (1)
Os(2)-C(24)	1.90 (1)	C(4)-C(9)	1.50 (1)
C(11)-O(11)	1.12 (1)	C(5)-C(10)	1.48 (1)

Angles

Os(2)-Ir-Os(1)	61.24 (1)	C(3)-Ir-C(2)	37.7 (4)
Os(2)-Os(1)-Ir	59.77 (1)	C(4)-Ir-C(1)	61.2 (3)
Os(1)-Os(2)-Ir	59.00 (1)	C(4)-Ir-C(2)	63.0 (4)
C(2)-C(1)-C(6)	124.2 (9)	C(4)-Ir-C(3)	38.2 (4)
C(5)-C(1)-C(6)	126.2 (9)	C(5)-Ir-C(1)	35.7 (3)
C(5)-C(1)-C(2)	109.0 (9)	C(5)-Ir-C(2)	61.3 (3)
C(1)-C(2)-C(7)	125.9 (10)	C(5)-Ir-C(3)	62.4 (4)

Table 2.1 cont'd.

C(3)-C(2)-C(7)	125.5 (11)	C(5)-Ir-C(4)	37.4 (4)
C(3)-C(2)-C(1)	108.2 (9)	C(12)-Os(1)-C(11)	174.7 (4)
C(2)-C(3)-C(8)	126.7 (12)	C(13)-Os(1)-C(11)	93.2 (4)
C(4)-C(3)-C(8)	124.4 (11)	C(13)-Os(1)-C(12)	90.3 (4)
C(4)-C(3)-C(2)	108.5 (9)	C(14)-Os(1)-C(11)	91.2 (4)
C(3)-C(4)-C(9)	126.3 (11)	C(14)-Os(1)-C(12)	91.6 (4)
C(5)-C(4)-C(9)	126.8 (11)	C(14)-Os(1)-C(13)	104.5 (4)
C(5)-C(4)-C(3)	106.5 (9)	C(22)-Os(2)-C(21)	174.3 (4)
C(1)-C(5)-C(10)	125.7 (10)	C(23)-Os(2)-C(21)	94.7 (4)
C(4)-C(5)-C(10)	124.1 (10)	C(23)-Os(2)-C(22)	90.7 (4)
C(4)-C(5)-C(1)	107.8 (9)	C(24)-Os(2)-C(21)	89.1 (4)
C(2)-Ir-C(1)	36.2 (4)	C(24)-Os(2)-C(22)	88.0 (4)
C(3)-Ir-C(1)	61.3 (4)	C(24)-Os(2)-C(23)	101.6 (4)

Ir(η^5-C_5Me_5)(CO). The carbonyl ligand on the iridium atom occupies an axial site. The structure of **1*** is similar to that of **1-Rh** except that the orientations of the cyclopentadienyl rings are slightly different: in **1*** two carbon atoms (C(1), C(5)) of the ring carbons are closest to the osmium atoms whereas in **1-Rh** only one of the carbon atoms is closest to these metal atoms.[46] Both molecules have close to (but not exact) mirror symmetry in the solid state. The Os-Os bond length in **1*** of 2.8536 (5) Å may be compared to 2.8455 (4) Å the Os-Os bond length in **1-Rh**,[46] and 2.877 Å the average Os-Os bond length in $Os_3(CO)_{12}$.[39] The Os-Ir bond lengths in **1*** (2.7902 (5) and 2.8124 (5) Å) are in the range 2.776 (5) - 2.881 (1) Å previously found for single, unbridged Os-Ir bonds in cluster compounds.[56] As in $Os_3(CO)_{12}$,[39] the axial Os-C bonds (average length = 1.96 Å) are longer than the equatorial Os-C bonds (average length = 1.91 Å). The geometry about the $Os_2(CO)_8$ unit in **1*** is similar to those of the $Os_2(CO)_8$ units in $Os_3(CO)_{12}$. The nearest nonbonding distances of a carbonyl carbon to a metal atom are Ir-C(12) = 3.25 (1) Å, Ir-C(21) = 3.28 (1) Å, and Os(1)-C(31) = 3.32 (1) Å. In other words, there is no evidence for semibridging carbonyls in the solid-state structure.

Carbonyl Exchange in 1 and 1*. The ^{13}C NMR spectrum of ^{13}CO-enriched **1** in CH_2Cl_2/CD_2Cl_2 at -48 °C exhibits five carbonyl resonances in the ratio 2:2:1:2:2 (Figure 2.2). The assignment of the resonances shown in Figure 2.2 and Chart 1 is based on the following arguments. The signal of intensity 1 at δ 174.3 is unambiguously assigned to the carbonyl on iridium on the basis of intensity; it also appears in the region associated with carbonyl ligands bound to iridium.[57] The two resonances to low field of this signal at δ 185.3 and 183.4 are attributed to the two types of axial carbonyls on osmium. In saturated trinuclear clusters of osmium the signals due to axial carbonyls invariably come to low field

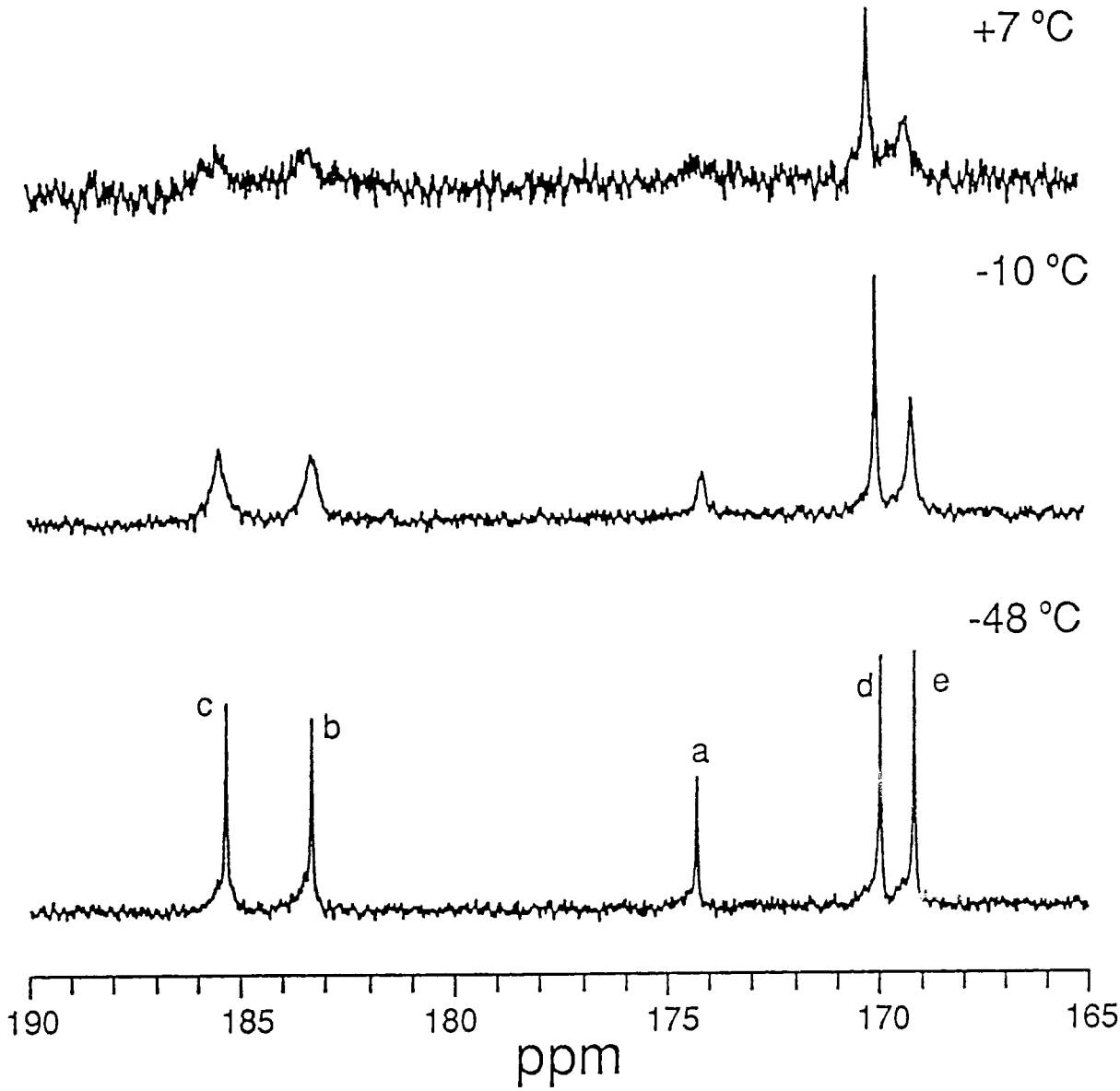

Figure 2.2 Variable-temperature ^{13}C NMR spectra of **1** in CH_2Cl_2/CD_2Cl_2.

to those of the equatorial carbonyls.[47,57,58] There is also evidence in the spectrum at -33 °C that these signals exhibit ^{13}C-^{13}C coupling as expected for a

Chart I

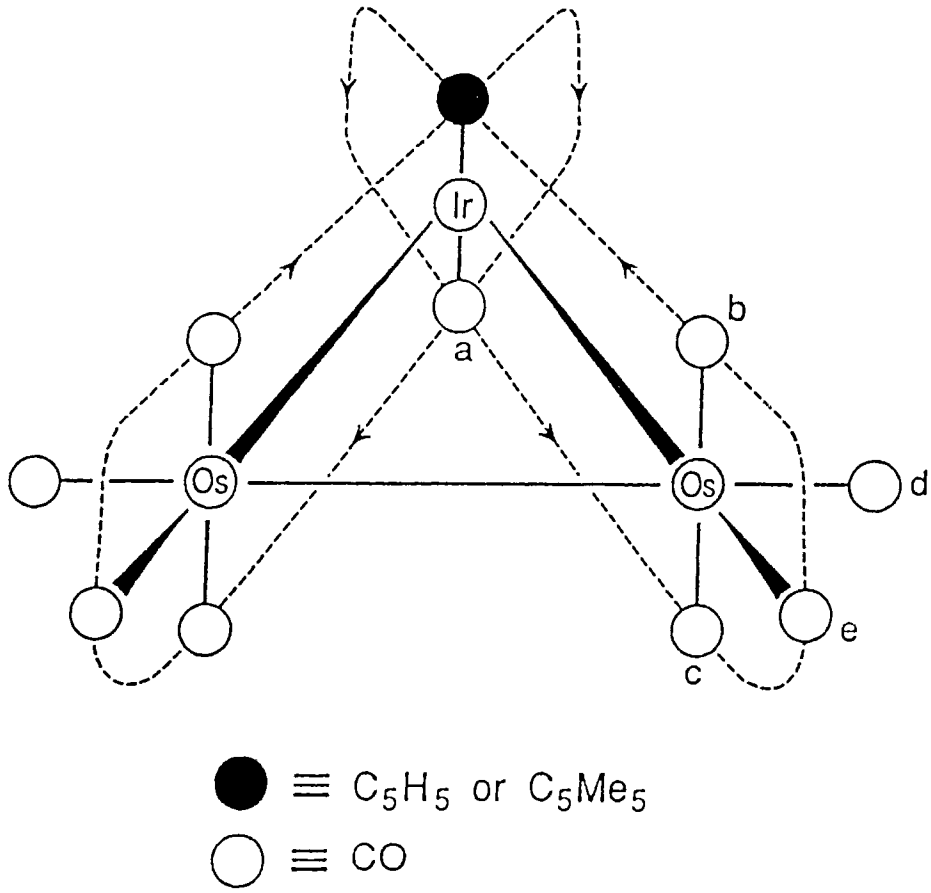

trans arrangement of two carbonyls that are chemically different.[59] (The level of ^{13}CO enrichment used in the sample was approximately 30%) The resonance at δ 185.3 is tentatively assigned to the carbonyls labelled c in the chart on the basis that the resonances due to the carbonyls on the opposite side of the Os_2Ir plane to that occupied by the cyclopentadienyl ligand should be less affected on going from **1** to **1***. (In **1*** the resonances of carbonyls b and c are degenerate and occur at δ 185.9.) The highest field signals, at δ 169.9 and 169.1, are assigned to carbonyls d and e, respectively, on the basis of the exchange mechanism (see below). The signals are in the region expected for equatorial carbonyls of $Os(CO)_4$ groupings in trinuclear clusters.[47,57,58] The changes in the

chemical shifts of the signals due to carbonyls d and e on going to **1*** are consistent with the argument used above to assign the resonances attributed to carbonyls b and c.

The presence of two signals for the axial carbonyls of the $Os(CO)_4$ units indicates that the $Ir(\eta^5\text{-}C_5H_5)(CO)$ unit in **1** is rigid at -48 °C. It is impossible to ascertain from the NMR evidence whether the Ir unit in **1** rotates with respect to the $Os_2(CO)_8$ moiety in solution at higher temperatures.

On warming the sample of **1** to +7 °C, four of the carbonyl resonances collapse to the base line (Figure 2.2). This behavior is interpreted in terms of partial merry-go-round CO exchanges that take place in those planes that are perpendicular to the plane containing the metal atoms and which pass through the iridium and one of the osmium atoms. The exchanges are illustrated in Chart I. Complete merry-go-round CO-exchanges have been proposed many times before to account for the coalescences of resonances in the variable temperature ^{13}C NMR spectra of metal carbonyl cluster and binuclear compounds.[60-64] It is only a partial merry-go-round in **1** since the cyclopentadienyl ligand remains coordinated to the iridium atom. For this reason, the mechanism requires that CO exchange takes place alternatively in the two planes so that the C_5H_5 group is always coordinated to the two equatorial sites on iridium but rocks back and forth between the two axial sites as each successive CO exchange occurs. After six individual exchanges each carbonyl of type a, b, c or e has visited each one of the other chemically different sites in this group of carbonyls. The signals assigned to carbonyls a , b, c and e should therefore coalesce to a singlet. This is observed for **1*** (see below), and for **1-Rh** where the same mechanism of CO exchange has been proposed.[49] The carbonyls labeled d do not take part in these exchanges (Chart I) and consequently the signal attributed to these carbonyls remains sharp as the

exchanges become fast on the NMR time scale. This is, however, more clearly seen in the spectra of **1*** (and **1-Rh**).[49]

The proposed exchange process leads to the following specific site exchanges in one plane: a ⟶ b , b ⟶ a , c ⟶ e , e ⟶ c. However, since the C_5H_5 ring moves from above to below the Os_2Ir plane, the other set of carbonyls labelled b and c also exchange whereas the remaining carbonyl labelled e is unchanged. If the rate of loss of spins from site a is k sec^{-1}, then it is also k from site e, but 2k from sites b and c. Since the amount of initial line broadening is proportional to the total rate of spin loss, the resonances attributed to carbonyls b and c should broaden faster than those due to carbonyls a and e. This is seen in the spectrum at -10 °C (Figure 2.2). (Both k and 2k were used in the simulation shown in Figure 2.3.)

In $Os_3(CO)_{11}(PR_3)$ clusters merry-go-round CO-exchanges are believed to occur in the two planes that are perpendicular to the Os_3 plane and that pass through two of the metal atoms, but not through the phosphorus atom (for PR_3 in equatorial position). In a similar manner to **1** (and **1***) one carbonyl does not take part in these exchanges and the ^{13}C NMR resonance due to this carbonyl in the variable temperature ^{13}C NMR spectra of these clusters remains sharp as the other resonances collapse.[47,62]

Simulation of the spectrum of **1** at -10 °C (Figure 2.3A) gave a rate constant for the CO exchange (i.e., k) of 9 ± 1 s^{-1} which corresponds to a $\Delta G^{\neq}$ of 14.2 ± 0.3 kcal mol^{-1} for the process at -10 °C. This value may be compared to a $\Delta G^{\neq}$ of 8.4 ± 0.4 kcal mol^{-1} found for the corresponding process in **1-Rh** (at -80 °C).[49] It is generally found that the barrier to carbonyl exchange in metal cluster compounds increases on going to the metal atom lower in the periodic table; the pair of molecules **1** and **1-Rh** illustrate this effect.

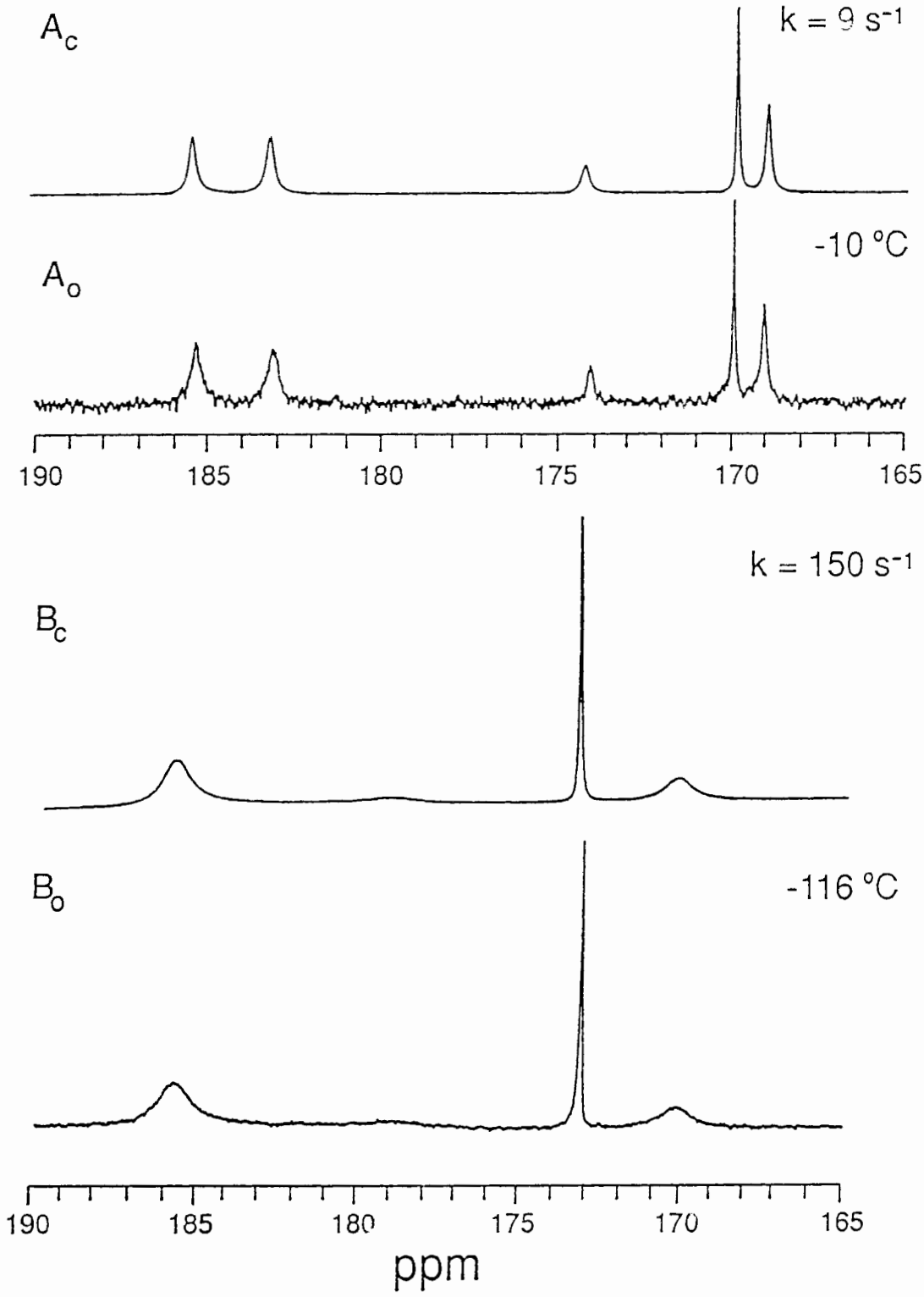

Figure 2.3 Calculated (A_c) and observed (A_o) ^{13}C NMR spectra for **1** at -10 °C; calculated (B_c) and observed (B_o) ^{13}C NMR spectra for **1*** at -116 °C.

The variable temperature ^{13}C NMR spectra of ^{13}CO-enriched **1*** in CH_2Cl_2/CD_2Cl_2 are shown in Figure 2.4. The assignment of the signals is based on similar arguments to those used in the assignment of the signals in **1**; note that the resonances attributed to the axial carbonyls on the $Os(CO)_4$ units in **1*** are degenerate.

As can be seen from Figures 2.2 and 2.4, there is a dramatic lowering of the barrier to carbonyl exchange in **1*** compared to that in **1**. Even with the sample of **1*** at -129 °C the carbonyl resonances are still somewhat broadened due to exchange. With the line width parameter used in the simulation of the spectrum of **1** (Figure 2.3A) it was possible to simulate the spectrum of **1*** at -116 °C (Figure 2.3B). This yielded a rate constant of 150 ± 15 s^{-1} which in turn gave a $\Delta G^{\neq}$ of 7.4 ± 0.2 kcal mol^{-1} for the carbonyl exchange in **1*** at -116 °C. The difference of 6.8 kcal mol^{-1} in the activation barriers to carbonyl exchange between **1** and **1*** is remarkable. A similar difference was observed in the variable temperature ^{13}C NMR spectra of **1-Rh** and **1*-Rh**.[49] The exchange of the carbonyls a, b, c, and e in **1*-Rh** at -100 °C was, however, so fast that a sharp singlet was still observed for these carbonyls. As for **1-Rh** and **1*-Rh**, the ^{13}C NMR spectra indicate that when **1** and **1*** are undergoing CO exchange at a comparable rate the temperature of the sample of **1** is some 100 degrees higher than that of the sample of **1***.

A similar, although not so dramatic, effect is observed in the barrier to carbonyl exchange in $Os_3(CO)_{11}[P(OMe)_3]$ compared to that in $Os_3(CO)_{12}$: in the phosphite derivative the barrier to the merry-go-round CO exchange in the plane that is perpendicular to the Os_3 plane and passes through the three carbonyls of the $Os(CO)_3[P(OMe)_3]$ was found to be 14.0 ± 0.4 kcal mol^{-1} at 20 °C.[47] The barrier to axial-equatorial carbonyl exchange in $Os_3(CO)_{12}$ has been estimated at 16.3 kcal mol^{-1} at 20 °C.[65] In order to rationalize these results it was reasoned

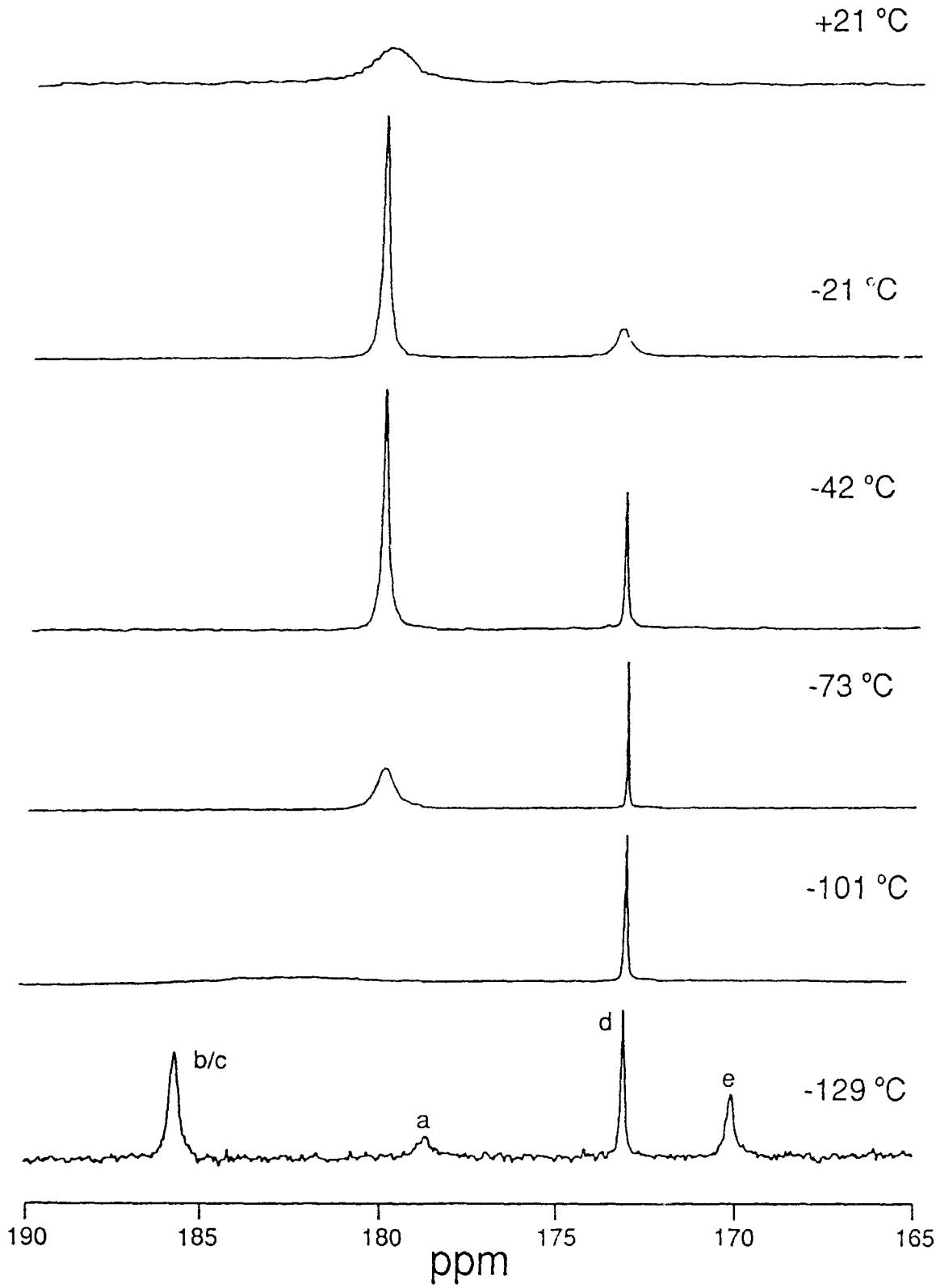

Figure 2.4 Variable-temperature ^{13}C NMR spectra of **1*** in CH_2Cl_2/CD_2Cl_2 except spectrum at -129 °C (in $CHFCl_2/CD_2Cl_2$).

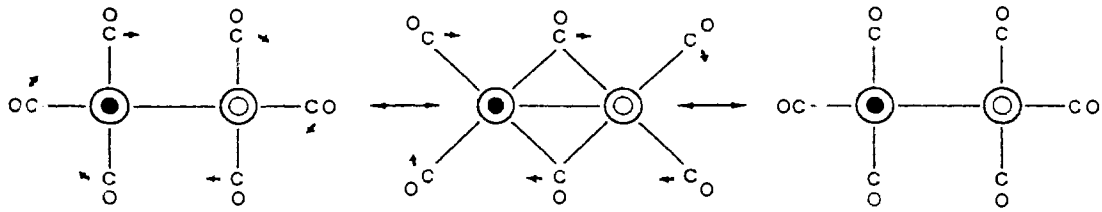

○=Os ●=P(OMe)$_3$ O=CO

that substitution of a carbonyl ligand in $Os_3(CO)_{12}$ by $P(OMe)_3$ would increase the electron density at the osmium atom where substitution had occurred, since $P(OMe)_3$ is a better donor ligand than CO. The increase in the electron density would cause expansion of the 5d orbitals on the osmium atom. This in turn could result in better overlap with the π^* orbitals of the axial carbonyls on the adjacent osmium atom and thus lower the activation energy needed to form the intermediate containing bridging carbonyls.[47]

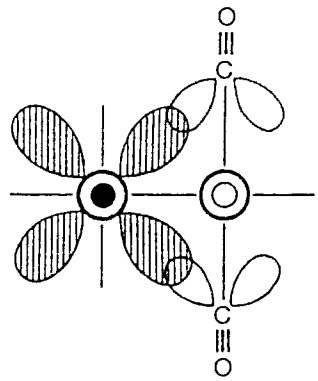

Similar arguments may be used to rationalize the much lower barrier to carbonyl exchange in **1*** compared to that in **1**.

As the temperature of **1*** was raised above -42 °C the signal assigned to the carbonyls labelled d (Chart I) broadened and collapsed to the base line as did, at a slower rate, the averaged signal due to the other carbonyls (Figure 2.4). This indicates that the carbonyls labelled d are now exchanging with the carbonyls designated a, b, c and e. Although there are several mechanisms that

can account for this behavior, the most probable is believed to be a (complete) merry-go-round CO exchange that occurs in the plane that is perpendicular to the Os_2Ir plane and passes through the two osmium atoms. As mentioned previously, this type of mechanism has been proposed to account for the CO exchange in trinuclear osmium carbonyl clusters.

It might be expected that the barrier to this exchange would be less sensitive to the third metal atom in the cluster (e.g. Rh or Ir) and to the substituents on that metal atom. Comparison of the variable temperature ^{13}C NMR spectra of **1*-Rh**[49] and **1*** shows that the temperature range for the collapse of the two signals, assigned to carbonyl d and the other carbonyls respectively, is similar for the two clusters. Comparison of the variable temperature ^{13}C NMR spectra for **1** and **1*** shows that the broadening of the signal assigned to carbonyl d in **1** occurs at about 40 - 50 °C higher than the same broadening in **1***. Thus although this CO exchange in the plane containing the two Os atoms shows some sensitivity to the substituents on the Ir atom, it is certainly less sensitive than the CO exchange in the IrOs plane (see above).

2.4 Conclusion

Trinuclear clusters of the type $(\eta^5\text{-}C_5R_5)(OC)Ir[Os(CO)_4]_2$ (R = H: **1**; R= Me: **1***) have been prepared from $Os(CO)_4(\eta^2\text{-cyclooctene})$ and $(\eta^5\text{-}C_5R_5)Ir(CO)_2$. Their spectroscopic properties in solution are similar to those of their Rh analogues.[49] In addition, the solid state structure of **1*** is similar to that of **1-Rh**.

Variable temperature ^{13}C NMR spectra of **1** and **1*** permitted the study of the carbonyl exchange processes in these clusters. Two different CO exchange processes occur; the one with the lower activation energy is believed to be the carbonyl exchange that takes place in the two vertical IrOs planes. Close to a 50% reduction in the activation barrier for this process was observed going from **1** to **1***: This reduction, which is believed to be due to a lowering of the energy of the transition state with bridging carbonyls, has been rationalized in terms of the greater electron releasing nature of C_5Me_5 compared to that of C_5H_5. In addition, the activation barrier for this CO exchange in **1** was found, as expected, to be considerably higher than that for **1-Rh**.

Concerning the ease of rotation of the $(\eta^5\text{-}C_5R_5)Ir(CO)$ unit, the ^{13}C NMR spectra showed that while the Ir unit of **1** was rigid at -48 °C, it was not possible determine this for **1*** since the ^{13}C NMR signals of the axial carbonyls of the $Os(CO)_4$ units in this cluster were degenerate.

Preliminary attempts to prepare the binary cluster $(OC)_5W[Os(CO)_4]_2$ were unsuccessful. Further investigations, however, that involve the use of $Os(CO)_4$-$(\eta^2\text{-cyclooctene})$ to rationally synthesize heterometallic clusters are warranted.

CHAPTER 3

SYNTHESIS, CARBONYL EXCHANGE, AND ISOMERIZATION IN $(\eta^5\text{-}C_5H_5)(OC)IrOs_2(CO)_7(L)$ (L = PMe_3, $P(OMe)_3$, $CNBu^t$)

3.1 Introduction

A strong impetus for the study of organometallic clusters has been the idea that clusters may serve as models for metal surface chemistry.[66] Triosmium carbonyl clusters have attracted much attention in this respect and a number of Os_3 compounds have been synthesized that contain ligands believed to be closely related to chemisorbed species. For most triosmium clusters, $Os_3(CO)_{12}$ is the starting material and hundreds of compounds have been formed by the direct reaction of organic and inorganic substrates with $Os_3(CO)_{12}$.[48b] It was therefore of interest to investigate some aspects of the chemistry of $(\eta^5\text{-}C_5R_5)(OC)Ir[Os(CO)_4]_2$ (R = H, Me), the preparation of which was described in Chapter 2. These clusters are related to $Os_3(CO)_{12}$ by the replacement of an $Os(CO)_4$ unit with the formally isolobal $(\eta^5\text{-}C_5R_5)Ir(CO)$ unit.

In this chapter the decarbonylation of $(\eta^5\text{-}C_5H_5)(OC)Ir[Os(CO)_4]_2$ by Me_3NO is described. From the resultant product, monosubstituted clusters were subsequently prepared by adding two electron donor ligands such as PMe_3, $P(OMe)_3$, and $CNBu^t$. Like the unsubstituted parent cluster, these three substituted clusters were found to undergo CO exchange. Also reported in this chapter is a study of this CO exchange to determine and compare the activation energy barriers of this exchange for the different clusters. The two dimensional NMR technique, NOESY, was used in an effort to obtain more information on the carbonyl exchange mechanism in one of the substituted clusters and to confirm the structure of the major isomer.

3.2 Experimental

Unless otherwise noted, manipulations of starting materials and products were carried out under a nitrogen atmosphere with the use of standard Schlenk techniques. The cluster $(\eta^5\text{-}C_5H_5)(OC)Ir[Os(CO)_4]_2$ was prepared as described in Chapter 2. Hexane and toluene were distilled over potassium while dichloromethane was distilled over P_2O_5. The phosphorus ligands and the *tert*-butyl isocyanide were obtained commercially. The Me_3NO was obtained commercially as the dihydrate and was sublimed before use.

Infrared spectra were recorded on a Perkin-Elmer 983 spectrometer; the internal calibration of the instrument was checked against the known absorption frequencies of gaseous CO. The room temperature ^1H NMR spectra were recorded on a Bruker SY-100 NMR spectrometer. The variable temperature NMR spectra and the NOESY spectrum were obtained with a Bruker WM400 NMR spectrometer (operating frequencies: 100.6 MHz for ^{13}C, 162 MHz for ^{31}P, and 400 MHz for ^1H). The ^{13}C NMR spectra were obtained on ^{13}CO-enriched samples (~30% ^{13}C). These samples were prepared from ^{13}CO-enriched $(\eta^5\text{-}C_5H_5)(OC)Ir[Os(CO)_4]_2$, the synthesis of which is described in Chapter 2. The NMR lineshape simulations shown in Figures 3.9, 3.11, and 3.13 were carried out by the use of the DNMR3 computer program of Kleier and Binsch.[67] The electron impact (70 eV) mass spectra were obtained with a Hewlett-Packard 5985 GC-MS instrument; the pattern of the ions at highest mass in each spectrum matched that calculated for the parent ion of the compound in question. Microanalyses were performed by M.K. Yang of the Microanalytical Laboratory of Simon Fraser University.

The NOESY spectrum was acquired with a relaxation delay of 3 s, an incremental evolution period of 0.14 ms, and a mixing period of 1 s. 128

experiments of 48 scans each were recorded with a sweep width of 3620 Hz in both F_1 and F_2.

Preparation of $(\eta^5\text{-}C_5H_5)(OC)IrOs_2(CO)_7(L)$ (L = PMe_3, $P(OMe)_3$, $CNBu^t$). A round-bottom flask (~80 mL capacity) fitted with a Teflon valve was charged with $(\eta^5\text{-}C_5H_5)(OC)Ir[Os(CO)_4]_2$ (50 mg, 0.056 mmol), CH_2Cl_2 (25 mL) and MeCN (~0.5 mL). A solution of Me_3NO in methanol was added dropwise until all the $(\eta^5\text{-}C_5H_5)(OC)Ir[Os(CO)_4]_2$ had been consumed (the progress of the reaction was monitored by the disappearance of the band at 2059 cm^{-1} in the infrared spectrum of the solution). The solution was evacuated to dryness leaving a dark red residue that presumably contained $(\eta^5\text{-}C_5H_5)IrOs_2(CO)_8(NCMe)$. The final step in the synthesis and the subsequent isolation of the substituted clusters will be discussed individually for each of the three derivatives.

$(\eta^5\text{-}C_5H_5)(OC)IrOs_2(CO)_7(PMe_3)$ (**1**): The residue thought to contain $(\eta^5\text{-}C_5H_5)IrOs_2(CO)_8(NCMe)$ was suspended in toluene (20 mL) and a solution of PMe_3 (6 μL, 0.058 mmol) in toluene (2 mL) was added. (The latter step was performed in a dry box.) The reaction solution was stirred at room temperature overnight after which the solvent was removed under vacuum. The residue was chromatographed on silica gel (15 x 1 cm). Elution with hexane gave a pale red band of unreacted $(\eta^5\text{-}C_5H_5)(OC)Ir[Os(CO)_4]_2$. Elution with hexane/$CH_2Cl_2$ (10/1) gave a bright red band of the desired product. The solvent was removed under vacuum to give $(\eta^5\text{-}C_5H_5)(OC)IrOs_2(CO)_7(PMe_3)$ (18 mg, 35%). The analytical sample was recrystallized from hexane/CH_2Cl_2 to give dark red, air-stable crystals: IR (hexane) ν(CO) 2085 (m), 2024 (s), 1993 (vs), 1975 (s), 1962 (m), 1950 (m), 1932 (w) cm^{-1}; MS (EI) *m/z* 940 (M^+); ^1H NMR ($CDCl_3$, -5 °C) major isomer δ 5.28 (s), 1.85 (d, J_{PH} = 10.2 Hz); minor isomer δ 5.38 (s), 1.80 (d, J_{PH} = 10.0 Hz); isomer ratio major:minor, 3.5:1; $^{31}P\{^1H\}$ NMR ($C_6D_5CD_3$, -50 °C) major isomer δ -57.0; minor isomer δ -58.5; ^{13}C NMR (CD_2Cl_2, CO region, -70 °C)

major isomer δ 196.3 (J_{PC} = 8.1 Hz), 193.9 (J_{PC} = 8.9 Hz), 186.7 (J_{CC} = 37.0 Hz), 185.3 (J_{CC} = 37.7 Hz), 176.2, 176.1, 172.2, 171.4; minor isomer δ 195.3 (J_{PC} = 8.8 Hz), 187.6, 186.1, 177.1, 175.5, 175.3, 170.3 (A low field doublet is believed to be obscured by the signals of the major isomer). Anal. Calcd for $C_{16}H_{14}IrO_8Os_2P$: C , 20.55; H, 1.57. Found: C, 20.51; H, 1.42.

(η^5-C_5H_5)(OC)$IrOs_2(CO)_7$[$P(OMe)_3$] (**2**): The synthesis of **2** was similar to that of **1** except $P(OMe)_3$ (7 μL, 0.056 mmol) replaced PMe_3. The reaction residue was chromatographed on silica gel (15 x 1 cm). Elution with hexane gave a pale red band of unreacted (η^5-C_5H_5)(OC)Ir[$Os(CO)_4$]$_2$ followed by a yellow band. Elution with hexane/CH_2Cl_2 (10:1) gave a bright red band of the desired product followed closely by a pale yellow band. The solvent was removed under vacuum to give (η^5-C_5H_5)(OC)$IrOs_2(CO)_7$[$P(OMe)_3$] (18 mg, 33%). The analytical sample was recrystallized from hexane/CH_2Cl_2 to give dark red, air-stable crystals: IR (hexane) ν(CO) 2090 (m), 2035 (s), 2012 (s), 1998 (vs), 1982 (s), 1970 (sh), 1944 (sh), 1939 (w) cm^{-1}; MS (EI) *m/z* 988 (M^+); ^1H NMR ($CDCl_3$, -20 °C) major isomer δ 5.32 (s), 3.61 (d, J_{PH} = 12.5 Hz); minor isomer δ 5.39 (s), 3.58 (d, J_{PH} = 13.6 Hz); isomer ratio major:minor 3.1:1; ^{31}P {^1H} NMR ($C_6D_5CD_3$, -50 °C) major isomer δ 99.3; minor isomer δ 97.9; ^{13}C NMR (CD_2Cl_2/CH_2Cl_2, 1/4; CO region, -50 °C) major isomer δ 190.9 (J_{PC} = 12.5 Hz), 190.1 (J_{PC} = 12.4 Hz), 186.4 (J_{CC} = 37.2 Hz), 184.4 (J_{CC} = 35.9 Hz), 175.5, 173.3, 171.3, 170.5; minor isomer δ 191.8 (J_{PC} = 11.2 Hz), 187.3, 185.4, 175.0, 174.8, 172.0, 169.7 (a low field doublet is believed to be obscured by signals of the major isomer). Anal. Calcd for $C_{16}H_{14}IrO_{11}Os_2P$: C, 19.49; H, 1.43. Found: C, 19.65; H, 1.46.

(η^5-C_5H_5)(OC)$IrOs_2(CO)_7$($CNBu^t$) (**3**): The synthesis of **3** was similar to that of **1** and **2** except $CNBu^t$ (6 μL, 0.063 mmol) was added in place of the phosphorus ligand. The reaction residue was chromatographed on silica gel

(15 x 1 cm). Elution with hexane gave a pale red band of unreacted $(\eta^5\text{-}C_5H_5)(OC)Ir[Os(CO)_4]_2$. Further elution with hexane gave a bright yellow band followed closely by a red band of the desired product. The solvent was removed under vacuum to give $(\eta^5\text{-}C_5H_5)(OC)IrOs_2(CO)_7(CNBu^t)$ (20 mg, 38%). The analytical sample was recrystallized from hexane/CH_2Cl_2 to give dark red, air-stable crystals: IR (hexane) ν(CN) 2182 (m,br); ν(CO) 2076 (m), 2032 (vs), 1995 (vs), 1979 (s), 1962 (m), 1948 (sh), 1936 (m) cm^{-1}; MS (EI) *m/z* 945 (M^+); ^1H NMR (CD_2Cl_2, -90 °C) major isomer δ 5.38 (s), 1.43 (s); minor isomer δ 5.32 (s), 1.51 (s); isomer ratio major:minor 9:1; ^{13}C NMR (CD_2Cl_2/CH_2Cl_2, 1/4; CO region, -80 °C) major isomer δ 187.4 (1, J_{CC} = 38 Hz), 186.5 (1), 185.3 (1, J_{CC} = 36 Hz), 175.6 (1), 172.9 (1), 172.7 (1), 171.9 (2); minor isomer δ 187.6, 185.5, 184.9, 172.4, 172.3, 171.7 (two signals were not observed). Anal. Calcd for $C_{18}H_{14}IrNO_8Os_2$: C, 22.88; H, 1.49; N, 1.48. Found: C, 23.10; H, 1.43; N, 1.36.

3.3 Results and Discussion

The clusters $(\eta^5\text{-}C_5H_5)(OC)IrOs_2(CO)_7(L)$ (L = PMe_3, **1**; L = $P(OMe)_3$, **2**; L = $CNBu^t$, **3**) were prepared in a two step process (eq 1):

$$(\eta^5\text{-}C_5H_5)(OC)Ir[Os(CO)_4]_2 \xrightarrow[2.\ L]{1.\ Me_3NO,\ MeCN} (\eta^5\text{-}C_5H_5)(OC)IrOs_2(CO)_7(L) \qquad (1)$$

(L = PMe_3, **1**; L = $P(OMe)_3$, **2**; L = $CNBu^t$, **3**)

In the initial step, $(\eta^5\text{-}C_5H_5)(OC)Ir[Os(CO)_4]_2$ in dichloromethane reacted with trimethylamine oxide in methanol in the presence of a small amount of acetonitrile. In the second step, the residue from the first step was suspended in toluene and a stoichiometric amount of ligand L was added. The residue was believed to contain $(\eta^5\text{-}C_5H_5)IrOs_2(CO)_8(NCMe)$, analogous to $Os_3(CO)_{11}(NCMe)$ formed under similar conditions by the reaction of Me_3NO with $Os_3(CO)_{12}$.[68] The residue was, however, not characterized. The cluster products **1**-**3** were isolated after chromatography in yields ranging from 33 to 38%.

Like the parent compound $(\eta^5\text{-}C_5H_5)(OC)Ir[Os(CO)_4]_2$, the substituted derivatives are deep red, air-stable crystalline solids. There is no evidence in the carbonyl region of the infrared spectra for bridging carbonyls.

Carbonyl Exchange in 1. The carbonyl region of the variable temperature ^{13}C NMR spectra of ^{13}CO-enriched **1** in CH_2Cl_2/CD_2Cl_2 is shown in Figure 3.1. The spectrum of **1** at -70 °C, shown in Figure 3.2, exhibits signals consistent with the presence of two isomers. In total, there are eight signals of intensity one assigned to the major isomer of **1** and seven signals attributed to a minor isomer.

Consideration of the spectrum of **1** at -70 °C (Figure 3.2) allows one to reduce the number of possible isomers that could give rise to the NMR

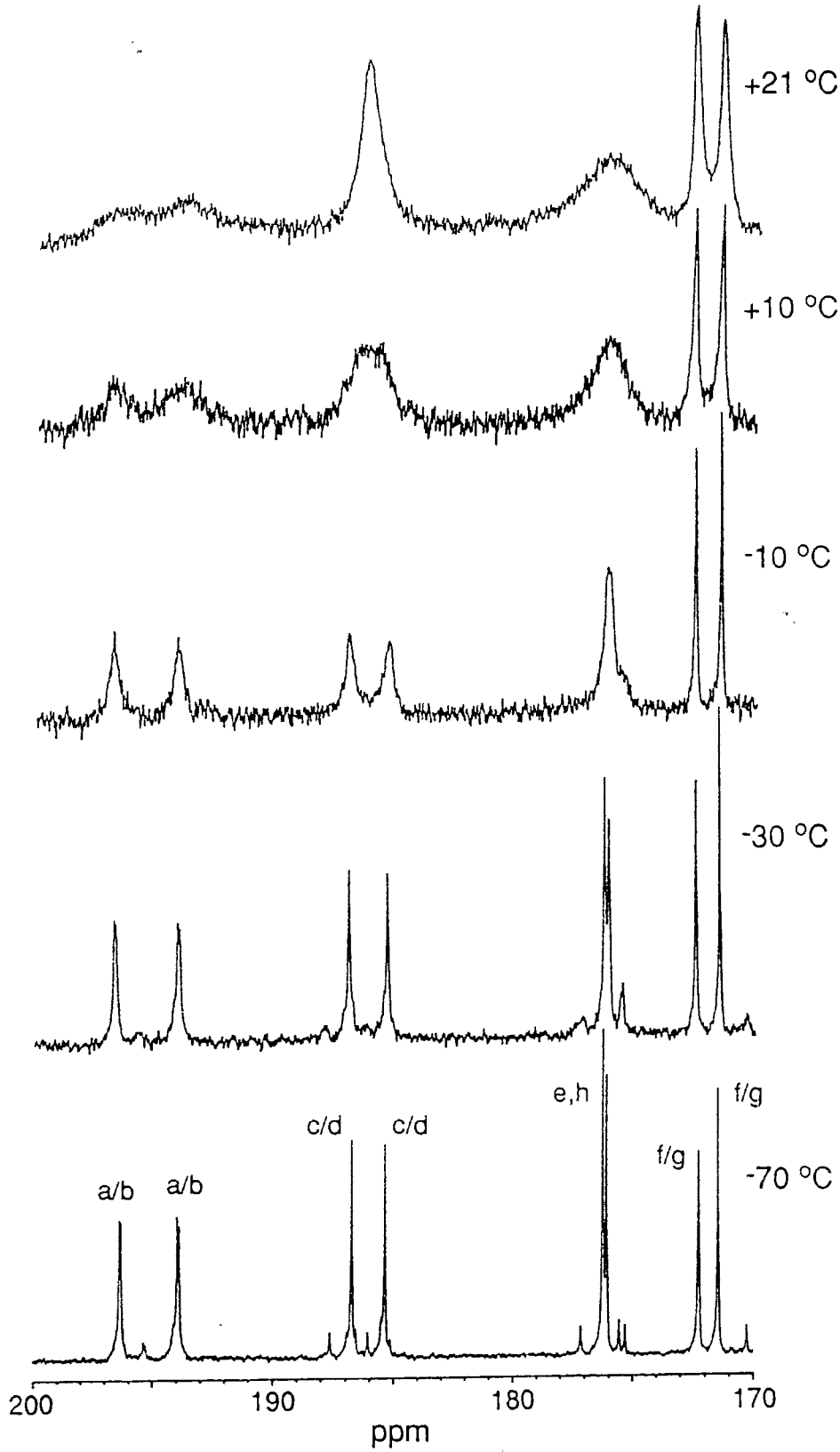

Figure 3.1 Variable temperature ^{13}C NMR spectra of **1** in CH_2Cl_2/CD_2Cl_2.

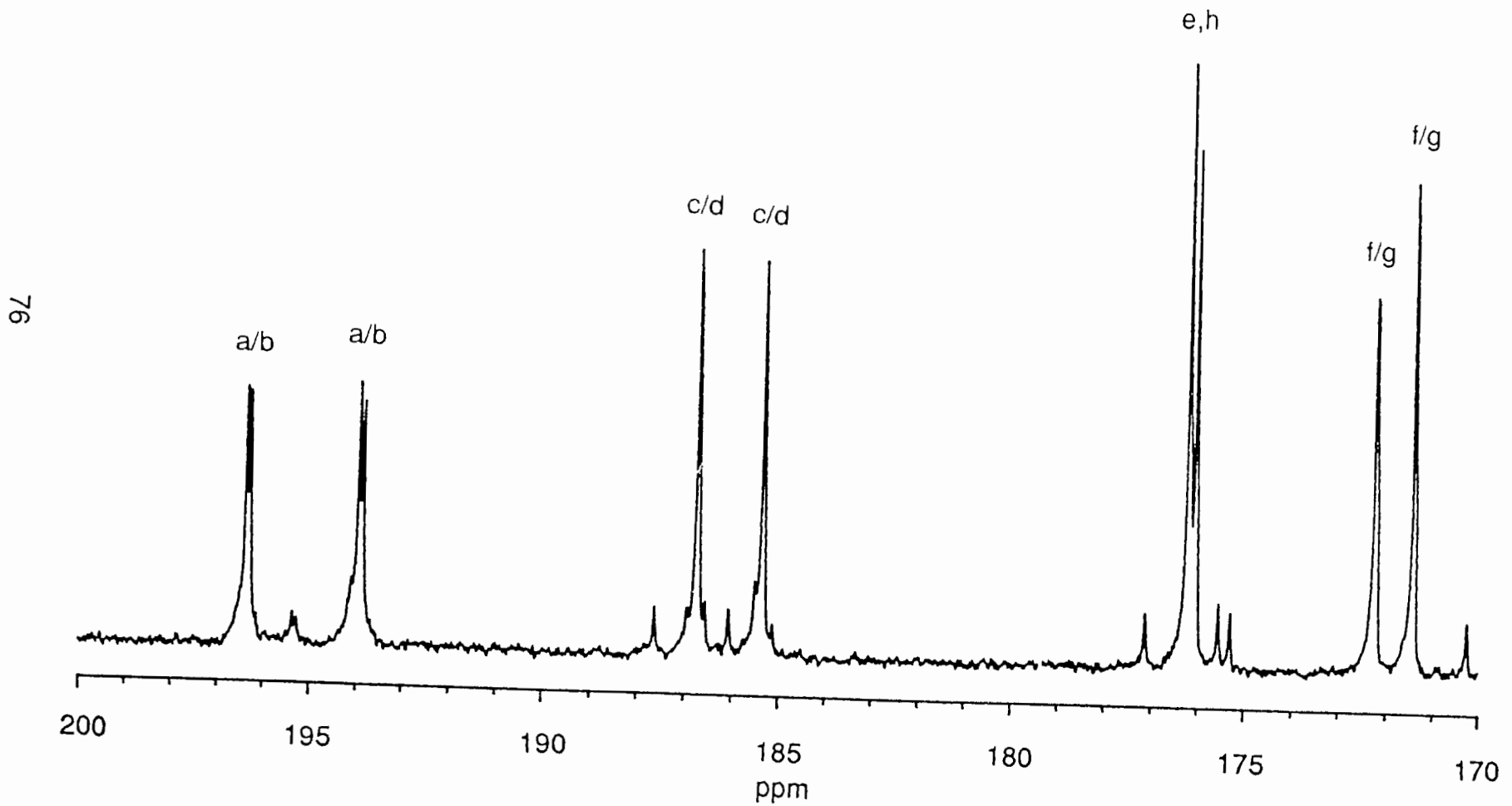

Figure 3.2 ^{13}C NMR spectrum of **1** at -70 °C in CH_2Cl_2/CD_2Cl_2.

resonances. The following discussion will focus on the signals due to the major isomer. Firstly, the presence of ^{31}P coupling to the two low field signals indicates that the phosphine ligand must be bound to an osmium atom. In addition, the ^{13}C NMR spectrum of $(\eta^5\text{-}C_5H_5)(Me_3P)Ir[Os(CO)_4]_2$ (i.e., the phosphine ligand bound to the iridium) would be expected to have only four carbonyl signals each of equal intensity . Secondly, bulky ligands such as phosphines invariably adopt the less sterically hindered equatorial sites in trinuclear clusters.[69] Further evidence that the phosphine does not adopt an axial site in **1** is that $^{31}P\text{-}^{13}C$ coupling is found for two signals (at δ 196.3 and 193.9) attributed to axial CO's. (In saturated trinuclear clusters of osmium, signals due to axial carbonyls invariably come to low field of those due to the equatorial carbonyls.[47,57,58]) If the PR_3 did adopt an axial site on an osmium atom, only one axial signal would be expected to have $^{31}P\text{-}^{13}C$ coupling. On this basis, it can be concluded that the major isomer of **1** has the phosphine bound in an equatorial site on one of the osmium atoms.

Thus the number of possible structures for the major isomer of **1** is narrowed to two: one in which the PR_3 is trans to the IrOs bond and one in which the phosphine is trans to the OsOs bond. These are shown in Chart 1 as A and B with L = PMe_3. (It will be assumed that the geometry around the iridium atom in **1** is similar to that found in Chapter 2 for $(\eta^5\text{-}C_5Me_5)(OC)Ir[Os(CO)_4]_2$ in that the carbonyl ligand on the iridium atom occupies an axial site.) It should be noted that when the L ligand is in an equatorial site, the position of the C_5H_5 ring (whether above or below the Os_2Ir plane) is not important with respect to the number of isomers detected. This is because the different isomers resulting from the change in position of the C_5H_5 ring would be mirror images of each other and therefore would not be detected by the NMR technique.

CHART 1

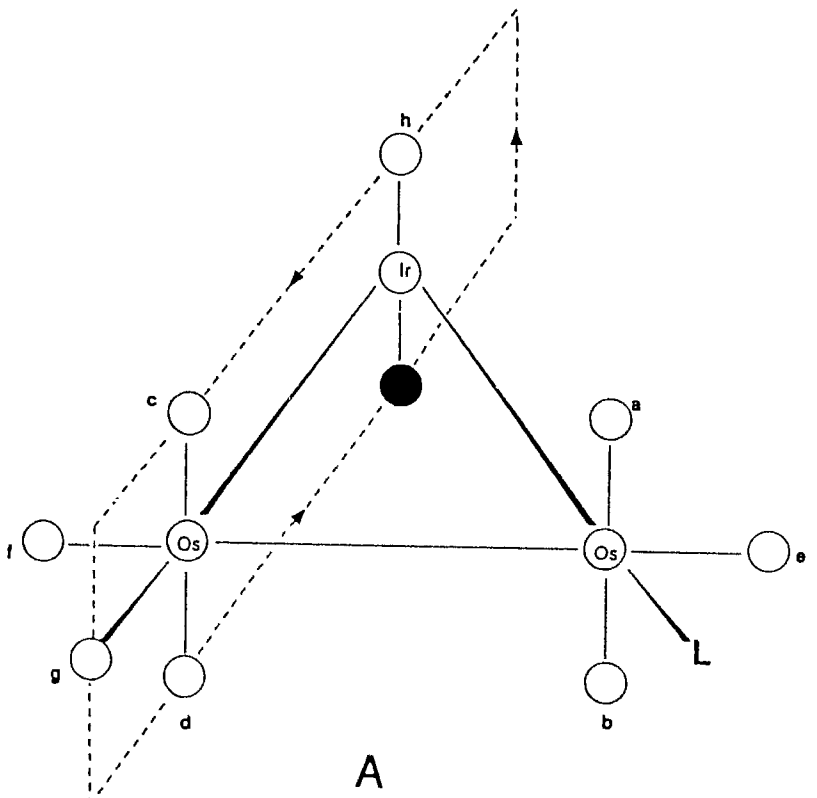

A

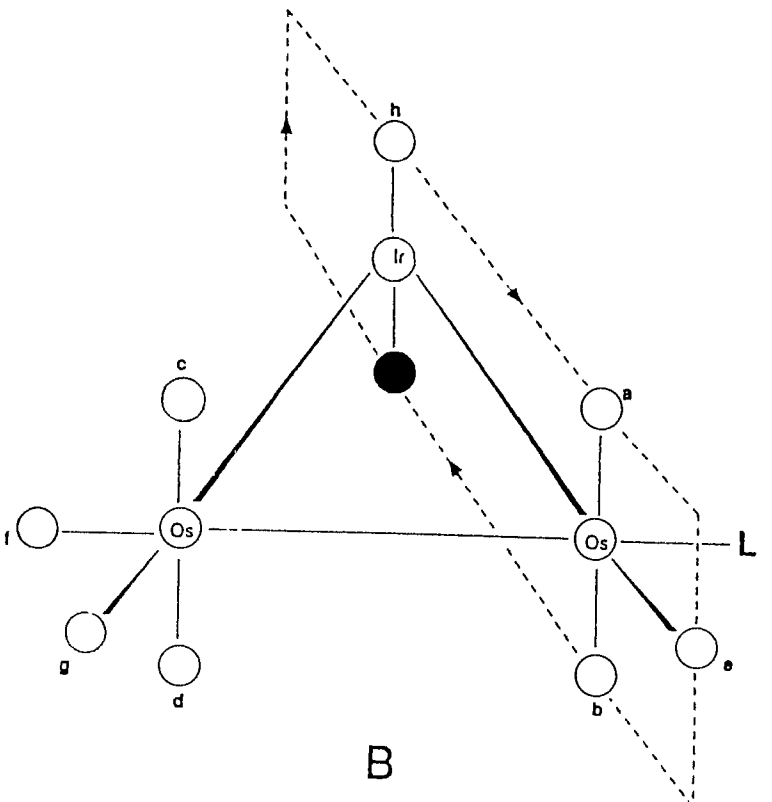

B

L = PMe_3, $P(OMe)_3$

○ = CO

● = C_5H_5

From the CO exchange discussed in detail below, it is believed that the major isomer in solution is B. The basis for the assignment of the signals would, however, be similar if A were the major isomer.

The assignment of the resonances shown in Figure 3.2 and Chart 1 is based on the following arguments. The four signals between δ 200 and 185 are attributed to the four axial carbonyls on the osmium atoms in **1** (see above). In particular, the two signals at δ 196.3 and 193.9 are doublets due to ^{31}P-^{13}C coupling and thus are assigned to carbonyls a and b . Likewise, the signals at δ 186.7 and 185.5 that exhibit ^{13}C-^{13}C coupling as expected for a trans arrangement of two carbonyls that are chemically different[59] are assigned to the axial carbonyls c and d. It is not surprising that the signals assigned to carbonyls a and b occur at a lower field than those assigned to carbonyls c and d since it has been observed that substitution of a carbonyl ligand in an $Os(CO)_4$ unit of a cluster by a phosphorus ligand causes a downfield shift of the resonances of the remaining carbonyls.[47,61,70]

The four remaining signals which occur between δ 177 and 171 (Figure 3.2) are attributed to the three equatorial carbonyls on the osmium atoms and the carbonyl on the iridium atom and can be tentatively assigned upon comparison of the spectrum with the analogous ^{13}C NMR spectrum of the parent compound, $(\eta^5\text{-}C_5H_5)(OC)Ir[Os(CO)_4]_2$ at -48 °C (Figure 2.2, Chapter 2). In the latter spectrum, the two high field signals are assigned to the equatorial carbonyls of the osmium atoms in $(\eta^5\text{-}C_5H_5)(OC)Ir[Os(CO)_4]_2$. On this basis the two high field signals at δ 172.2 and 171.4 in Figure 3.2 are tentatively assigned to the equatorial carbonyls of the $Os(CO)_4$ unit (carbonyls f and g) in **1**. The signals are in the region expected for equatorial carbonyls of $Os(CO)_4$ groupings in trinuclear clusters.[47,47,58] Since substitution by a phosphorus ligand on an $Os(CO)_4$ unit shifts the ^{13}C resonance of the carbonyl to lower field (see above),

one of the pair of signals at δ 176.2 and 176.1 is tentatively assigned to carbonyl e. Finally, one of these signals is tentatively assigned to the carbonyl on iridium (carbonyl h); it appears in the region associated with carbonyl ligands bound to iridium.[57]

The presence of two signals for the axial carbonyls on both the $Os(CO)_4$ and the $Os(CO)_3(PMe_3)$ units (Figure 3.2) indicates that the $Ir(\eta^5\text{-}C_5H_5)(CO)$ unit of **1** is rigid at -70 °C. Similar behavior was found for the parent compound, $(\eta^5\text{-}C_5H_5)(OC)Ir[Os(CO)_4]_2$ (Figure 2.2, Chapter 2). As with the parent cluster, it is impossible to determine whether the Ir unit in **1** rotates relative to the $Os_2(CO)_7(L)$ moiety at higher temperatures (see below). It should be noted that rotation of the Ir unit alone cannot account for all the changes in the ^{13}C NMR spectra of **1** (Figure 3.1). Such a rotation would require the signal assigned to carbonyl e to remain sharp with an increase in temperature. This is not the case as is seen in Figure 3.1.

The variable temperature ^{13}C NMR spectra (Figure 3.1) can be used to determine whether the major isomer of **1** has structure A or B (Chart 1) in solution. On warming the sample to -10 °C, six of the carbonyl resonances begin to collapse leaving two sharp signals at high field. This behavior is interpreted in terms of a partial merry-go-round CO exchange in those planes that are perpendicular to the Os_2Ir plane and that pass through the iridium and one of the osmium atoms. These exchange processes are illustrated for A and B in Chart 1. According to this mechanism, the C_5H_5 group in **1** will rock back and forth between axial sites on the iridium atom. A similar partial merry-go-round exchange was proposed for the parent compound $(\eta^5\text{-}C_5H_5)(OC)Ir\text{-}[Os(CO)_4]_2$ as discussed in Chapter 2.

For structure A, this exchange process leads to the following specific site interconversions: c ⟶ g, g ⟶ c, d ⟶ h, h ⟶ d. However, since the Cp ring moves from above to below the Os_2Ir plane, the carbonyls labelled a and b would also become magnetically equivalent. In this mechanism, the carbonyls labelled e and f remain static and the two signals attributed to these carbonyls would remain sharp even as the exchange process becomes fast on the NMR time scale. The presence of the PMe_3 ligand prevents CO exchange in the other IrOs plane. Similar behavior has been noted in $Os_3(CO)_{10}(PEt_3)_2$ where the phosphines prevent CO exchange in the vertical planes containing two osmium atoms and a phosphine ligand.[61] Such an exchange if it occurred would require the phosphine ligand to enter an axial site and this would be prevented by steric interactions with the neighboring axial CO ligands.

For isomer B, the CO exchange leads to the following site interconversions: a ⟶ e, e ⟶ a, b ⟶ h, h ⟶ b. Movement of the Cp ring across the Os_2Ir plane would also cause carbonyls c and d to become magnetically equivalent. In this mechanism, carbonyls f and g remain static, and the two signals attributed to them would therefore remain sharp as the exchange became fast.

There is also a possibility of having exchange in the other IrOs plane of isomer B, but this mechanism gives rise to the same specific site exchanges as outlined for isomer A and thus this process would not be distinguishable from that for isomer A. In addition, for isomer B, the exchange would more likely occur in IrOs plane that contained the $Os(CO)_3(PMe_3)$ unit, since phosphorus donor ligands are known to lower the barrier to carbonyl exchange (see below).[47,71]

The variable temperature ^{13}C NMR spectra (Figure 3.1) are more consistent with the major isomer of **1** having structure B in solution. Firstly, the signals assigned to carbonyls f and g are sharp to -10 °C. Secondly, the spectra at +10 and +21 °C show the closely separated signals assigned to carbonyls c and d coalescing to a singlet at δ 186; this is consistent with exchange between these two carbonyls. This would not be expected for isomer A. In addition, the signals assigned to carbonyls a, b, e and h continue to collapse into the base line in the spectrum at +21 °C as one would expect for the coalescence of widely separated signals of isomer B. Further evidence to support this conclusion is found in the two dimensional NOESY spectrum of **1** at -30 °C (see below).

Due to the low intensity of the signals due to the minor isomer and the observation of only seven of the expected eight signals, the structure of the minor isomer of **1** in solution could not be unambiguously determined. However, the spectrum at -70 °C (Figure 3.2) is consistent with the minor isomer having Structure A (Chart 1). Firstly, there are four high field signals that can be attributed to carbonyls e, f, g and h. Secondly, the signals at δ 187.6 and 186.1 can be attributed to carbonyls c and d of the $Os(CO)_4$ unit. Lastly, the low field doublet at δ 195.3 can be attributed to either carbonyl a or b. The doublet due to the other carbonyl of the $Os(CO)_3(PMe_3)$ unit is believed to be obscured by signals of the major isomer.

From the chemical shift separation of the ^{13}C resonances assigned to carbonyls c and d, $\Delta G^{\neq}$ for the barrier to CO exchange in the IrOs plane was calculated to be 13.2 ± 0.3 kcal mol^{-1} for **1** at the coalescence temperature (about 10 °C). This value may be compared to a $\Delta G^{\neq}$ of 14.2 ± 0.3 kcal mol^{-1} for the unsubstituted parent cluster, $(\eta^5\text{-}C_5H_5)(OC)Ir[Os(CO)_4]_2$ (Chapter 2). This lowering of the energy barrier for carbonyl exchange is attributed to an electronic effect of the PMe_3 ligand. Replacement of a carbonyl by the better σ-donor

phosphine causes an increase in electron density on the osmium center and a subsequent expansion of its 5d orbitals. This in turn results in better overlap of the 5d orbitals with axial carbonyls on adjacent metal atoms, as shown on page 66 of this thesis, and should lower the activation barrier to formation of the intermediate with bridging carbonyls.[47] For example, $Os_3(CO)_{11}(PEt_3)$ was found to have a lower barrier to axial-equatorial exchange than $Os_3(CO)_{12}$.[61,71]

In addition to the previously mentioned collapse of six low field signals, a broadening of the two high field signals at δ 172 and 171 is apparent in the spectra of **1** at +10 and +21 °C. This is believed to be due to the onset of isomerization between the major and minor isomers of **1** (see below). It is concluded from the spectra shown in Figure 3.1 that the CO exchange process in **1** has a lower activation barrier than does the isomerization process. (The isomerization may cause some line broadening to occur in the spectrum at +10 °C, but if it is assumed that the minor isomer of **1** has structure A, then isomerization cannot result in the coalescence of the resonances assigned to carbonyls c and d.)

In addition to the one dimensional ^{13}C NMR spectra, a two dimensional NOE (NOESY) ^{13}C spectrum of **1** at -30 °C (Figure 3.3) was obtained. (The conventional one dimensional spectrum and the carbonyl assignments are reproduced at the top of Figure 3.3.) NOESY experiments involving the ^1H, ^{13}C and ^{31}P nuclei have been used to examine the chemical exchange mechanisms of organometallic complexes.[36a,72,73] For example, an analysis of the carbonyl scrambling in $Os_3(\mu\text{-}H)_2(CO)_{10}$ has been performed from a ^{13}C NOESY experiment.[73b] As well, strong evidence that the exchange pathway between two isomers of $Cr(CO)_2(CS)[P(OMe)_3]_3$ involves a trigonal twist mechanism was provided by a ^{31}P NOESY experiment.[36a] A detailed background of NOESY

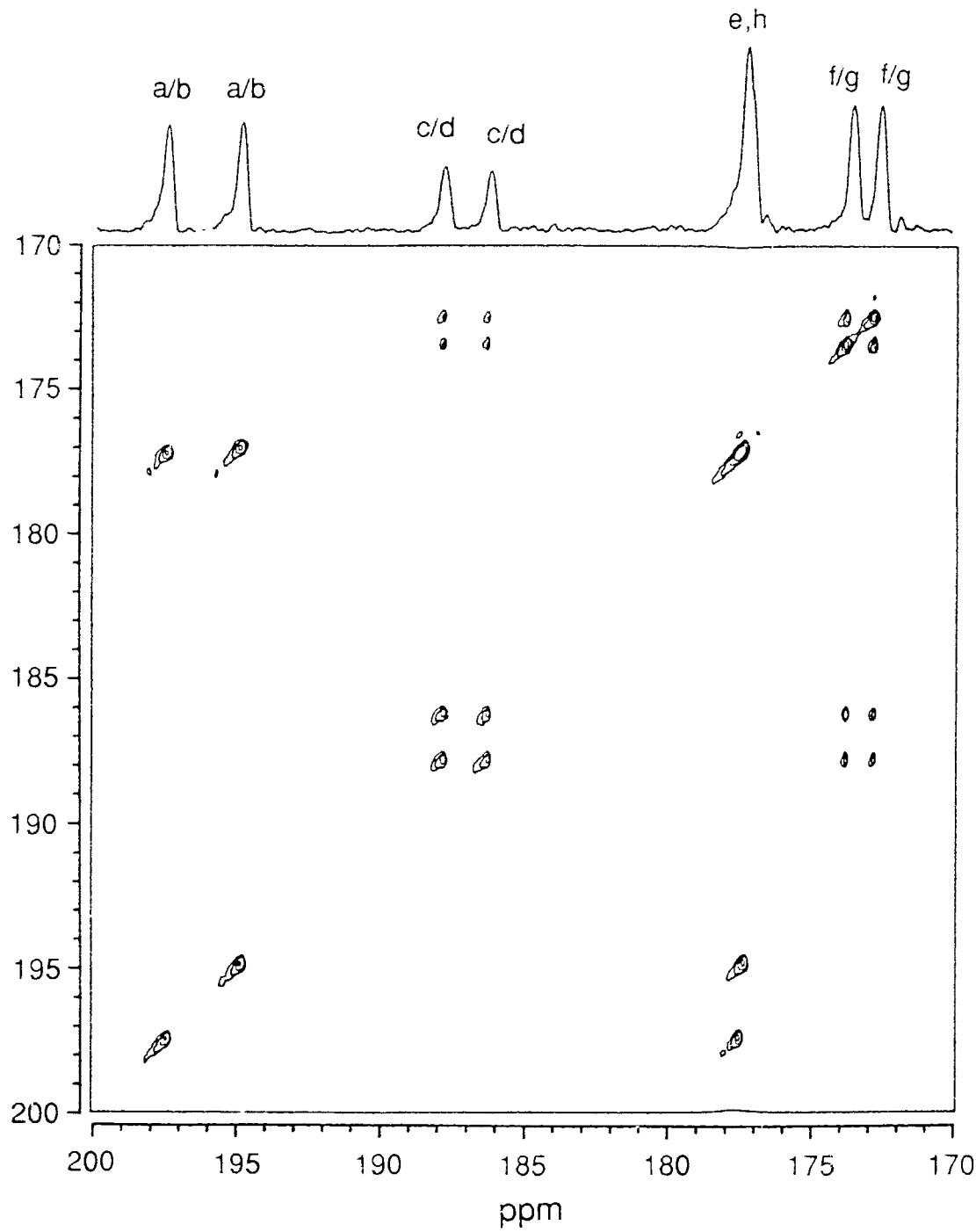

Figure 3.3 ^{13}C NOESY spectrum for **1** in CH_2Cl_2/CD_2Cl_2 at -30 °C.

spectroscopy will not be presented here. Such a treatment can be found in a number of sources.[74]

The NOESY spectrum of **1** was obtained, in order to assist in the assignment of the resonances found in the one dimensional spectrum. It was also hoped that the NOESY spectrum would show which carbonyls were exchanging with each other and in this way support the proposed mechanism for the exchange. Since the structure of the major isomer of **1** can be deduced from the variable temperature ^{13}C NMR spectra alone, the NOESY spectrum will be used only to confirm the exchange mechanism proposed for the major isomer of **1** (Chart 1). This two dimensional spectrum was carried out at -30 °C since this was the temperature at which exchange began to cause broadening of the signals in the one dimensional spectrum. (The spectrum at -50 °C, which is not shown in Figure 3.1, is similar in appearance to that at -70 °C.)

In general, the off-diagonal cross peaks in a NOESY spectrum are due to one of two effects: namely, chemical exchange or the nuclear Overhauser effect (NOE). As proposed earlier, the two possible structures for the major isomers of **1**, structures A and B, have different CO exchange mechanisms and therefore should show different cross peaks. For structure A, the NOESY spectrum would be expected to show cross peaks due to exchange between carbonyls a and b, and between carbonyls d and h. On the other hand, a major isomer of **1** with structure B would be expected to show cross peaks due to exchange between carbonyls c and d, between carbonyls a and e , and between carbonyls b and h. The NOESY spectrum has cross peaks consistent with the earlier conclusion that the major isomer of **1** has structure B and that the CO exchange is as shown in Chart 1 for B.

There are off-diagonal peaks that cannot be accounted for by the exchange mechanism for isomer B. For example, there are off-diagonal peaks

between resonances assigned to carbonyls f and g, c and f, c and g, d and f, and d and g. These cross peaks are thought to be due to ^{13}C-^{13}C NOE interactions. Since the signals attributed to carbonyls f and g remain fairly sharp up to +10 °C, these two carbonyls must not be involved in any CO exchange process at -30 °C. Thus according to this interpretation, there are NOE's occurring between the carbon atoms of the two equatorial carbonyls and between those of the axial and equatorial carbonyls of the $Os(CO)_4$ unit. The observation of an NOE is not unexpected since these carbonyls are fairly close in space (~2.8 Å) and from the level of ^{13}CO enrichment used (~30 %), roughly one fifth of the clusters are estimated to have ^{13}C atoms in these sites.

Carbonyl Exchange in 2. Variable temperature ^{13}C NMR spectra in the carbonyl region of ^{13}CO enriched $(\eta^5\text{-}C_5H_5)(OC)IrOs(CO)_7[P(OMe)_3]$ (**2**) are shown in Figure 3.4. The spectrum of **2** at -50 °C is shown in Figure 3.5. Not surprisingly, many features of the low temperature limiting ^{13}C NMR spectrum of the phosphine derivative (Figure 3.2) are also found in that of the phosphite analogue (Figure 3.5).

The deduction of the structure of the major isomer of **2** in solution follows the same reasoning as outlined for **1**. In short, the presence of ^{31}P-^{13}C coupling exhibited by the two low field signals in the spectrum at -50 °C (Figure 3.5) indicates that the relatively bulky phosphite ligand is bound in an equatorial site on an osmium atom in **2**. Therefore, as for **1**, there are two possible structures for the major isomer of **2**. These are shown in Chart 1 (L = $P(OMe)_3$). The resonance assignments for **2** shown in Figure 3.5 are based on the same arguments as discussed for **1**. The four signals between δ 195 and 180 are attributed to the four axial osmium carbonyls of **2**. The two doublets at δ 190.9 and 190.1 are assigned to the axial carbonyls of the $Os(CO)_3[P(OMe)_3]$ unit. The singlets at δ 186.4 and 184.4 that exhibit ^{13}C-^{13}C coupling are assigned to

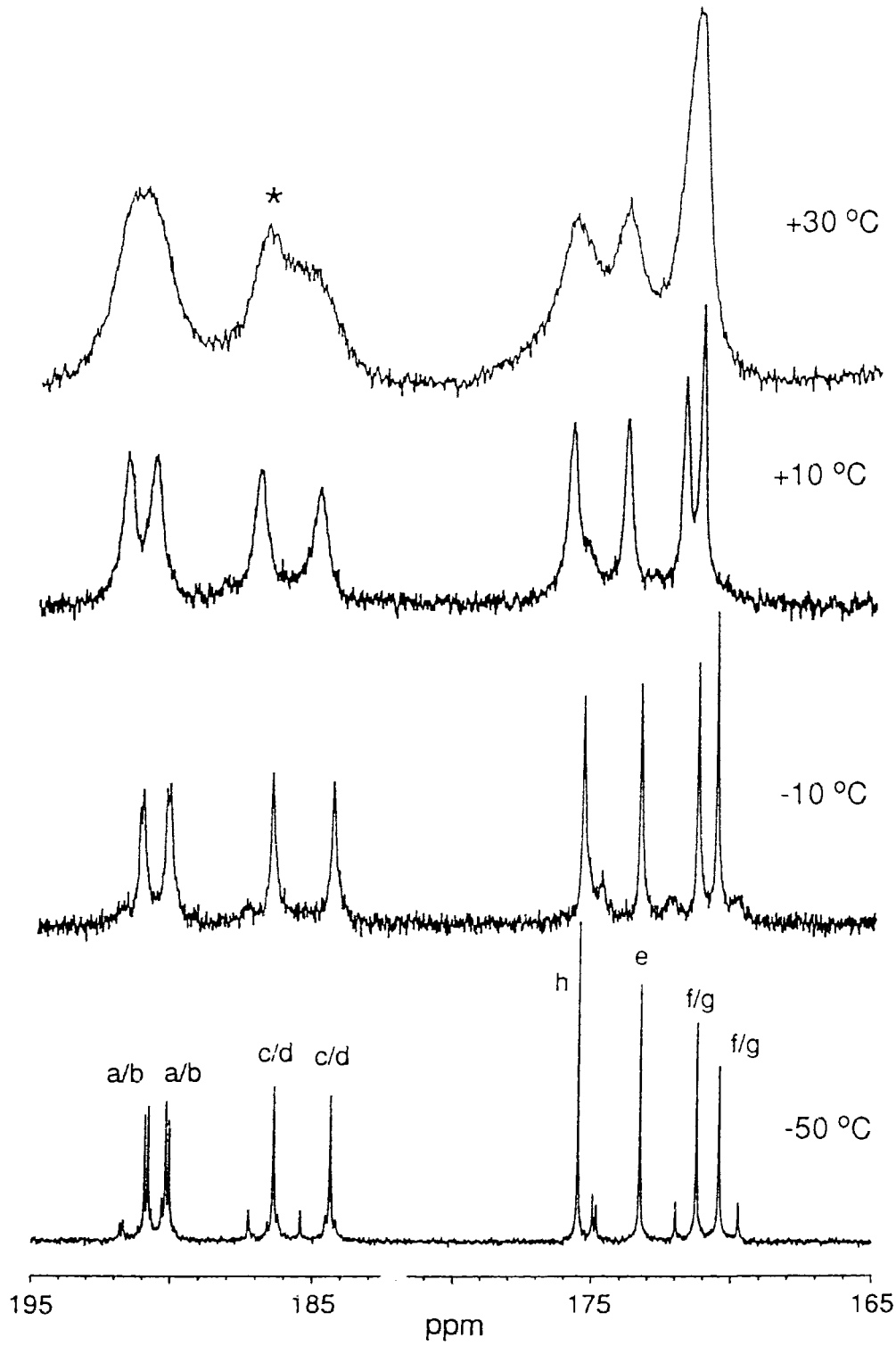

Figure 3.4 Variable Temperature ^{13}C NMR spectra of **2** in CH_2Cl_2/CD_2Cl_2. (peak marked with an asterisk is due to an impurity.)

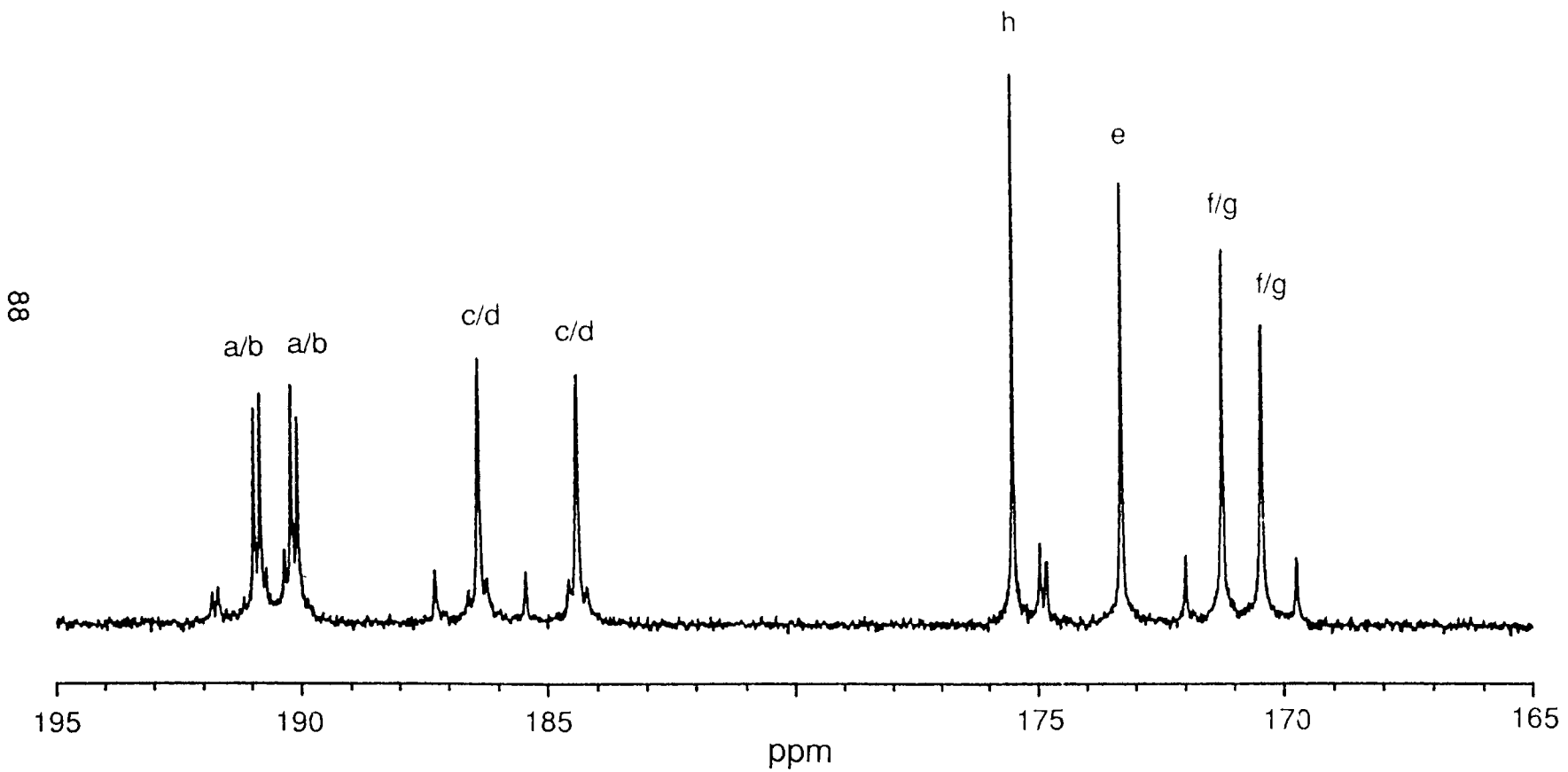

Figure 3.5 ^{13}C NMR spectrum of **2** at -50 °C in CH_2Cl_2/CD_2Cl_2.

the axial carbonyls of the $Os(CO)_4$ unit of **2**. The trans ^{13}C-^{13}C coupling constants for **2** (35.9, 37.2 Hz) were comparable to those observed in **1** (37.0, 37.7 Hz).

The four signals between δ 176 and 170 in the spectrum of **2** at -50 °C are assigned to the three equatorial carbonyls on the osmium atoms and the carbonyl on the iridium atom. Comparison of the low temperature limiting spectrum of **2** (Figure 3.5) with that of **1** (Figure 3.2) and $(\eta^5\text{-}C_5H_5)(OC)Ir\text{-}[Os(CO)_4]_2$ (Figure 2.2, Chapter 2) allowed the tentative assignment of these four signals. The two signals at δ 171.3 and 170.5 are tentatively assigned to the equatorial carbonyls of the $Os(CO)_4$ unit of **2**. On the basis that the resonances for the iridium carbonyl in **1** and the parent cluster $(\eta^5\text{-}C_5H_5)(OC)Ir[Os(CO)_4]_2$ occurred at δ 176 and 174.3, respectively, the resonance at δ 175.5 (Figure 3.5) is tentatively assigned to the corresponding carbonyl of **2** (i.e., carbonyl h). As a result, the resonance at δ 173.3 is tentatively attributed to carbonyl e of **2**. It has been found for $Os_3(CO)_{11}(L)$ that when L = $P(OMe)_3$ the ^{13}C NMR resonances of the carbonyls of the $Os(CO)_3(L)$ unit are not shifted to as high field as those for L = PMe_3.[75] The assignment of the corresponding carbonyl resonances in **1** and **2** are consistent with this observation.

While the low temperature limiting ^{13}C NMR spectra of **1** and **2** were similar, the variable temperature spectra of **2** (Figure 3.4) shows some significant differences compared to that of **1** (Figure 3.1). On warming the sample of **2** to -10 °C all eight signals began to broaden and collapse, although the two high field signals at δ 171.4 and 170.7 appeared to collapse at a somewhat slower rate than the other six signals (Figure 3.4). This behavior is interpreted in terms of two exchange processes with similar activation energies. One process is the partial merry-go-round CO exchange (proposed previously for **1**) that would cause the collapse of six of the signals. The second process is

believed to be isomerization between the major and minor isomers of **2** (see below); this would result in the broadening and collapse of the two signals attributed to carbonyls f and g and further broadening of the other signals. The former process appears to have a slightly lower energy barrier than the latter process in **2**, though there is certainly less of a difference between the two processes than was seen for **1** (see below).

Since the isomerization process in **2** occurs in the temperature range needed for the CO exchange process to cause coalescence, it was not possible to determine an accurate activation energy barrier for the exchange in **2**. This is because the broadening of the signals due to CO exchange cannot be separated from that due to isomerization. It should be noted that the small peak at about δ 187 in the +30 °C spectrum for **2** (Figure 3.5) is believed to be due to an impurity.

Since the two exchange processes occur almost simultaneously, it is not possible to determine whether the major isomer of **2** has structure A or B in solution. However, the signals assigned to carbonyls f and g remain fairly sharp during the CO exchange process, as can be seen in the spectrum at -10 °C (Figure 3.4). This suggests that, like **1**, the major isomer of **2** has structure B (Chart 1, L = $P(OMe)_3$) in solution.

The pattern of the ^{13}C NMR signals attributed to the minor isomer of **2** (Figure 3.5) is similar to that found for the minor isomer of **1** (Figure 3.2). By using the same reasoning that was applied to **1**, the spectrum of **2** at -50 °C (Figure 3.5) is consistent with the minor isomer of **2** having either structure A or B (Chart 1, L = $P(OMe)_3$). In accord with this reasoning, a further doublet due to the minor isomer should be observed at low field but is believed obscured by signals due to the major isomer.

Carbonyl Exchange in 3. Variable temperature ^{13}C NMR spectra in the carbonyl region of ^{13}CO-enriched $(\eta^5\text{-}C_5H_5)(OC)IrOs(CO)_7(CNBu^t)$ (**3**) are shown in Figure 3.6 and the spectrum of **3** at -80 °C is shown in Figure 3.7. The low temperature limiting spectrum of **3** exhibits signals consistent with the presence of two isomers. There are six resonances of intensity one and one resonance of intensity two assigned to the major isomer. In addition there are six much weaker signals assigned to a minor isomer. Two signals due to the minor isomer are believed to be obscured by those due to the major isomer.

Examination of the spectrum of **3** at -80 °C (Figure 3.7) allows a number of structural isomers to be eliminated. Firstly, the isocyanide ligand must be bound to an osmium atom since the ^{13}C NMR spectrum of $(\eta^5\text{-}C_5H_5)(Bu^tNC)Ir\text{-}[Os(CO)_4]_2$ would only have four signals of equal intensity. Secondly, ligands that are sterically undemanding such as isocyanides are, unlike phosphorus ligands, normally found in axial sites in trinuclear osmium carbonyl clusters.[32a,76] (It should, however, be mentioned that the ^{13}C NMR spectrum of $Os_3(CO)_{11}(CNBu^t)$ at -60 °C indicated the presence of a small amount of the equatorially substituted isomer.[32]) That there are only three signals for the major isomer of **3** in the low field region that is associated with axial carbonyls (see above) is consistent with the isocyanide occupying an axial site on an osmium atom in **3**. If the isocyanide ligand was bound in an equatorial site, four low field signals would be expected (e.g., as found for **1** and **2**).

The number of possible structures for the major isomer of **3** in solution is therefore reduced to two; one in which the $CNBu^t$ is on the same side of the Os_2Ir plane as the C_5H_5 ring and one in which the isocyanide is on the opposite side of the plane as the Cp ring. These are shown in Chart 2 as A and B with L = $CNBu^t$. It will be assumed that the major isomer of **3** has structure B in solution. This structure is expected to be slightly preferred on steric grounds

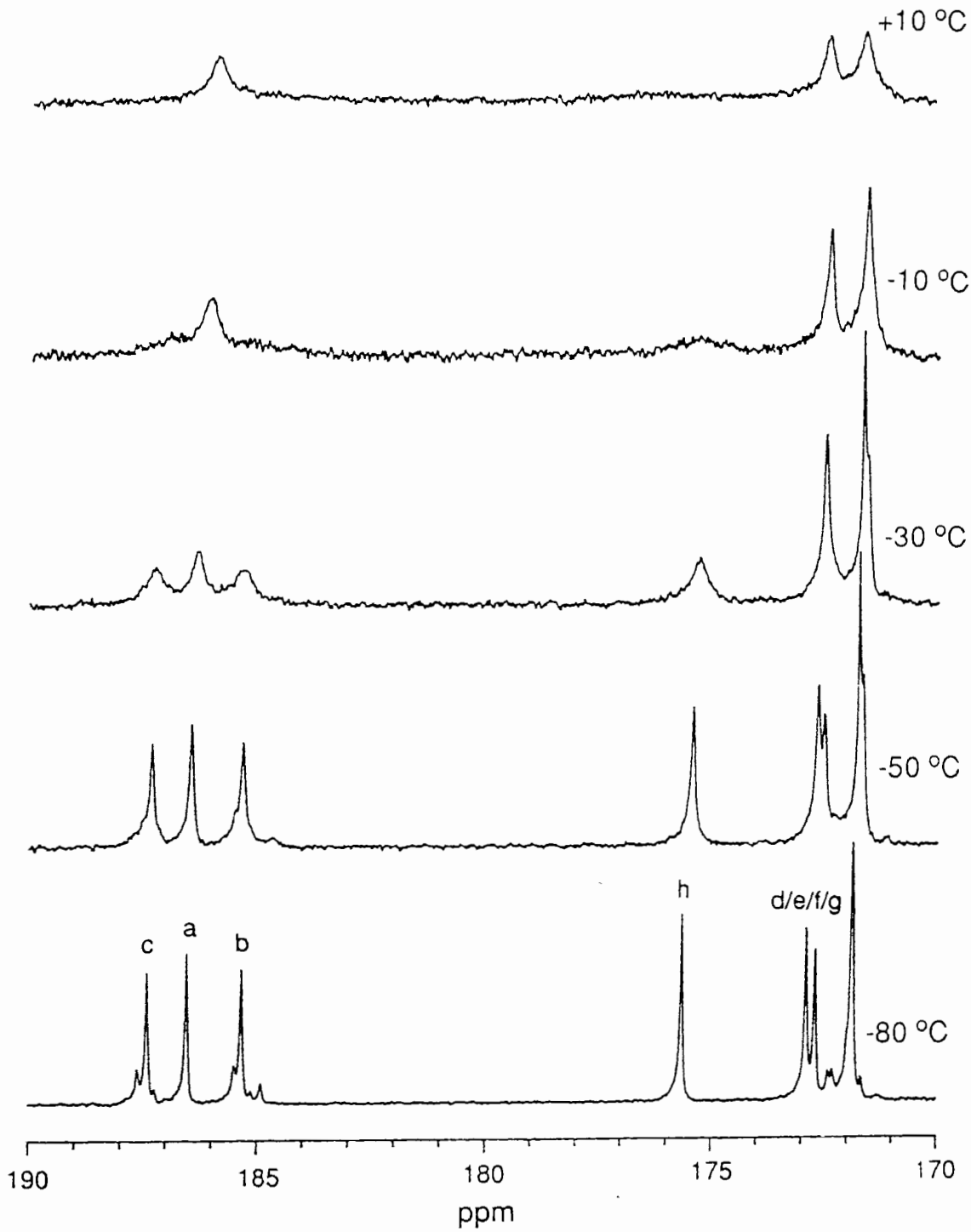

Figure 3.6 Variable temperature ^{13}C NMR spectra of **3** in CH_2Cl_2/CD_2Cl_2.

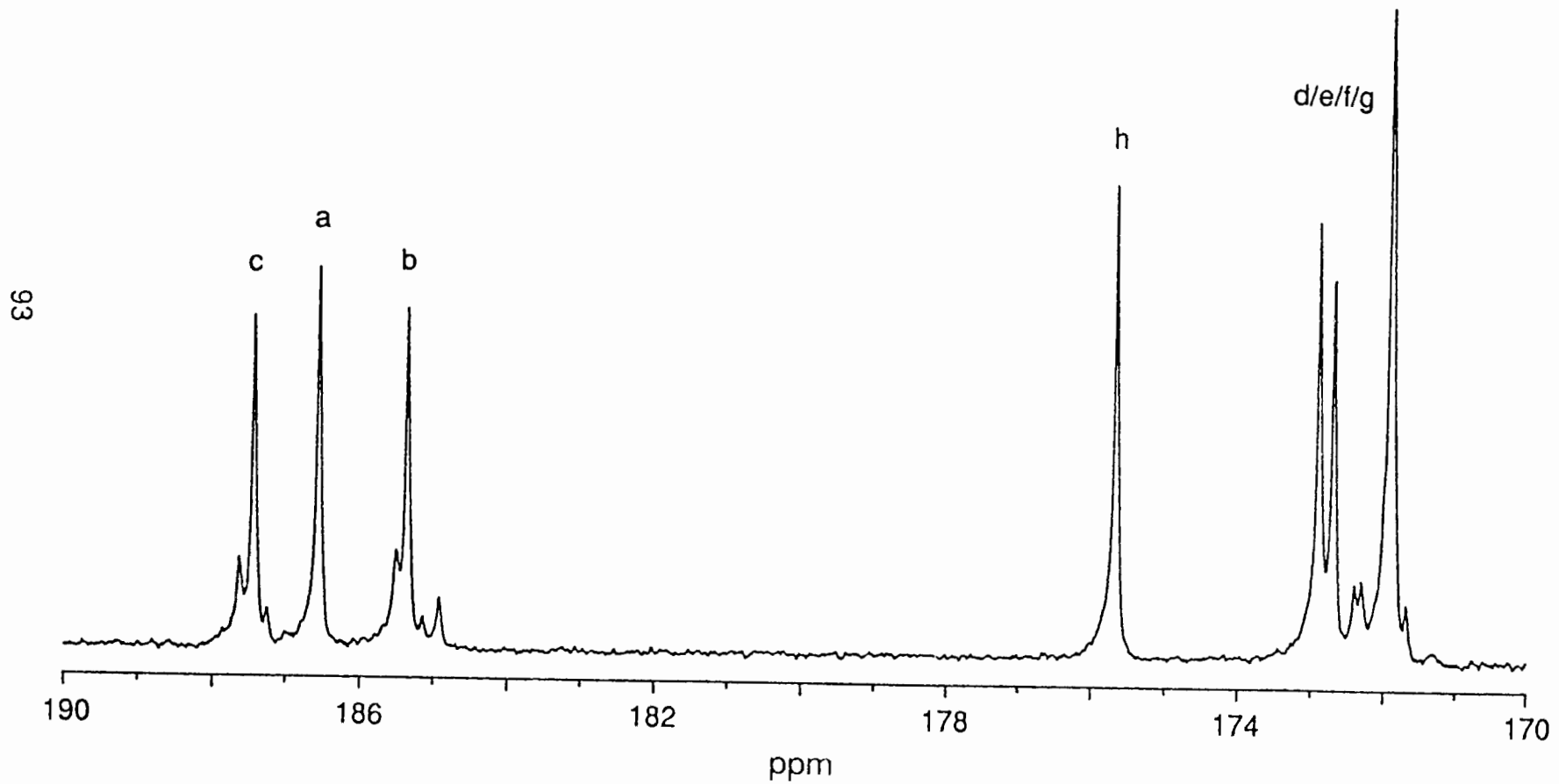

Figure 3.7 ^{13}C NMR spectrum of **3** at -80 °C in CH_2Cl_2/CD_2Cl_2.

CHART 2

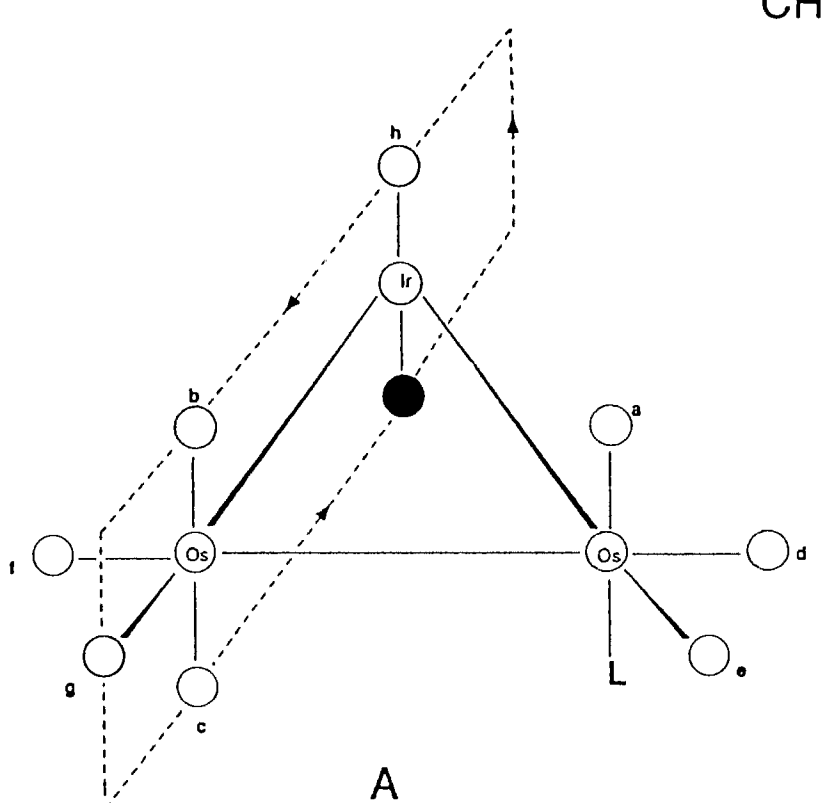

A

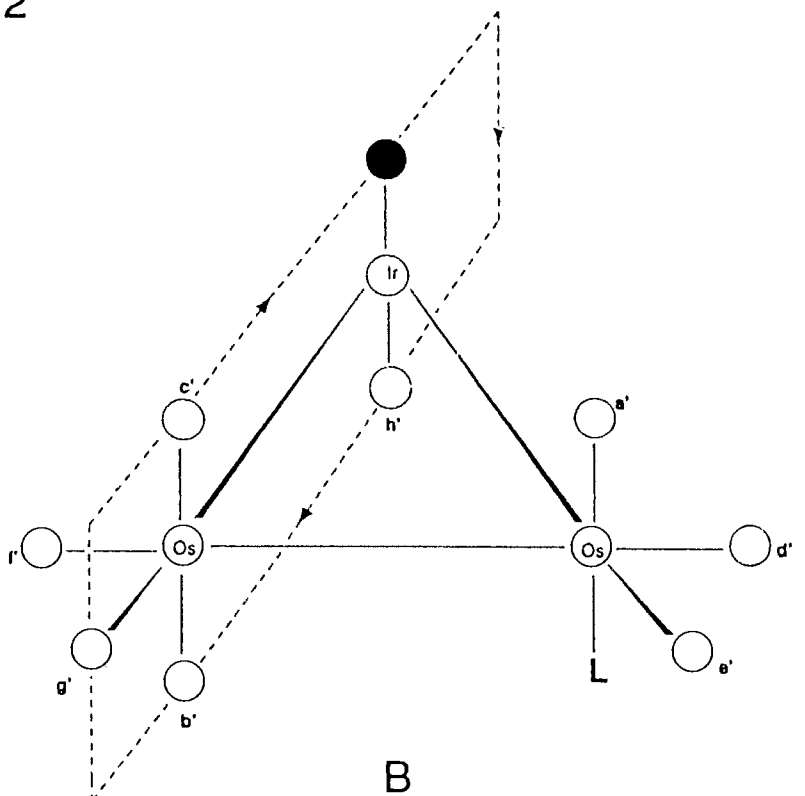

B

L = CNBu^t

○ = CO

● = C_5H_5

since the more bulky ligands, the C_5H_5 ring and the $CNBu^t$ group are on opposite sides of the Os_2Ir plane.

The assignment of the resonances for the major isomer of **3** shown in Figure 3.7 is based on the following arguments. As mentioned previously, the three signals between δ 188 and 185 are attributed to the three axial carbonyls on the osmium atoms. In particular, the two signals at δ 187.4 and 185.3 that exhibit ^{13}C-^{13}C coupling (see above) are assigned to the axial carbonyls b and c. It is known that CN triple bonds possess particularly strong magnetic anisotropies and it has been found that in regions near the triple bond that deshielding occurs.[77] For example, it has been found for three isomers of $Os_3(\mu\text{-}H)_2(CO)_9(CNBu^t)$ that with one exception, the NMR resonances of the carbonyls nearest the $CNBu^t$ ligand were shifted downfield.[32b] On this basis, the resonances at δ 185.3 and 187.4 in the spectrum of **3** at -80 °C are tentatively assigned to carbonyls b and c, respectively. The resonance at δ 186.5 is therefore assigned to carbonyl a. As expected, this resonance does not exhibit ^{13}C-^{13}C coupling.

The four high field signals in Figure 3.7 are assigned to the four equatorial carbonyls on osmium atoms and the carbonyl on the iridium atom. On the basis of the iridium carbonyl resonances of **1**, **2**, and $(\eta^5\text{-}C_5H_5)(OC)Ir[Os(CO)_4]_2$ which occur at δ 176, 175.5 and 174.3, respectively, the resonance at δ 175.6 is tentatively assigned to the corresponding carbonyl in **3** (i.e., carbonyl h). Since this leaves four carbonyls to be accounted for by three signals, two of the carbonyls must have degenerate signals. Consistent with this view is that the peak to highest field is of intensity two. Further assignment of the resonances due to carbonyls d, e, f, and g in **3** is currently not possible.

Due to the low intensity of the signals and the observation of only six of the possible eight signals attributed to the minor isomer of **3**, its structure in

solution could not be ascertained. Three possible structures for this minor isomer are thought most probable. The first has the same structure as A in Chart 2. The remaining two have the isocyanide ligand in an equatorial site, where it can be trans to either the IrOs or the OsOs bonds,analogous to the isomers of **1** and **2**. After consideration of the exchange process (see below), the isomer having structure A is thought most likely to be the minor isomer of **3**.

On warming the sample of **3** to -30 °C, four of the signals collapse while two high field signals remain relatively sharp (Figure 3.6). This behavior is interpreted in terms of a partial merry-go-round CO exchange in the IrOs plane that contains the $Os(CO)_4$ unit as illustrated in Chart 2. Such a CO exchange results in conversion between the two isomers of **3** with the isocyanide ligand in an axial site (A and B in Chart 2). (This is in contrast to **1** and **2**, where the CO exchange process does not result in isomerization.)

It is possible that a small amount of **3** could exist as the equatorially substituted isomer (see above). Any exchange between it and the major isomer would necessarily involve some other mechanism such as a trigonal twist mechanism. However, the trigonal twist mechanism was thought unlikely for the lowest energy CO exchange process for **3** since it has been found for triosmium clusters that trigonal twist mechanisms have an energy barrier equal to or greater than that for bridge-terminal CO exchange processes (see below).

Two other mechanisms that could account for the observed changes in the ^{13}C NMR spectra of **3** are a rotation of the $Ir(\eta^5\text{-}C_5H_5)(CO)$ unit with respect to the rest of molecule and an isomerization process that involves movement of the isocyanide ligand between the two axial sites on the osmium atom it is attached to. However, given the proposed CO exchange processes for **1**, **2** and the parent $(\eta^5\text{-}C_5H_5)(OC)Ir[Os(CO)_4]_2$ cluster it is believed that the merry-go-

round process illustrated in Chart 2 for **3** is the most likely. The discussion that follows is based on that assumption.

The exchange process between structures A and B of **3** leads to the following specific site exchanges: a ⟶ a', b ⟶ g', g ⟶ b', c ⟶ h', h ⟶ c', d ⟶ d', e ⟶ e', f ⟶ f' (see Chart 2). In such a mechanism, all eight carbonyls should exchange with each other. That two high field signals appear to remain fairly sharp in the spectrum at -30 °C (Figure 3.6) probably indicates that the resonances arising from equatorial carbonyls d, e, and f are sufficiently close to those from d', e' and f' that the broadening prior to yielding averaged signals was quite small. Upon further warming of **3** to -10 °C and +10 °C, a low field signal at δ 186 grows in intensity. Since it appears in the low field region of the spectrum, it is attributed to a resonance arising from the axial carbonyls. From the appearance of the spectrum of **3** at -10 °C, one can rule out the possibility that this new peak is the result of exchange between the signals formerly at δ 187.4 and 185.3 since at -10 °C, these signals appear to be still collapsing into the base line. Furthermore, in accord with the exchange process proposed for **3** (Chart 2), carbonyls b and c do not exchange with c' and b' respectively. The new signal is therefore attributed to carbonyls a and a'.

Consideration of the two high field signals in the spectra of **3** at -10 °C and +10 °C (Figure 3.6), reveals that they are beginning to broaden and collapse indicative of further exchange. There are a number of exchange processes that could be invoked to account for this collapse in the resonances due to the equatorial carbonyls. Two possibilities that were considered were a trigonal twist of the $Os(CO)_3(L)$ unit and a merry-go-round exchange in the vertical plane that passes through the two osmium atoms. Either of these possibilities may involve movement of the isocyanide to an equatorial site.

Since the two isomers of **3** have different ^{1}H NMR chemical shifts for the methyl groups of their CNBu^t ligands, the isomerization process can also be studied with ^{1}H NMR spectroscopy. The methyl resonances in the variable temperature ^{1}H NMR spectra of **3** are shown in Figure 3.8. The spectrum at -60 °C (213 ± 3 K) was simulated with the DNMR3 computer program.[67] The calculated and observed lineshapes for **3** are shown in Figure 3.9. The rate constant (i.e., *k*) used for the simulated spectrum of 50 ± 6 s^{-1} yields a $\Delta G^{\neq}$ value of 10.7 ± 0.2 kcal mol^{-1} at -60 °C. Since the isomerization process involves CO exchange, this is also the activation barrier for CO exchange in the IrOs plane of **3**. This is a somewhat low barrier for CO exchange for an Os_2Ir cluster. As mentioned earlier, **1** and $(\eta^5\text{-}C_5H_5)(OC)Ir[Os(CO)_4]_2$ have barriers to CO exchange in the IrOs plane of 13.2 and 14.2 kcal mol^{-1}, respectively. That the barrier in **3** should be lower than that for the unsubstituted $(\eta^5\text{-}C_5H_5)(OC)Ir\text{-}[Os(CO)_4]_2$ is not unexpected since it has been found for $Os_3(CO)_{12}$ that substitution of a CO by the better donor ligands, PEt_3, $P(OMe)_3$, or CNBu^t, lowers the activation energy barrier for CO exchange.[32,47,71,75]

However, the significant difference between the activation energy barriers of the phosphine substituted cluster, **1,** and the isocyanide substituted cluster, **3,** is not as easily explained. It is particularly surprising given that for **1**, the CO exchange apparently involves the phosphine-substituted Os atom, while for **3**, the proposed CO exchange does *not* involve the isocyanide-substituted Os atom. One would expect that the effect of the substituted σ-donor ligand (i.e., PMe_3 or CNBu^t) would be felt to the greatest extent if the CO exchange included the metal atom to which it is bonded.

Isomerization of 1 and 2. As noted earlier, the variable temperature ^{13}C NMR spectra of **1** (Figure 3.2) gave evidence of a second fluxional process, in addition to CO exchange in the IrOs plane, that occurs at higher temperatures

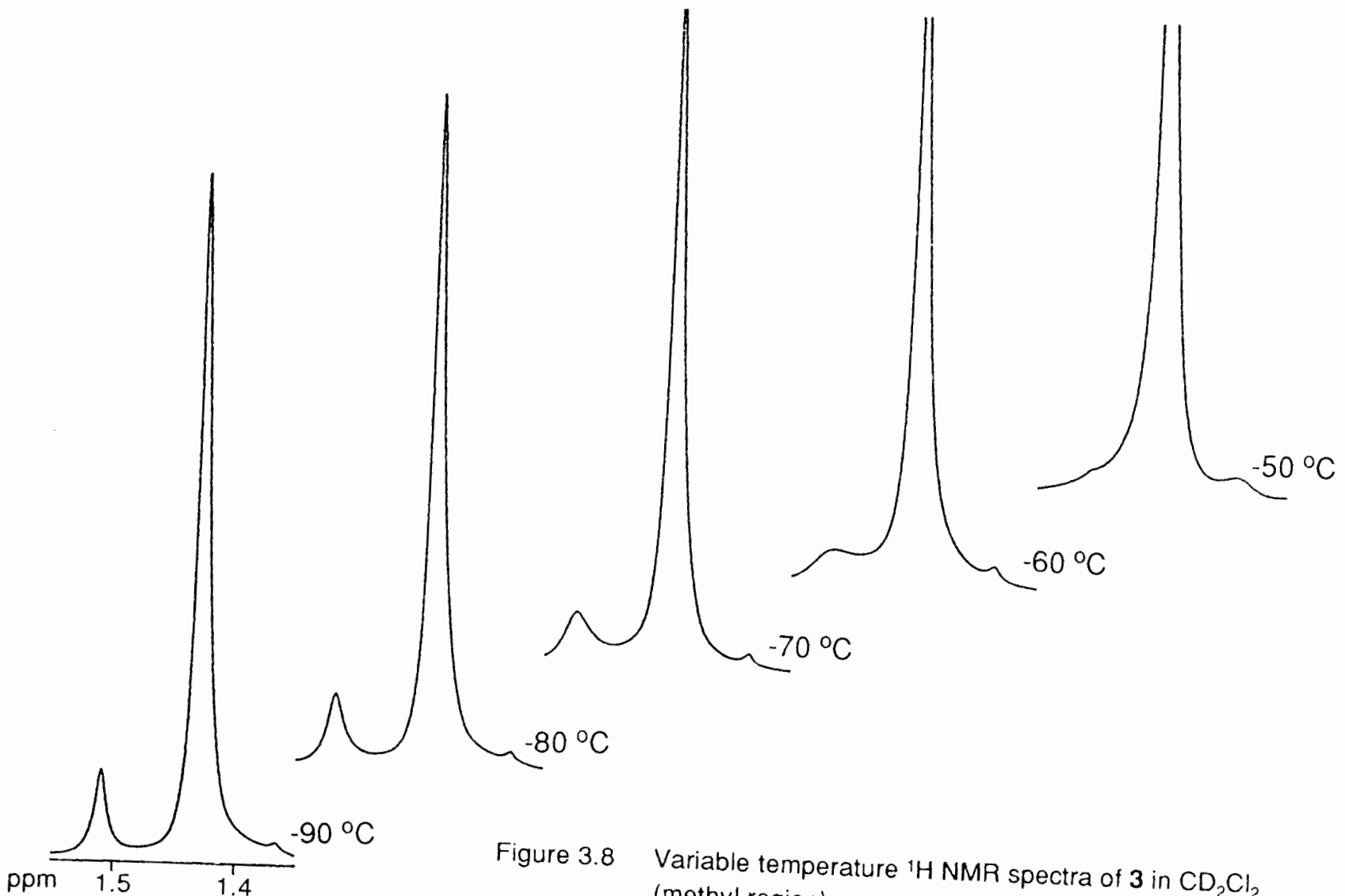

Figure 3.8 Variable temperature ^1H NMR spectra of **3** in CD_2Cl_2 (methyl region).

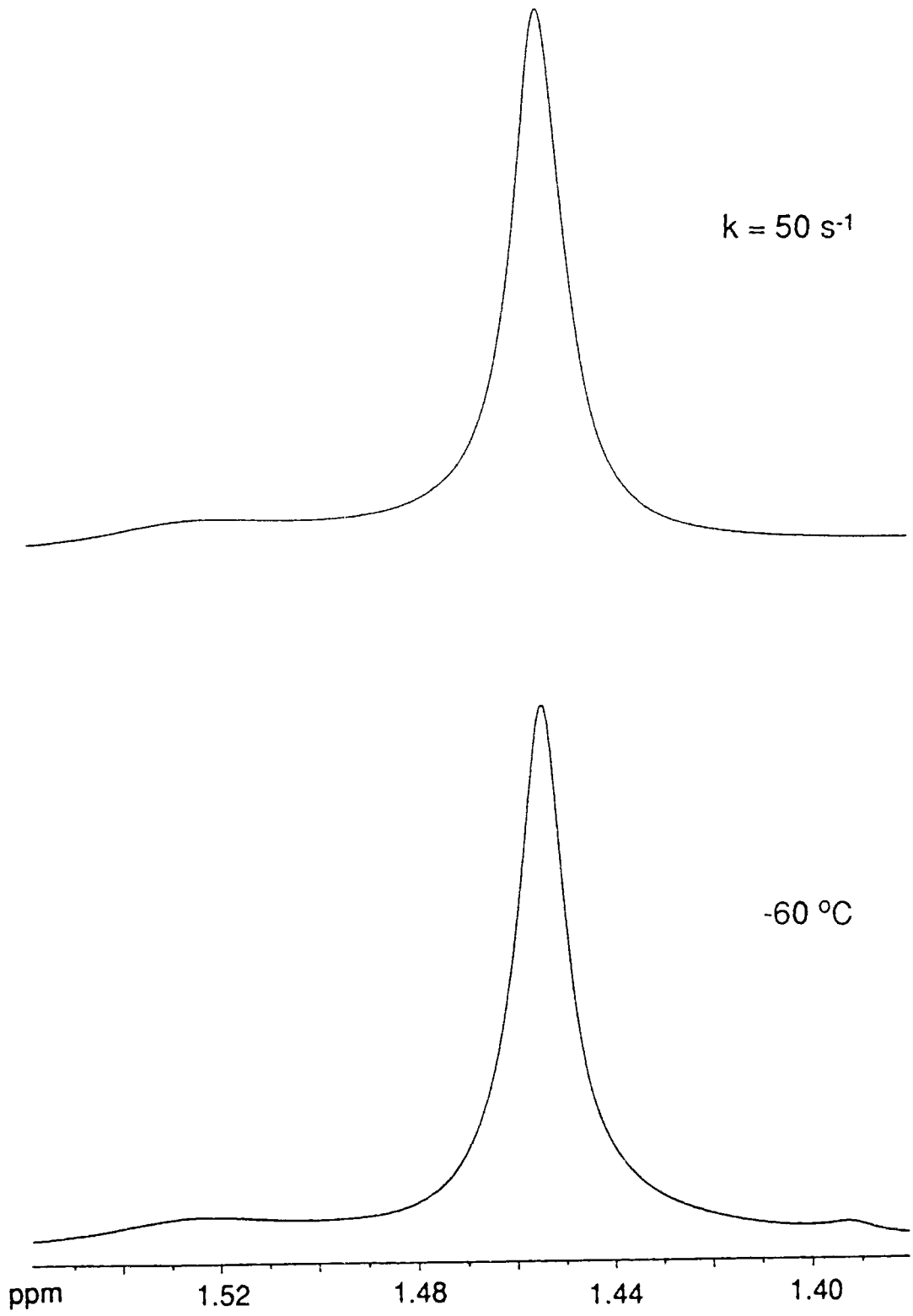

Figure 3.9 Calculated and observed ^{1}H NMR spectra for **3** at -60 °C. (methyl region)

(i.e., 10 and 21 °C). One possibility for this higher energy process is the isomerization process between the major and minor isomers of **1**. To check this possibility, variable temperature ^1H NMR spectra of **1** in $CDCl_3$ were obtained. The C_5H_5 resonance signals of these spectra are shown in Figure 3.10. The spectra are consistent with exchange occurring between the two isomers.

The spectrum of **1** at 35 °C (308 ± 3 K) was simulated; the calculated and observed lineshapes are shown in Figure 3.11. The rate constant used for the simulated spectrum of 60 ± 4 s^{-1} yields a $\Delta G^{\neq}$ value of 15.5 ± 0.2 kcal mol^{-1} at 35 °C.

As determined earlier, the major isomer of **1** has structure B, while the minor isomer most likely has structure A (Chart 1, L = PMe_3). The mechanism of exchange between these two isomers of **1** is believed to involve a trigonal twist of the $Os(CO)_3(PMe_3)$ unit (Chart 3, L = PMe_3). Trigonal twist mechanisms have been implicated before in various metal clusters.[47,70,78] A twist similar to this was proposed to account for some of the nonrigid processes in $Os_3(CO)_{12-x}[P(OMe)_3]_x$ (x = 2, 4, 5).[47,70] In the proposed mechanism, the phosphite ligand, for steric reasons, never enters an axial site but rocks back and forth between the two equatorial positions, which simultaneously causes axial-equatorial carbonyl exchange. This rocking motion is also referred to as a turnstile or pinwheel mechanism in the literature. It should be noted that this mechanism could involve either the carbonyl above the Os_2Ir plane (i.e., carbonyl a) or the one below the plane (i.e., carbonyl b).

As mentioned earlier, it was inferred from the variable temperature ^{13}C NMR spectra of **1** that the activation barrier for the CO exchange process was lower than that for the isomerization process. The activation barriers of **1**, 13.2 ± 0.3 kcal mol^{-1} for the partial bridge-terminal CO exchange in the IrOs plane and 15.5 ± 0.2 kcal mol^{-1} for the trigonal twist barrier, are consistent with this view. In

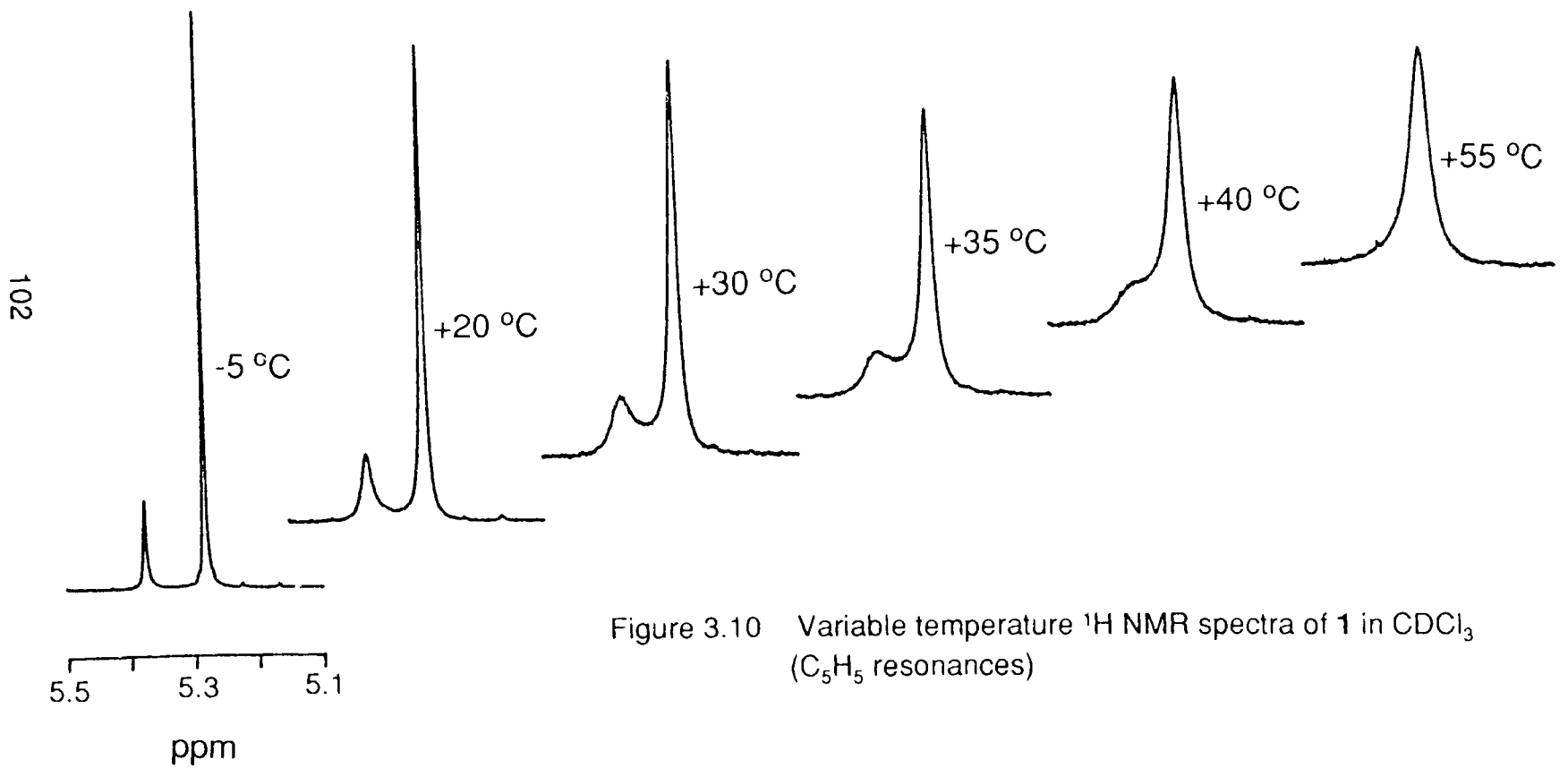

Figure 3.10 Variable temperature ^1H NMR spectra of **1** in $CDCl_3$ (C_5H_5 resonances)

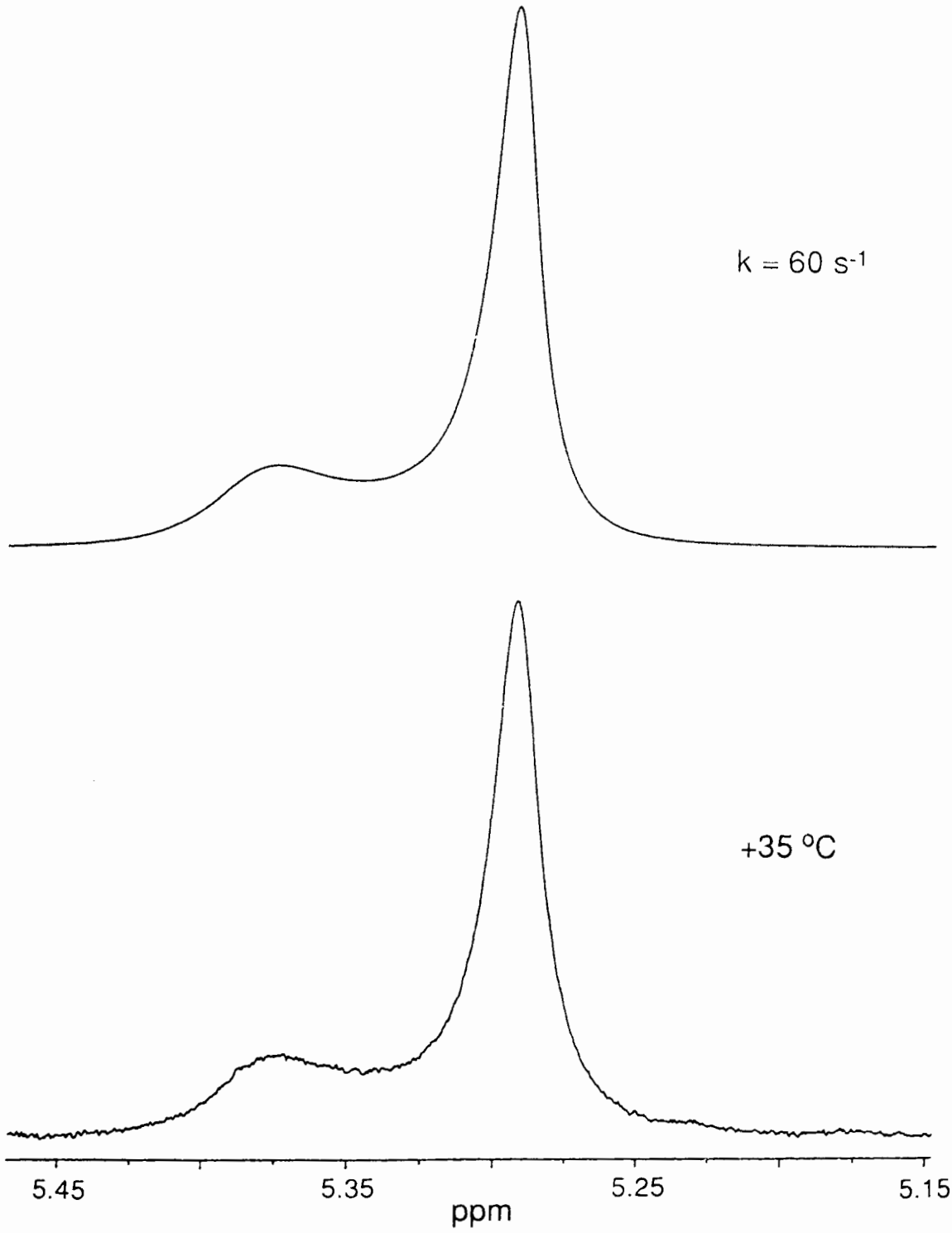

Figure 3.11 Calculated and observed ^1H NMR spectra for **1** at +35 °C. (C_5H_5 resonances)

CHART 3

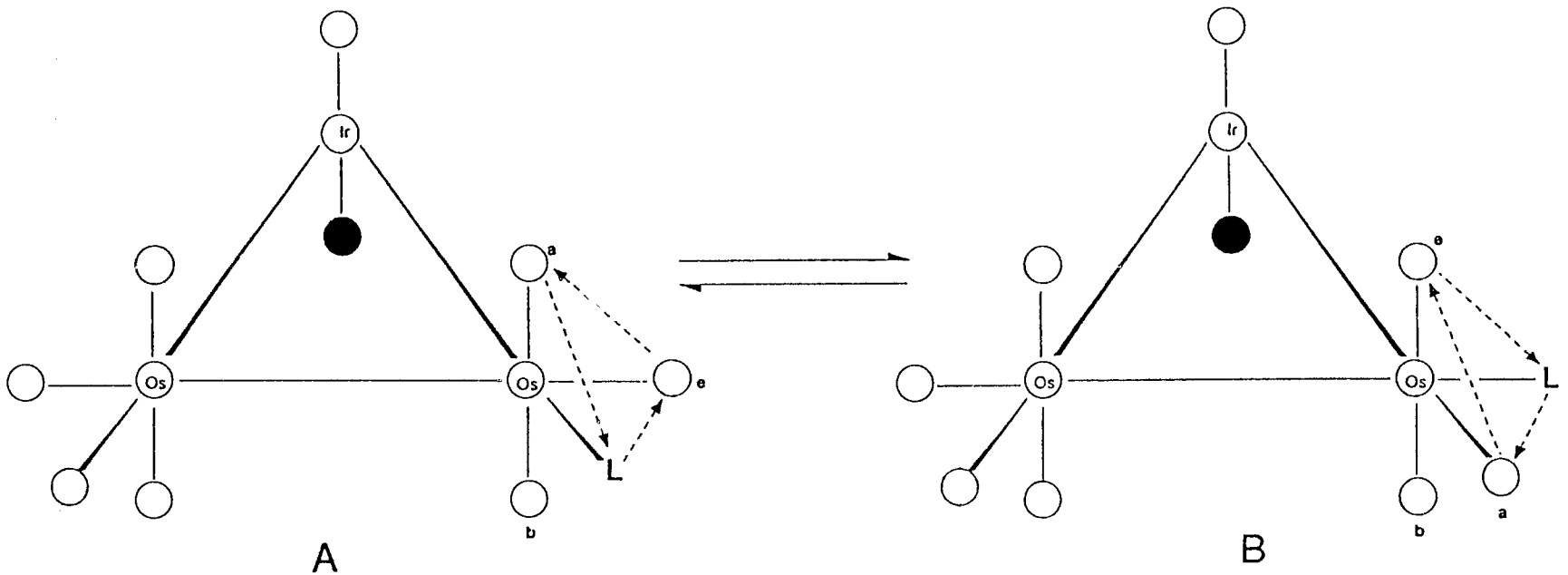

$L = PMe_3, P(OMe)_3$ ○ = CO ● = C_5H_5

the study of the $Os_3(CO)_{12-x}[P(OMe)_3]_x$ (x = 2,4) compounds, it was found that the barrier to the trigonal twist rearrangement was equal to or greater than that for the bridge-terminal CO exchange.[47] For $Os_3(CO)_8[P(OMe)_3]_4$, the barriers were roughly equal: 10.6 ± 0.4 kcal mol^{-1} for the trigonal twist and 10.3 kcal mol^{-1} for bridge-terminal CO exchange. However, for $Os_3(CO)_{10}[P(OMe)_3]_2$, the barrier for the trigonal twist rearrangement (15.0 ± 0.4 kcal mol^{-1}) was much higher than that for the bridge-terminal CO exchange (12.4 ± 0.5 and 12.7 ± 0.4 kcal mol^{-1}).

Variable temperature ^1H NMR spectra of **2** in $CDCl_3$ were also obtained and the C_5H_5 resonances of these spectra are shown in Figure 3.12. As found for **1**, the spectra were consistent with exchange between the two isomers. The spectrum of **2** at 25 °C (298 ± 3K) was simulated; the calculated and observed lineshapes are shown in Figure 3.13. The rate constant used for the simulated spectrum of 45 ± 4 s^{-1} yields a $\Delta G^{\neq}$ of 15.2 ± 0.2 kcal mol^{-1} at 25 °C.

Although the structures of the major and minor isomers of **2** could not be unambiguously determined from their ^{13}C NMR spectra (see above), the spectra were consistent with one of the isomers having structure A and the other having structure B (Chart 1, L = $P(OMe)_3$). The same mechanism proposed to account for isomerization in **1**, namely the trigonal twist rearrangement, may be invoked to account for the isomerization in **2** (Chart 3, L = $P(OMe)_3$).

Since the activation energy barrier for the CO exchange in **2** could not be determined (see above), a comparison between CO exchange and isomerization barriers for **2** was not possible. A comparison between the activation energy barriers for isomerization in **1** and **2** is possible, however, and there is no significant difference between them. This is somewhat surprising since PMe_3 and $P(OMe)_3$ are considered to have different electronic properties.[38]

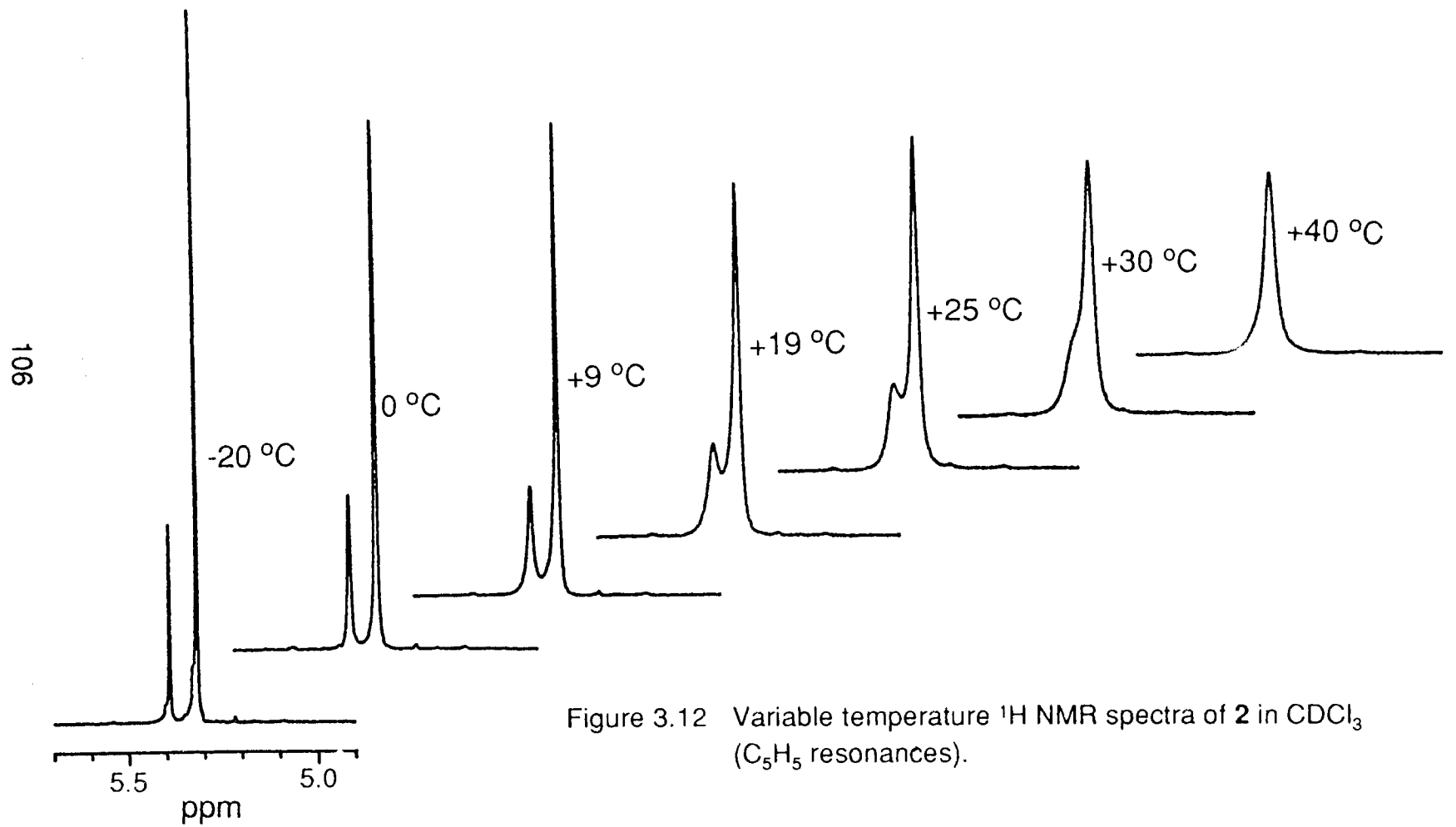

Figure 3.12 Variable temperature ^1H NMR spectra of **2** in $CDCl_3$ (C_5H_5 resonances).

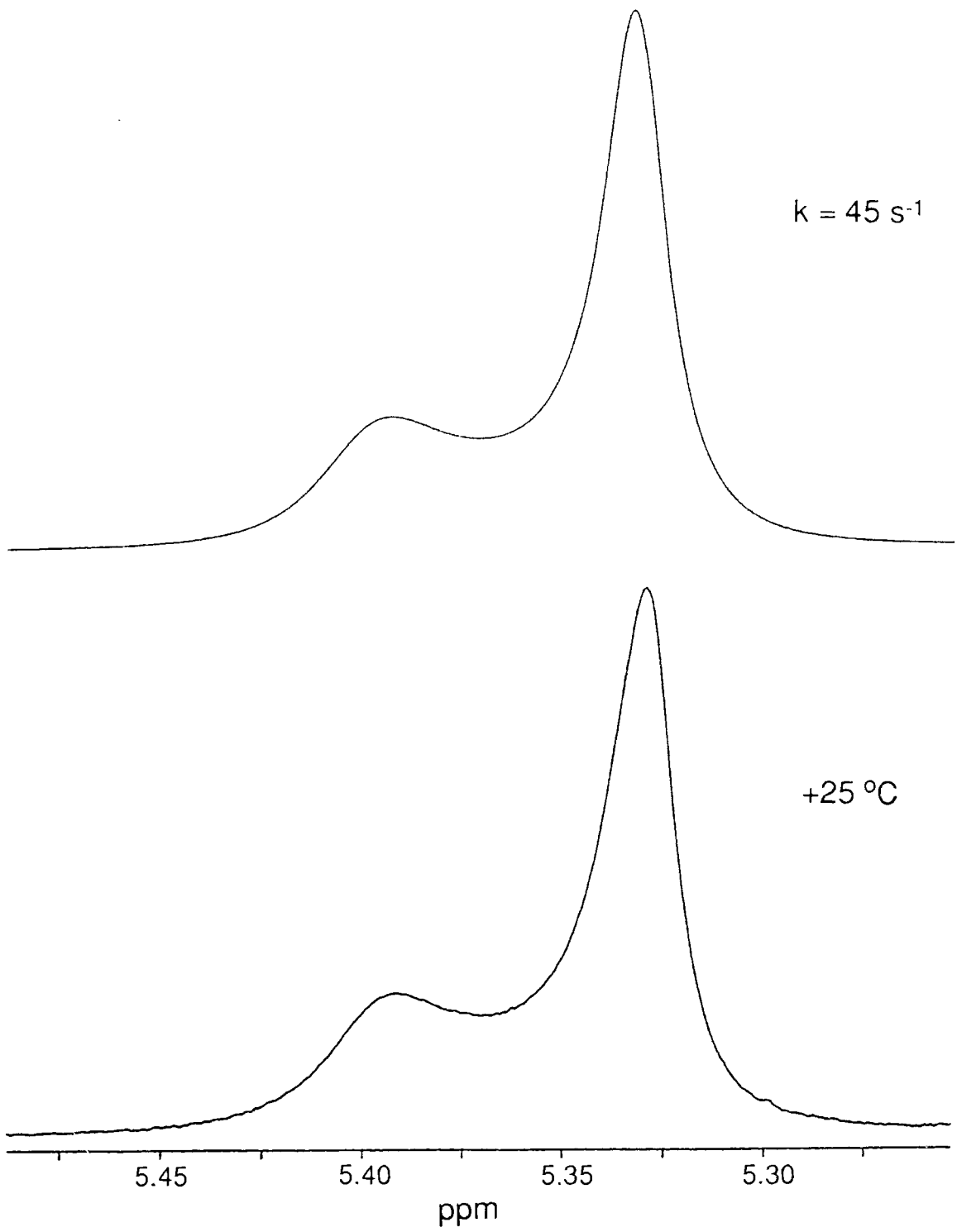

Figure 3.13 Calculated and observed ^1H NMR spectra of **2** at +25 °C (C_5H_5 resonances).

3.4 Conclusion

The $(\eta^5\text{-}C_5H_5)(OC)IrOs(CO)_3(L)$ (L = PMe_3, **1**; L = $P(OMe)_3$, **2**; L = $CNBu^t$, **3**) clusters were prepared by the substitution of a CO ligand from $(\eta^5\text{-}C_5H_5)\text{-}(OC)Ir[Os(CO)_4]_2$ with L, with Me_3NO as the decarbonylation agent.

The variable temperature ^1H and ^{13}C NMR spectra of these clusters was examined in order to determine their structure in solution and to study their fluxionality.

For **1**, the spectroscopic data strongly indicated that the PMe_3 ligand was trans to the OsOs bond in the major isomer. However, the structures of the major isomers of the phosphite and isocyanide analogues could not be unambiguously determined.

The low temperature ^{13}C NMR limiting spectra of these compounds indicated that the $(C_5H_5)Ir(CO)$ unit in these clusters is rigid (with the exception of free rotation of the C_5H_5 ring). This was found earlier for the unsubstituted parent cluster.

The CO exchange process with the lowest energy for the three clusters was interpreted in terms of a partial merry-go-round in one of the vertical IrOs planes, analogous to the parent cluster. The activation energy barriers for this process in **1** and **3** were determined from the variable temperature ^{13}C and ^1H NMR, respectively. As expected, the barriers for these clusters were lower than that for the unsubstituted cluster. The isocyanide analogue had a particularly low barrier.

The activation energy barriers for the isomerization process in the two clusters with a phosphorus ligand were determined by variable temperature ^1H NMR; there was no significant difference between the barriers. Further study of the effect of the L ligand on the barrier to the trigonal twist exchange as the steric and electronic properties of L are changed, is obviously needed.

Finally, the results of the ^{13}C NOESY spectrum of **1** were consistent with those results of the one dimensional spectra and confirmed the identity of the major isomer.

CONCLUSIONS

In this thesis, osmium has been found to form both complexes with dative metal-metal bonds and trinuclear clusters.

In the former area, the 18-electron $Os(CO)_{5-x}(CNBu^t)_x$ (x = 1,2) acts as a two electron donor ligand to the $M(CO)_5$ fragment. One reason for the ready formation of these complex is that the $Os(CO)_{5-x}(CNBu^t)_x$ molecules are coordinatively unsaturated. This thesis extends the work previously carried out in this laboratory on the phosphorus-ligand analogues. The site preference for the isocyanide ligand was different to that found for the phosphorus ligand. In addition, a second example of a structurally-characterized trimetallic complex with two, unbridged dative metal-metal bonds in tandem was prepared.

There are number of studies on these complexes that are either in progress or have recently been completed. For example, an investigation of whether the dative metal-metal bond undergoes heterolytic cleavage when photolyzed is presently underway.[79] In addition, molecular orbital calculations on the electronic nature of dative metal-metal bonds in $(OC)_5OsM(CO)_5$ (M = Cr, Mo, W) have recently been carried out by another group.[80] This study confirmed that the complexes do indeed have dative metal-metal bonds.

There are a number of directions that future studies on complexes with dative metal-metal bonds could take. Firstly, compounds of the type $Os(CO)_4(L)$ (where L = carbene, CS, olefin, and pyridine) could be studied in order to determine their ability to form complexes with dative metal-metal bonds, and also to determine the site preference of L and the ability of L to migrate. Secondly, kinetic studies to quantitatively determine the metal-metal bond strengths in these complexes could be carried out.

Concerning the trinuclear clusters, the rational synthesis of the parent $IrOs_2$ clusters involved the use of mononuclear starting materials. The lowest energy carbonyl exchange process for both the substituted and unsubstituted clusters appeared to be the same: namely a partial merry-go-round between the carbonyls on the iridium atom and one of the osmium atoms. The barrier to this exchange varied depending on the substituents on the Ir and Os atoms. In addition, the $(C_5R_5)Ir(CO)$ fragment of these clusters was found to be rigid relative to the Os_2 moiety when the carbonyls are not exchanging.

In terms of future directions for studies of $IrOs_2$ clusters, one obvious area would be further exploration of the chemistry of the parent clusters. In particular, reactions of the these clusters with small molecules such as H_2, HX, X_2, C_2H_4, allene, and C_2R_2 could be studied. Another area to explore would be the synthesis of substituted $IrOs_2$ clusters where the substituted ligand (e.g., L = PF_3, $P(OR)_3$, or olefin) would be on the iridium atom. Such a synthesis would probably involve the use of $(C_5R_5)Ir(CO)(L)$ as one of the starting materials. In these clusters, the carbonyl exchange process would be expected to involve exchange only between the osmium centers. Lastly, the potential usefulness of the ^{13}C NOESY technique in examining the structure and chemical exchange processes in metal carbonyl clusters could be explored further. For example, it would be of interest to do further NOESY experiments on the two phosphorus-ligand substituted clusters at different temperatures. This technique may prove very useful in assigning the ^{13}C NMR resonances and in elucidating the carbonyl exchange mechanisms of metal carbonyl clusters. Further studies of the use of the ^{13}C NOESY technique are currently planned.

REFERENCES

1. Stranges, A.N. *J. Chem. Ed.* **1984**, *61*, 185.

2. Haaland, A. *Angew. Chem., Int. Ed. Engl.* **1989**, *28*, 992.

3. Khasnis, D.V.; Le Bozec, H.; Dixneuf, P.H.; Adams, R.D. *Organometallics* **1986**, *5*, 1772.

4. Mayer, J.M.; Calabrese, J.C. *Organometallics* **1984**, *3*, 1292.

5. Hock, D.A.; Mills, O.S. *Acta. Crystallogr.* **1961**, *14*, 139. See also: Casarin, M.; Ajo, D.; Granozzi, G.; Tendello, E.; Aime, S. *Inorg. Chem.* **1985**, *24*, 1241.

6. a) Geoffroy, G.L.; Rosenberg, S.; Whittle, R.R. *J. Am. Chem. Soc.* **1984**, *106*, 5934. b) Mercier, W.C.; Whittle, R.R.; Burkhardt, E.W.; Geoffroy, G.L. *Organometallics* **1985**, *4*, 68.

7. Arndt, L.W.; Darensbourg, M.Y.; Delord, T.; Bancroft, B.T. *J. Am. Chem. Soc.* **1986**, *108*, 2617.

8. Anders, U.; Graham, W.A.G. *J. Am. Chem. Soc.* **1967**, *89*, 539.

9. Halpin, C.; Hall, M.B. *J. Am. Chem. Soc.* **1986**, *108*, 1695.

10. Einstein, F.W.B.; Pomeroy, R.K.; Rushman, P.; Willis, A.C. *J. Chem. Soc., Chem. Commun.* **1983**, 854.

11. a) Einstein, F.W.B.; Jones, T.; Pomeroy, R.K.; Rushman, P. *J. Am. Chem. Soc.* **1984**, *106*, 2707. See also: Davis, H.B.; Einstein, F.W.B.; Glavina, P.G.; Jones, T.; Pomeroy, R.K.; Rushman, P. *Organometallics* **1989**, *8*, 1030. b) Fleming, M.M.; Pomeroy, R.K.; Rushman, P. *J. Organomet. Chem.* **1984**, *273*, C33. c) Einstein, F.W.B.; Pomeroy, R.K.; Rushman, P.; Willis, A.C. *Organometallics* **1985**, *3*, 250. d) Einstein, F.W.B.; Jennings, M.C.; Krentz, R.; Pomeroy, R.K.; Rushman, P.; Willis, A.C. *Inorg. Chem.* **1987**, *26*, 1341. e) Davis, H.B.; Einstein, F.W.B.; Johnston, V.J.; Pomeroy, R.K. *J. Organomet. Chem.* **1987**, *319*, C25. f) Davis, H.B.; Einstein, F.W.B.; Martin, L.R.; Pomeroy, R.K.; Wong, E.A. to be submitted for publication.

12. a) Del Paggio, A.A.; Muetterties, E.L.; Heinekey, D.M.; Day, V.W.; Day, C.S. *Organometallics* **1986**, *5*, 575. b) Uson, R.; Fornies, J.; Espinet, P.;

Fortuno, C.; Tomas, M.; Welch, A.J. *J. Chem. Soc., Dalton Trans.* **1988**, 3005.

13. a) Einstein, F.W.B.; Martin, L.R.; Pomeroy, R.K.; Rushman, P. *J.Chem. Soc., Chem. Commun.* **1985**, 345. See also: Martin, L.R.; Einstein F.W.B.; Pomeroy, R.K. *Organometallics* **1988**, *7*, 294. b) Einstein, F.W.B.; Johnston, V.J.; Ma, A.K.; Pomeroy, R.K. *Organometallics* **1990**, *9*, 52.

14. Adams, R.D.; Selegue, J.P. in *Comprehensive Organometallic Chemistry*; Wilkinson, G.; Stone, F.G.A.; Abel, E.W. Eds; Pergamon; Elmsford, NY, 1982; Vol. 4 p 981-2.

15. The crystal structures of $(OC)_4(Bu^tNC)OsCr(CO)_5$ (**1-Cr**) and [*cis-dieq*-$(OC)_3(Bu^tNC)_2Os]Cr(CO)_5$ (**2b-Cr**) were determined by R.J. Batchelor and F.W.B. Einstein.

16. Batchelor, R.J.; Davis, H.B.; Einstein, F.W.B.; Pomeroy, R.K. *J. Am. Chem. Soc.* **1990**, *112*, 2036.

17. The crystal structure of $(OC)_4(Bu^tNC)OsOs(CO)_3(CNBu^t)W(CO)_5$ (**3a**) was determined by R.J. Batchelor and F.W.B. Einstein.

18. Shipley, J.A.; Batchelor, R.J.; Einstein, F.W.B.; Pomeroy, R.K. *Organometallics* **1991**, *10*, 3620.

19. Batchelor,R.J.; Einstein, F.W.B.; Pomeroy, R.K.; Shipley, J.A. *Inorg. Chem.* (in press).

20. Rushman, P; van Buuren, G.N.; Shiralian, M.; Pomeroy, R.K. *Organometallics* **1983**, *2*, 693.

21. Burke, M.R. Ph.D. Thesis, University of Alberta, 1987.

22. Albers, M.O.; Singleton, E.; Coville, N.J. *J. Chem. Ed.* **1986**, *63*, 444.

23. Albers, M.O.; Coville, N.J.; Singleton, E. *J. Chem. Soc., Dalton Trans.* **1982**, 1069

24. Martin, L.R.; Einstein, F.W.B.; Pomeroy, R.K. *Inorg. Chem.* **1985**, *24*, 2777.

25. Cotton, F.A.; Parish, R.V. *J. Chem. Soc.* **1960**, 1440.

26. (a) Bodner, G.M. *Inorg. Chem.* **1975**, *14*, 2694. (b) Mann, B.E.; Taylor, B.F. *^{13}C NMR Data for Organometallic Compounds* Academic: New York 1981; p 14.

27. Adams, D.M. *Metal-Ligand and Related Vibrations* St. Martin's: New York, 1968; p 98 - 101.

28. (a) Jetz, W.; Graham, W.A.G. *J. Am. Chem. Soc.* **1967**, *89*, 2773. (b) Cotton, F.A.; Wilkinson, G. *Advanced Inorganic Chemistry*, 5th ed.; Wiley: New York, 1988, p 1037. (c) Klahn, A.H.; Sutton, D. *Organometallics* **1989**, *8*, 198. d) Chalk, K.L.; Pomeroy, R.K. unpublished results.

29. $Mn_2(CO)_{10-x}(PR_3)_x$ complexes:(a) Giordano, R.; Sappa,E.; Tiripicchio, A.; Tiripicchio Camillini, M.; Mays, M.J.; Brown, M.P. *Polyhedron*, **1989**, *8*, 1855. (b) Treichel, P.M. In *Comprehensive Organometallic Chemistry*; Wilkinson, G., Stone, F.G.A., Abel, E.W., Eds.; Pergamon: Elmsford NY, 1982, Vol.4 p 11 and references therein. $Re_2(CO)_{10-x}(PR_3)_x$ complexes: Boag, N.M.; Kaesz, H.D. In *Comprehensive Organometallic Chemistry*; Wilkinson, G., Stone, F.G.A.; Abel, E.W. Eds.; Pergamon; Elmsford, NY, 1982, Vol. 4 p 171 and references therein.

30. Harris, G.W.; Boeyens, J.C.A.; Coville, N.J. *Organometallics*, **1985**, *4*, 914.

31. (a) Benfield, R.E.; Johnson, B.F.G.; Raithby, P.R.; Sheldrick, G.M. *Acta Crystallogr., Sect. B: Struct. Crystallogr. Cryst. Chem.* **1978**, *B34*, 666. (b) Alex, R.F.; Einstein, F.W.B.; Jones, R.H.; Pomeroy, R.K. *Inorg. Chem.* **1987**, *26*, 3175.

32. Mays, M.J.; Gavins, P.D. *J. Chem. Soc., Dalton Trans.* **1980**, 911. See also (a) Bruce, M.I.; Matisons, J.G.; Wallis, R.C.; Patrick, J.M.; Skelton, B.W.; White, A.H. *J. Chem. Soc. Dalton Trans.*, **1983**, 2365. (b) Ma, A.K.; Einstein, F.W.B.; Johnston, V.J.; Pomeroy, R.K. *Organometallics*, **1990**, *9*, 45.

33. Treichel, P.M. *Adv. Organomet. Chem.* **1973**, *11*, 21.

34. (a) Yamamoto, Y. *Coord. Chem. Rev.* **1980**, *32*, 193. (b) Harvey, P.D.; Butler, I.S.; Harris, G.W.; Coville, N.J. *Inorg. Chem.* **1986**, *25*, 3608.

35. Batchelor, R.J.; Davis, H.B.; Einstein, F.W.B.; Johnston, V.J.; Jones, R.H.; Pomeroy, R.K.; Ramos, A.F. *Organometallics* (accepted for publication).

36. (a) Ismail, A.A.; Sauriol, F.; Sedman, J.; Butler, I.S. *Organometallics* **1985**, *4*, 1914. (b) Dixon, D.T.; Kola, J.C.; Howell, J.A.S. *J. Chem. Soc., Dalton Trans.* **1984**, 1307. (c) Darensbourg, D.J. *Inorg. Chem.* **1979**, *18*, 14.

37. Yamamoto, Y.; Aoki, K.; Yamazaki, H. *Inorg. Chem.* **1979**, *18*, 1681.

38. Tolman, C.A. *Chem. Rev.* **1977**, *77*, 313.

39. Churchill, M.R.; DeBoer, B.G. *Inorg. Chem.* **1977**, *16*, 878.

40. Willis, A.C.; van Buuren, G.N.; Pomeroy, R.K.; Einstein, F.W.B. *Inorg. Chem.* **1983**, *22*, 1162.

41. Cook, N.; Smart, L.; Woodward, P. *J. Chem. Soc., Dalton Trans.* **1977**, 1744.

42. Hoffmann, R. *Angew. Chem. Int. Ed. Engl.* **1982**, *21*, 711.

43. Stone, F.G.A. *Angew. Chem. Int. Ed. Engl.* **1984**, *23*, 89.

44. a) Knight, J.; Mays, M.J. *J. Chem. Soc. A* **1970**, 654. b) Howell, J.A.C.; Matheson, T.N.; Mays, M.J. *J. Organomet. Chem.* **1975**, *88*, 363.

45. Aldridge, M.L.; Green, M.; Howard, J.A.K.; Parin, G.N.; Porter, S.J.; Stone, F.G.A.; Woodward, P. *J. Chem. Soc.; Dalton Trans.* **1982**, 1333.

46. Hsu, L.-Y.; Hsu, W.-L.; Marshall, A.G.; Shore, S.G. *Organometallics* **1984**, *3*, 591.

47. Alex, R.F.; Pomeroy, R.K. *Organometallics* **1987**, *6*, 2437 and references therein.

48. a) Mann, B.E. In *Comprehensive Organometallic Chemistry*; Wilkinson, G.; Stone, F.G.A.; Abel, E.W. Eds. Pergamon: New York, 1982. Vol. 3, p 89. b) Deeming, A.J. *Adv. Organomet. Chem.* **1986**, *26*, 1.

49. Washington, J.; Takats, J. *Organometallics*, **1990**, *9*, 925.

50. Davis, H.B.; Einstein, F.W.B.; Johnston, V.J.; Pomeroy, R.K. *J. Am. Chem. Soc.* **1988**, *110*, 4451.

51. The crystal structure of $(\eta^5\text{-}C_5Me_5)(OC)Ir[Os(CO)_4]_2$ (**1***) was determined by A. Riesen and F.W.B. Einstein.

52. Riesen, A.; Einstein, F.W.B.; Ma, A.K.; Pomeroy, R.K.; Shipley, J.A. *Organometallics*, **1991**, *10*, 3629.

53. Hoyano, J.K.; Graham, W.A.G. personal communication.

54. Kang, J.W.; Moseley, K.; Maitlis, P.M. *J. Am. Chem. Soc.* **1969**, *91*, 5970. See also: Ball, R.G.; Graham, W.A.G.; Heinekey, D.M.; Hoyano, J.K.;

McMaster, A.D.; Mattson, B.M.; Michel, S.T. *Inorg. Chem.* **1990**, *29*, 2023.

55. Johnston, V.J.; Einstein, F.W.B.; Pomeroy, R.K. *J. Am. Chem. Soc.* **1987**, *109*, 7220.

56. Johnson, B.F.G.; Lewis, J.; Raithby, P.R.; Azman, S.N.; Syed-Mustaffa, B.; Taylor, M.J.; Whitmire, K.H.; Clegg, W. *J. Chem. Soc., Dalton Trans.* **1984**, 2111.

57. See ref 26b, p 176 and 180.

58. Aime, S.; Osella, D.; Milone, L.; Rosenberg, E. *J. Organomet. Chem.* **1981**, *213*, 207.

59. (a)Tachikawa, M.; Richter, S.I.; Shapley, J.R. *J. Organomet. Chem.* **1977**, *128*, C9. (b) Aime, S.; Osella, D. *J. Chem. Soc., Chem. Commun.* **1981**, 300.

60. (a) Cotton, F.A.; *Inorg. Chem.* **1966**, *5*, 1083. (b) Cotton, F.A.; Hunter, D.L. *Inorg. Chim. Acta* **1974**, *11*, L9.

61. Johnson, B.F.G.; Lewis, J.; Reichert, B.E.; Schorpp, K.T. *J. Chem. Soc., Dalton Trans.* **1976**, 1403.

62. Deeming, A.J.; Donovan-Mtunzi, S.; Kabir, S.E.; Manning, P.J. *J. Chem. Soc., Dalton Trans.* **1985**, 1037.

63. (a) Adams, H.; Bailey, N.A.; Bentley, G.W.; Mann, B.E. *J. Chem. Soc., Dalton Trans.* **1989**, 1831. (b) Lijuan, L.; D'Agostino, M.F.; Sayer, B.G.; McGlinchey, M.J. *Organometallics* **1992**, *11*, 477.

64. For example: (a) Adams, R.D.; Cotton, F.A. *J. Am. Chem. Soc.* **1973**, *95*, 6589. (b) ref 11a.

65. Ma, A.K,; Pomeroy, R.K. unpublished results. See also: (a) Forster, A.; Johnson, B.F.G.; Lewis, J.; Matheson, T.W.; Robinson, B.H.; Jackson, W.G. *J. Chem. Soc., Chem. Commun.* **1974**, 1042. (b) Aime, S.; Gambino, O.; Milone, L.; Sappa, E.; Rosenberg, E. *Inorg. Chim. Acta* **1975**, *15*, 53.

66. Band, E; Meutterties, E.L.; *Chem. Rev.* **1978**, *78*, 639.

67. Kleier, D.A.; Binsch, G. *QCPE* **1970**, *11*, 165.

68. Johnson, B.F.G.; Lewis, J.; Pippard, D.A. *J. Chem. Soc., Dalton Trans.* **1981**, 407.

69. For example: a) Bruce, M.I.; Matisons, J.G.; Skelton, B.W.; White, A.H. *J. Chem. Soc., Dalton Trans.* **1983**, 2375. b) Keister, J.B.; Shapley, J.R. *Inorg. Chem.* **1982**, *21*, 3304. c) Churchill, M.R.; DeBoer, B.F. *Inorg. Chem.* **1977**, *16*, 2397.

70. Alex, R.F.; Pomeroy, R.K. *J. Organomet. Chem.* **1985**, *284*, 379.

71. See ref 65a and 65b.

72. Kook, A.M.; Nicklas, P.N.; Selegue, J.P.; Smith, S.L.; Aime, S. *Organometallics* **1984**, *3*, 499.

73. a) Benn, R. *Angew. Chem., Int. Engl. Ed.* **1982**, *21*, 626. b) Hawkes, G.; Lian, L.Y.; Randall, E.W.; Sales, K.D. *J. Chem. Soc., Dalton Trans.* **1985**, 225.

74. a) Bodenhausen, G.; Ernst, R.R. *J. Am. Chem. Soc.* **1982**, *104*, 1304. b) Derome, A.E. *Modern NMR Techniques for Chemistry Research* Pergamon, Oxford, 1987, p 239-44. c) Mann, B.E. In *Advances in Organometallic Chemistry*; Stone, F.G.A., West, R., Eds; Academic: San Diego, 1988; Vol 28, p 431-3.

75. Ma, A.K.; Pomeroy R.K. unpublished results.

76. Adams, R.D.; Golembeski, N.M. *Inorg. Chem.* **1979**, *18*, 1909.

77. Gunther, H. *NMR Spectroscopy*; Wiley: New York, 1980; p 73.

78. For example: a) Zuffa, J.L.; Kivi, S.J.; Gladfelter, W.L. *Inorg. Chem.* **1989**, *28*, 1888. b) Beringhelli, T.; D'Alfonso, G.; Molinari, H.; Marri, B.E.; Pickup, B.T.; Spencer, C.M. *J. Chem. Soc., Chem. Commun.* **1986**, 796. c) Rosenberg, E.; Thorsen, C.B.; Milone, L.; Aime, S. *Inorg. Chem.* **1985**, *24*, 231. d) Johnson, B.F.G.; Lewis, J.; Mace, J.; Raithby, P.R.; Stevens, R.E.; Gladfelter, W.L. *Inorg. Chem.* **1984**, *23*, 1600. e) Bruce, M.I.; Schultz, D.; Wallis, A.C.; Redhouse, A.D. *J. Organomet. Chem.* **1979**, *169*, C15. f) Gavins, P.D.; Mays, M.J. *J. Organomet. Chem.* **1978**, *162*, 389. g) Bryan, E.G.; Forster, A.; Johnson, B.F.G.; Lewis, J.; Matheson, T.W. *J. Chem. Soc., Dalton. Trans.* **1978**, 196.

79. Male, J.L.; Pomeroy, R.K. ; Tyler, D.R. unpublished results.

80. Nakatsuji, N.; Hada, M.; Kawashima, A. *Inorg. Chem.* **1992**, *31*, 1740.